ISOLATION AND STRUCTURE ELUCIDATION OF NEW MARINE NATURAL PRODUCTS ISOLATED FROM HAWAIIAN INVERTEBRATES

A DISSERTATION SUBMITTED TO THE GRADUATE DIVISION OF THE UNIVERSITY OF HAWAIʻI AT MĀNOA IN PARTIAL FULFILMENT OF THE REQUIREMENTS FOR THE DEGREE OF

DOCTOR OF PHILOSOPHY

IN

CHEMISTRY

May 2017

By

Stephen M. Parrish

Thesis Committee:

Philip G. Williams, Chairperson
Thomas K. Hemscheidt
Joseph T. Jarrett
Ho L. Ng
Wei-Wen Winston Su

Keywords: Natural Products, BACE1, Polyacetylene, Diterpene, Estrogen Receptor, Secondary Metabolite, Cytotoxicity, Bioactivity Guided Isolation

We certify that we have read this thesis and that, in our opinion, it is satisfactory in the scope and quality as a thesis for the degree of Doctor of Philosophy in Chemistry.

THESIS COMMITTEE

_____

Philip G. Williams, Chairperson

_____

Thomas K. Hemscheidt

_____

Joseph T. Jarrett

_____

Ho L. Ng

_____

Wei-Wen Winston Su

ACKNOWLEDGMENTS

During my tenure at the University of Hawai‘i at Mānoa I’ve had the pleasure to be a part of many different organizations and met many fabulous individuals whom have helped support and shape me to whom I am. To H.U.L.A. and Hawaii Jitterbugs. Memberships to these groups gave me a balance and raised my spirits when the science was not so accommodating. After all, lindy hop was developed during the Great Depression.

Although there are far too many people to thank for their wisdom and help, I would like to take a moment to acknowledge a few. I would like to acknowledge Dr. Philip Williams for his general support. For finding collaborators even if they didn’t always work out and for correcting my poor grammar. To Wes Yoshida for teaching me repetitively how to run 2D NMR experiments. To Ram Neupane, who let me use him as a trouble shooting guide when I needed to bounce ideas or do reactions and for teaching me some computation chemistry. However, I have to give my greatest acknowledgement to Dr. Jinqiu Dai for all of her wonderful snippets of advice and encouragement; the constant reinforcement to not take the shortcuts and reminders to “be patient.” For telling me to call my mother. For being my second mother.

I lastly would like to acknowledge all those family members whom have passed during my studies when this doctorate assumed priority. To my father, his mother and sister, my παπού, and Uncle Bob. This is, in part, for you.

ABSTRACT

Extracts of three species of sponge and an egg mass of the nudibranch *Hexabranchus sanguineus* were examined because they displayed biological activity against either BACE1 or HSV-1 and VSV. In some cases bioactivity guided isolation led to the purified active agent, while in others a loss in activity led to chemical investigations of the extract. The fruits of this labor were the identification, characterization, and, in most cases, biological evaluation of 7 new and 10 known compounds from four separate structural classes. The structures of these compounds were elucidated through analyses of NMR experiments (^{1}H, ^{13}C, TOCSY, HMBC, HSQC, COSY, ROESY, and NOESY), HR-MS data, computational simulations, and optical rotations. For reference, the structures of these compounds are on the next page.

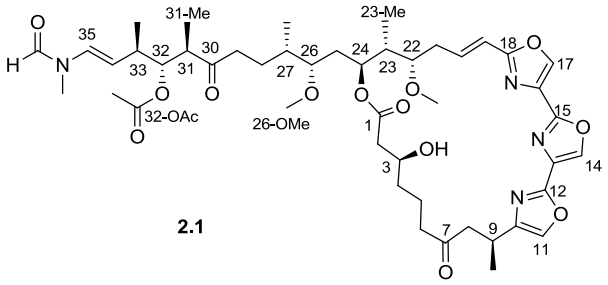

2.1

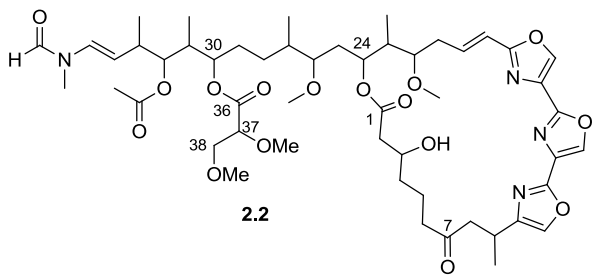

2.2

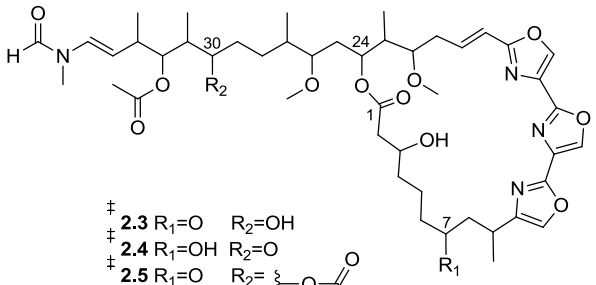

‡ **2.3** R_1=O R_2=OH
‡ **2.4** R_1=OH R_2=O
‡ **2.5** R_1=O R_2=

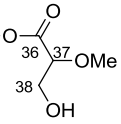

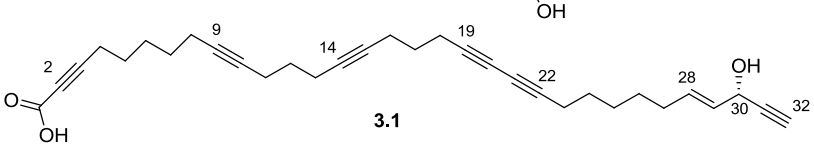

3.1

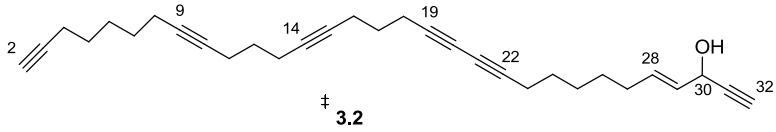

‡ **3.2**

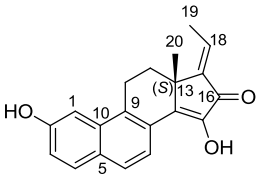

‡ **4.1**

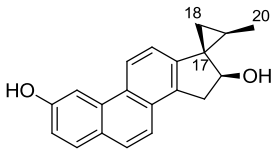

4.2

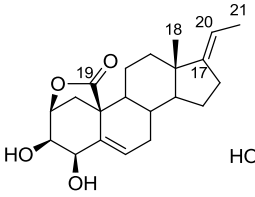

4.3

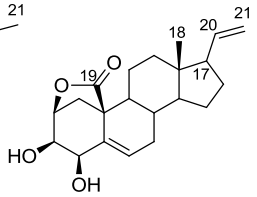

4.4

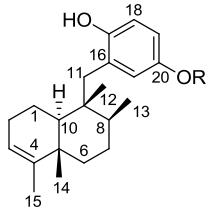

5.1 R=H
5.3 R=$COCH_3$

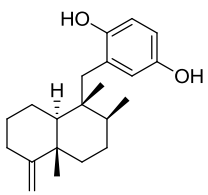

5.2

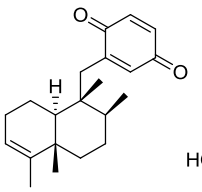

5.4

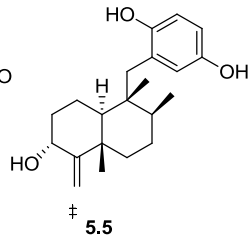

‡ **5.5**

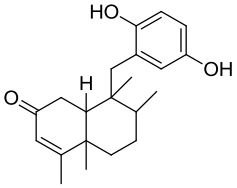

‡ **5.6**

‡ Denotes New Compound

TABLE OF CONTENTS

List of Figures

List of Tables

List of Abbreviations

$[\alpha]_D^T$	specific rotation at 589 nm and temperature T in ºC
$AB_{40/42}$	beta amyloid protein fragments contacting 40 or 42 amino acids
AChEI	acetylcholinesterase inhibitor
ACN	acetonitrile
AD	Alzheimer's disease
AMU	atomic mass unit
APP	amyloid precursor protein
BACE1	beta amyloid cleavage enzyme one
brd	broad doublet

brs	broad singlet
c	concentration in g/100 mL
°C	degrees in Celsius
C8	octylsilyl
calcd	calculated
CD	circular dichroism
$CDCl_3$	deuterated chloroform
^{13}C NMR	nuclear magnetic resonance of carbon isotope with mass 13 Daltons
COSY	correlation spectroscopy
δ	chemical shift
d	doublet
1D	one dimensional
2D	two dimensional
DCM	dichloromethane
dd	doublet of doublets
ddd	doublet of doublet of doublets
dddd	doublet of doublet of doublet of doublets
ddt	doublet of doublet of triplets
DMSO	dimethyl sulfoxide
dq	doublet of quartets
dt	doublet of triplets
EFC	enzyme fragment complementation
ESI	electrospray ionization
FDA	Food and Drug Administration
HMBC	heteronuclear multiple bond coherence
^{1}H NMR	nuclear magnetic resonance of carbon isotope with a mass of 1 Dalton
HPLC	high pressure liquid chromatography
HSQC	heteronuclear single quantum coherence
IC_{50}	inhibitor concentration of 50%
IR	infrared
^{n}J	coupling constant via n bonds

LC-MS	liquid chromatography mass spectrometry
m	multiplet
$[M+H]^+$ /$[M+Na]^+$	protonated molecule/sodium adduct
m/*z*	mass to charge ratio
MHz	megahertz
MS	mass spectrometry
MW	molecular weight
NIH	National Institute of Health
NMR	nuclear magnetic resonance
NOE	nuclear Overhauser effect
[O]	oxidation
p*	pi antibonding orbital
q	quartet
qC	quaternary carbon
qd	quartet of dublets
ROESY	rotating frame Overhauser effect spectroscopy
s	singlet
S	sinister (descriptor in Cahn-Ingold-Prelog system)
sAPP	soluble amyloid precursor protein
SCUBA	self-contained underwater breathing apparatus.
Si	silica
sp.	species
sp^2	sp^2 hybridization state
t	triplet
tdd	triplet of doublet of doublets
TDDFT	Time Dependent Density Function Theory
TOCSY	total correlation spectroscopy
TRPM7	transient receptor potential cation channel, subfamily M, member 7
UV	ultra violet

CHAPTER 1

1. Introduction[1]

1.1. A Brief History of Natural Products

For centuries, mankind has looked towards Nature for inspiration. We have used Nature's chemistry to increase our effectiveness in both taking and preserving life. In warfare, tribes would coat their weaponry in toxins to make them more dangerous. For example, native Hawaiians on Maui would dip their spears in a sacred pool, rubbing the tips against the seaweed-like soft coral, thereby coating them with the deadly toxin palytoxin.[2] This is not an isolated example, as South American natives would rub the ends of their weapons on poison dart frogs, essentially applying lethal or paralysis-inducing alkaloids like epibatidine,[3] to help ensure the kill.

The use of Nature's bounty as traditional medicines has flourished, as well. Almost all ancient civilizations used plants and herbs as a means to remedy their ailments and/or enhance other characteristics. Ancient Egyptians would apply honey to wounds knowing that it helped promote healing and prevent festering.[4] Other cultures, such as the Incans, used plants to combat hunger and fatigue, unaware they were ingesting the powerful narcotic cocaine by chewing on coca leaves.[5] While the use of these traditional medicines flourished, one thing was certain, most knew nothing about the active components these medicines contained.

As civilizations and technology became more advanced, there was a shift from traditional medicines to pharmacognosy. Scientists began isolating and identifying the bioactive components of these traditional medicines and poisons. This work led to many well-known

molecules that are still used today. These were molecules like morphine,[6] extracted from opium poppy, or salicin,[7] a precursor to the drug aspirin from willow bark. During the first half of the 1900's, the major families of antibiotics were identified including the penicillins[8] and tetracyclines.[9] The discovery of these compounds fundamentally changed modern medicine. With these antibiotics widely available, mortality rates gradually decreased,[10] as influenza and pneumonia were no longer within the top five leading causes of death.[11]

Buoyed by these successes, screenings campaigns were conducted using these traditional medicines and poisons to identify compounds that could alleviate other ailments such as hypertension, malaria, or cancer. This work produced many drug leads and a plethora of FDA approved agents such as the anticancer drugs paclitaxel,[12] daunorubicin,[13] and camptothecin.[14] Artemisinin[15] (an antimalarial agent) and lovastatin[16] (cholesterol lowering agent) are fruits of natural product chemistry that currently generate billions in revenue every year.

Up until the 1950's, most natural product research was conducted on terrestrial organisms. It was not until the advent of SCUBA that researchers began intense investigations of the marine environment. Being able to spend prolonged periods underwater allowed researchers to explore new ecological niches and collect new organisms including sponges, tunicates, mollusks, and marine cyanobacteria. These organisms have become extremely productive sources of new chemistry.[17] Having this "new" environment to peruse has yielded seven approved marine drugs,[18] e.g. the anticancer alkaloid trabectedin,[19] isolated from a tunicate, which binds to the minor groove of DNA. Ziconotide,[20] a peptide obtained from a cone snail's poison used to treat severe chronic pain, is another fruit of this labor. Currently there are approximately two dozen marine-derived compounds in clinical trials.[21,22]

According to Newman and Cragg, approximately 46% (558) of all small molecule approved drugs are natural products or their derivatives.[23] This indicates that screening Nature's creations

for molecular scaffolds is a viable strategy for the discovery of new leads. Given the impressive track-record, it is no wonder that we still look to Mother Nature to cure us.

1.2. Selected Target of Current Pathology: BACE1 and Alzheimer's Disease

Human life expectancies are increasing, in part, due to advances in modern medicine. A byproduct of longer lifespans is that other pathologies which often take a longer time to develop begin to manifest. One such disease is Alzheimer's disease (AD). In the United States alone, an estimated 5.4 million people have AD and in 2016, it was expected to have cost over $236 billion (not including the enormous amount of unpaid family care).[24]

While the exact cause of AD is not known, there are several hypotheses. The two major hallmarks of AD are tau tangles and Aβ plaques located in the brain. One hypothesis being investigated deals with the development of tau tangles in the brain,[25,26] which are caused by hyperphosphorylation of tau protein abundant in neurons of the central nervous system.[27] When this hyperphosphorylation occurs, the tau proteins can self-assemble tangles, or if the protein is misfolded, the usually soluble protein can now become insoluble and form aggregates.[28] These tangles, which occur within the neuron, are thought to be toxic to neurons by preventing intracellular transport of nutrients and other essential molecules throughout the cell.[29] The jury is still out on whether the tau tangles are a causative function of AD, or if they are an effect.

The Amyloid Cascade hypothesis is a second AD hypothesis that is strongly supported.[30,31,32] In this hypothesis, amyloid precursor protein (APP) is cleaved by the enzyme β-secretase, also known as BACE1 (beta-amyloid cleavage enzyme one), to generate peptide fragments which may then be cleaved by γ-secretase to form 40 or 42 amino acid insoluble peptide fragments. These insoluble proteins then aggregate, forming $A\beta_{42}$ plaques within the brain (Figure 1.1). The

$A\beta_{42}$ plaques can block neuronal connections and at elevated levels become toxic to the neurons, leading to neuronal degeneration and overall loss of cognitive function. Therefore BACE1 and γ-secretase are potential targets for the treatment of Alzheimer's; the inhibition would lead to diminished levels of insoluble Aβ proteins, preventing the formation of new plaques in the brain and hopefully slowing/halting the onset of Alzheimer's disease. While γ-secretase is not a good drug target, because it plays a major role in the NOTCH signaling pathway that is important in cell differentiation, neuronal function, and cell-cell communication,[33] BACE1 is a suitable target for the treatment of Alzheimer's as knockout mice deficient of BACE1 don't have any overtly abnormal phenotypes.[34] The inhibition of BACE1 would lead to diminished levels of insoluble Aβ proteins, preventing the formation of new plaques in the brain and hopefully slowing/halting the onset of Alzheimer's disease.

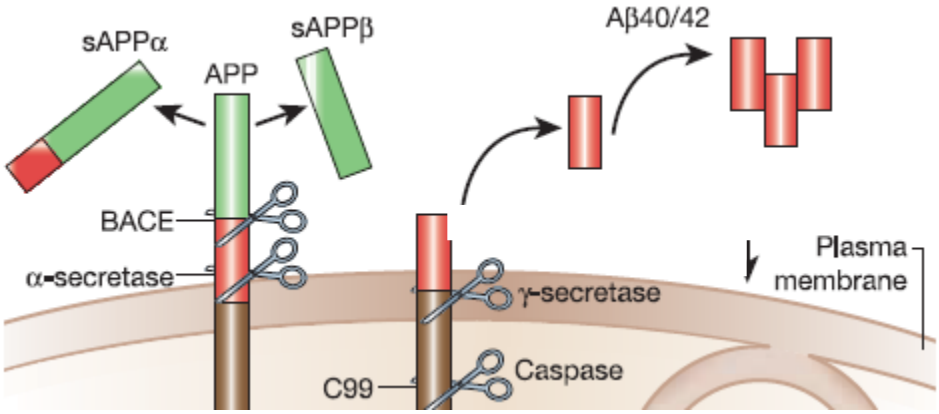

Figure 1.1 Formation of Amyloid Plaques Found in AD. Cleavage of amyloid precursor protein (APP) by a-secretase forms soluble fragments where-as cleavage by both BACE and γ-secretase yields insoluble Aβ40/42 proteins that aggregate to form plaques. Image modified from Mattson, M. P. *Nature*. **2004**, 430, 631.

Currently, five drugs are approved by the FDA to treat AD. However, these drugs only treat the cognitive symptoms, and none target the possible cause. For instance, four of the drugs are acetylcholinesterase inhibitors (AChEI), including galantamine, a natural product drug derived from the bulbs of the lily, daffodil and related plants. AChEIs works by inhibiting the hydrolysis

of acetylcholine, allowing for the neurotransmitter to continue activating neurons.[35] The fifth, memantine, is an *N*-methyl D-aspartate antagonist, which works by regulating glutamate levels in the brain, preventing them from rising to cytotoxic levels.[36] Since these drugs do not treat the cause, neurological deterioration due to AD continues, and unless a medical breakthrough occurs, the incidence rate of AD is expected to double in twenty years.[24]

1.3. Research Objectives and Strategies

When a new drug target arises, such as BACE1, there are typically two major approaches in drug discovery from nature; bioactivity guided isolation and high-throughput screening of libraries of pure, previously isolated compounds (Figure 1.2). In the bioactivity guided approach, samples are collected, extracted, and fractionated with each fraction tested in an assay for activity. The assay is dependent upon the researcher's interest and goals. Any fractions that display activity are checked for purity by ^{1}H NMR and LCMS. An impure fraction then goes back to the fractionation stage, being fractionated under different conditions. This could be anything from changing the chromatography stationary phase, the mobile phase gradient, or even using liquid-liquid partitionings or dialysis. The new fractions are tested again for activity and the active fractions checked for purity. This loop continues until a pure and active compound is isolated. Then the compound is characterized and its structure elucidated. As a lower priority, inactive fractions are then sometimes subject to fractionation in order to isolate other pure compounds. Usually this approach is directed by an interesting mass, ^{1}H NMR, or UV chromatogram. The pure compounds are then screened against various assays often in a directed fashion based on substructures.

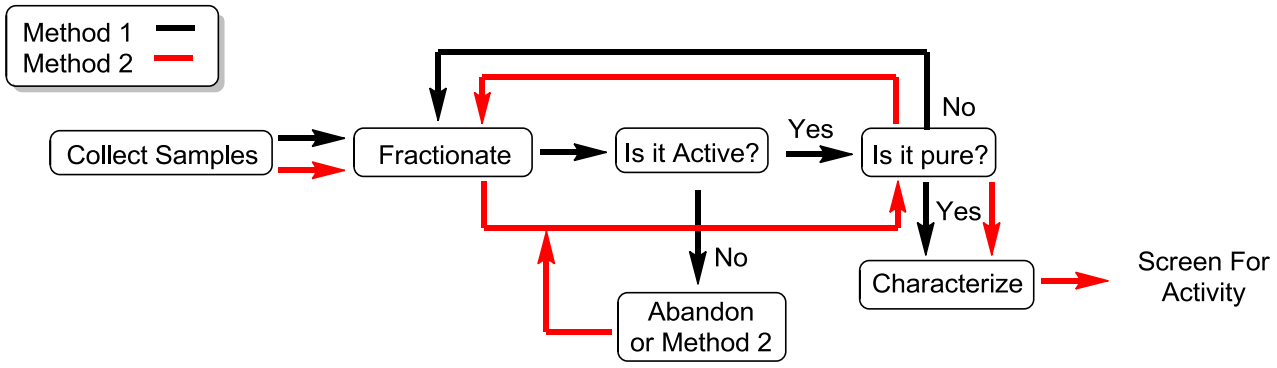

Figure 1.2 Two General Strategies for Drug Discovery. Method 1 is the path of bioactivity guided isolation is described by following the black arrows. The red arrows, method 2, is the path of purity guided isolation where the goal is the collection of pure compounds followed by screening. Method 2 either starts from the sample stage, or more commonly if activity is lost during method 1.

The intent of this research was primarily the identification of new and interesting natural products drug leads. Focusing first on the bioactivity guided isolation of strong inhibitors of BACE1, sometimes subsequent purification proves the initial activity was a false positive. In these cases, a secondary goal was the identification of new compounds based on interesting ^{1}H NMR, MS, or UV chromatograms and then evaluating biological activities inferred by knowledge of their analogues.

Samples of marine organisms were collected from a variety of locations around the Hawaiian Islands. Biological samples were extracted and subjected to a crude fractionation based on polarity with all fractions stored in 96 well plates for easy screening and distribution to collaborators. Preliminary data was collected by screening these samples against BACE1 and projects were chosen based on their strength of inhibition. Samples displaying less than 60% activity and within three standard deviations of the negative control were deemed "active," while samples displaying less than 40% activity were deemed "very active."

The BACE1 EFC assay worked as follows. A circular peptide containing both an enzyme donor (ED) and BACE1 cleavage site was incubated with our sample and BACE1 enzyme. After incubation, an enzyme acceptor reagent was added followed by the chemiluminescent substrate.

If BACE1 is uninhibited it will cleave the circular peptide such that the ED domain is now available for binding to the enzyme acceptor (EA) reagent. When ED and EA bind properly, a working β-galactosidase enzyme is formed which can cleave the chemiluminescent substrate thereby producing light. This light is monitored as a proxy for activity where less light equates to more inhibition and therefore greater "activity." The overall process can be seen in Figure 1.3.

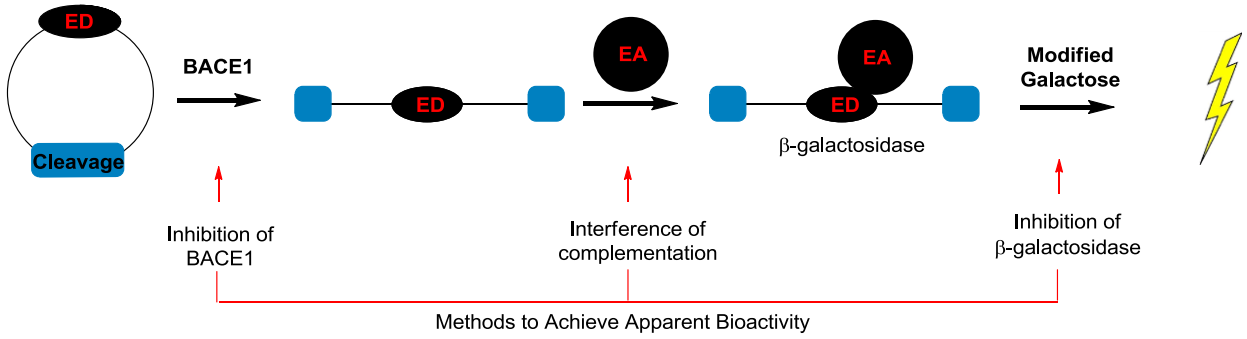

Figure 1.3 BACE1 EFC Assay System. Modes and points of apparent inhibition of BACE1 can be seen at the red arrows. Cleavage is the BACE1 cleavage site, ED is the enzyme donor, EA is the enzyme acceptor, and the lightning bolt represents chemiluminescence.

Since any disruption in light will be interpreted as inhibition, it is important to note the ways this could happen. These ways include if the targeted enzyme BACE1 is inhibited, if the sample disrupts the complementation process of EA and ED, or if the resulting β-galactosidase is inhibited. Therefore, active fractions originating from the 100% MeOH or other very lipophilic fractions were deemed lower priority since they are likely to disrupt the complementation process or form promiscuous aggregators and sequester away enzyme. Likewise, 25% MeOH fractions were deemed lower priority due to their typical large sugar content which is more likely to inhibit or compete for the β-galactosidase.

From 2010-2014 over 500 biological samples have been collected, extracted, and fractionated into over 3,000 samples. Each sample has been screened in the aforementioned EFC BACE1 assay to provide about 51 very active fractions (< 40% enzyme activity; 1.6% of total samples),

and an additional 87 somewhat active fractions (60% to 40% enzyme activity; 2.7% of total samples). This is displayed in Figure 1.4A. A second way to visualize this data is by fraction where it becomes easier to prioritize the samples Figure 1.4B.

A)

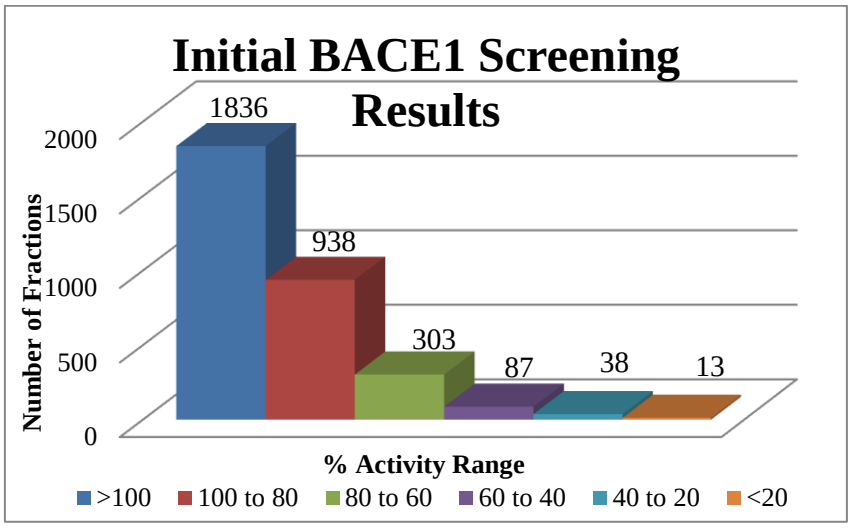

B)

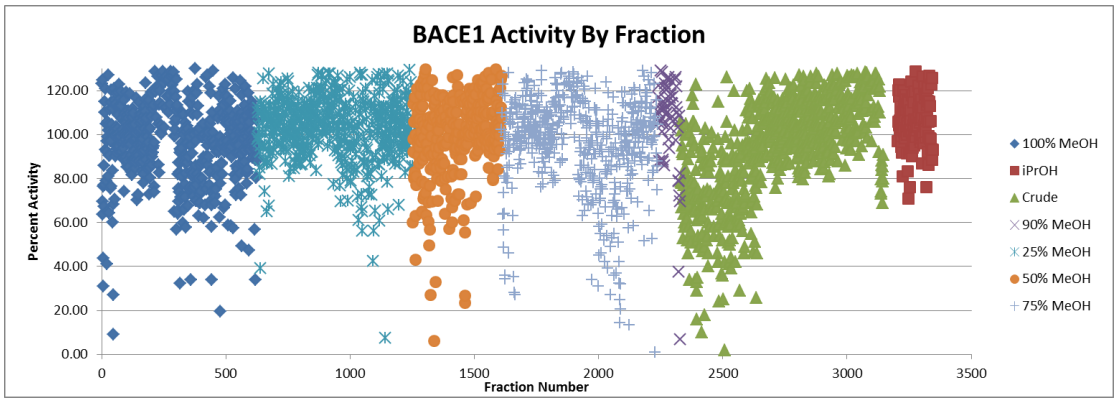

Figure 1.4 EFC BACE1 Assay Screening Results. A) All fractionated samples tested are lumped into six categories based upon % DMSO control activity in their respective assay. Blue, red, and green bars (>60%) are considered inactive. Purple represents moderate activity samples (60%< >40%), while blue and orange are strong activity samples(<40%). B) Same data as above displayed as a scatterplot by fraction to infer polarity of the sample. From left to right the fractions in % MeOH are: 100, 25, 50, 75, 90, crude, iPrOH

Here-in we report the results of three projects chosen based on the BACE 1 results above, and a fourth project based on inhibition of herpes simplex virus 1 (HSV-1) and vesicular stomatitis virus (VSV). In two of these cases bioactivity is lost after fractionation which resulted in the chemical investigation of the animal. In all cases, new secondary metabolites have been isolated,

their structures determined, and the compounds subjected to varying degrees of biological evaluation.

CHAPTER 2

2. Ulapualides C-E Isolated From a Hawaiian *Hexabranchus sanguineus* Egg Mass[37]

2.1. Overview of *Hexabranchus sanguineus* metabolites

Originally isolated in 1986 from egg masses of the nudibranch *Hexabranchus sanguineus*, the ulapualides[38] derive their Hawaiian name from the flowerlike appearance of the Spanish dancer's eggs underwater (ula=red and pua=flower). The ulapualides contain a characteristic tris-oxazole moiety and a long aliphatic tail similar to the mycalolides[39] and kabiramides.[40] These compounds exhibit strong cytotoxicity which is proposed to protect the egg masses from predation. The cytotoxicity arises from the conserved aliphatic tail region that irreversibly binds to G-actin and behaves as a molecular mimic of the actin severing protein gelsolin.[41] Taking advantage of this strong affinity allowed co-crystallization with G-actin that provided the absolute configuration of ulapualide A (**2.1**) via X-ray crystallography.[42,43]

As part of our ongoing search for BACE1 inhibitors, preliminary data in our BACE1 affinity assay suggested the ulapualides in crude extracts bound to that enzyme. After purification, however, ulapualides A (**2.1**) and B (**2.2**) showed no significant inhibition of BACE1 when tested at concentrations up to 30 μM. Further chemical investigation of the extract led to the isolation and identification of three new analogs, ulapualides C-E (**2.3**-**2.5**), described within.

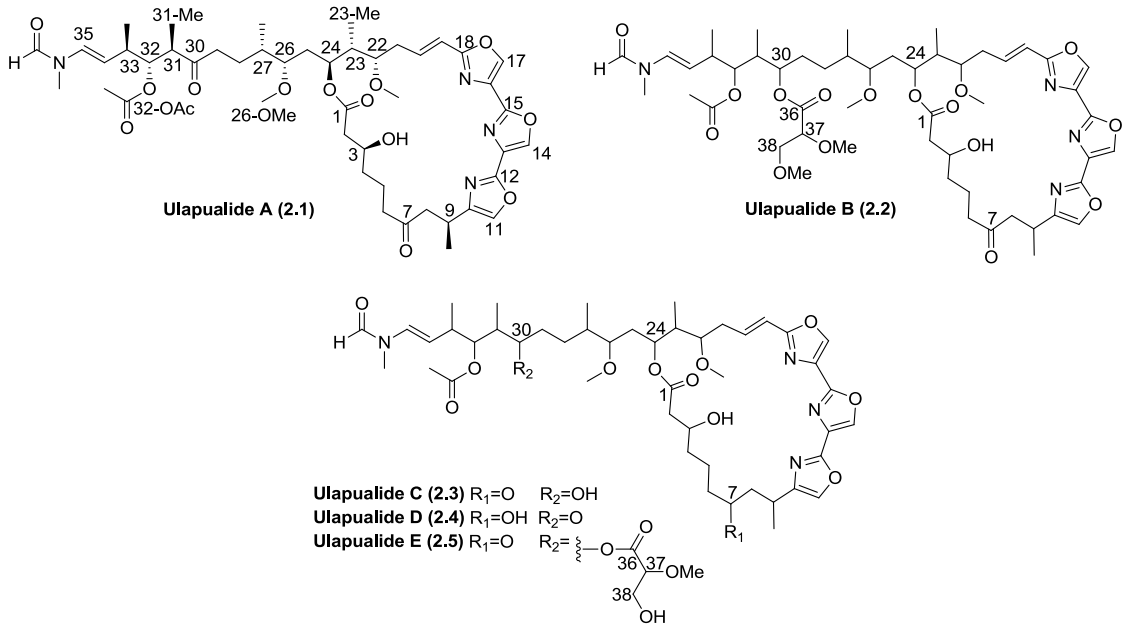

Figure 2.1 Ulapualides Isolated From *Hexabranchus sanguineus* Egg Mass

2.1.1. Isolation and Structure Determination Ulapualides A-E

Two egg masses from the west shore of Oahu (Electric Beach) were extracted with 1:1 MeOH:CH_2Cl_2 overnight three times. The resultant extract was dry loaded on C8 silica gel and subjected to a stepped gradient of MeOH:H_2O. The 75% MeOH fraction was separated by reversed-phase HPLC leading to the isolation of ulapualides A and B (**2.1**-**2.2**), along with ulapualide C (**2.3**) and a mixture of two other analogs. Subjecting this mixture to further HPLC using a different eluent afforded ulapualides D (**2.4**) and E (**2.5**). ^{1}H and ^{13}C NMR data were collected on all isolated compounds (Tables 2.1 and 2.2, respectively), but insufficient sample was available for direct detection of ^{13}C NMR for **2.4** and **2.5**. Consequently, ^{13}C chemical shifts were obtained from indirect HSQC and HMBC experiments for these two compounds.[44]

Table 2.1. ^{1}H NMR Chemical Shifts of Ulapualides C-E (2.3-2.5) in $CDCl_3$

	Ulapualide C (3)	Ulapualide D (4)	Ulapualide E (5)
position	δ_H (J in Hz)[a] [minor][b]	δ_H (J in Hz)[a] [minor][b]	δ_H (J in Hz)[a] [minor][b]
2	2.45, m	2.49, m	2.46, m
3	4.23, septet (4.1)	4.17, m	4.23, septet (4.1)
4	1.65, m	1.72, m	1.72, m
	1.55, m		1.60, m
5	1.95, m	1.25, m	1.96, m
	1.79, m		1.76, m
6	2.55, m	1.76, m	2.57, m
		1.41, m	
7		4.07, br t (8.4)	
8	3.10, m	1.76, m	3.01, m
	2.51, dd (4.9, 16.3)	1.71, m	2.51, dd (15.5, 3.7)
9	3.41, m	2.98, m	3.42, m
9-Me	1.31, d (7.0)	1.32, d (7.0)	1.32, d (6.9)
11	7.41, d (1.0)	7.40, d (1.3)	7.40, s
14	8.06, s	8.08, s	8.06, s
17	8.06, s	8.06, s	8.06, s
19	6.38, d (16.0)	6.31, d (15.7)	6.39, d (16.5)
20	7.05, dt (16.0, 7.4)	7.09, ddd (15.3, 8.9, 6.0)	7.01, m
21	2.66, ddt (14.4, 4.6, 1.8)	2.70, m	2.65, br d (14.5)
	2.44, m	2.36, dd (14.3, 8.2)	2.42, m
22	3.41, m	3.66, t (6.1)	3.40, m
22-OMe	3.37, s	3.38, s	3.37, s
23	1.85, m	1.61, t (7.1)	1.81, m
23-Me	0.91, d (7.0)	0.88, d (6.9)	0.87, d (6.9)
24	5.24, t (8.2)	5.26, t (9.6)	5.23, m
25	1.54, m	1.69, m	1.49, m
		1.41, m	
26	2.95, br d (9.4)	2.98, m	2.93, dt (8.8, 3.3)
26-OMe	3.30, s	3.31, s	3.28, s
27	1.71, m	1.70, m	1.72, m
27-Me	0.832, d (6.7) [0.828, d]	0.792, d (6.7) [0.788, d]	0.83, d (6.9) [0.82, d]
28	1.65, m	1.70, m	0.94, m
	0.90, m	1.25, m	
29	1.25, br s	2.44, m	1.57, m
30	3.44, m		5.10, t (7.2)
31	1.54, m	2.77, dd (8.8, 7.3)	1.81, m
31-Me	0.85, d (7.0) [0.84, d]	1.06, d (7.1) [1.05, d]	0.954, d (6.9) [0.947, d]
32	4.80, td (9.8, 2.9)	5.12, dd (8.9, 3.9) [5.13 dd]	4.75 dd (10.4, 2.4)
32''32-OAc	2.16, s [2.15, s]	2.00, s [1.99, s]	2.11, s [2.10, s]
33	2.56, m	2.48, m	2.53, m
33-Me	1.05, d (6.8) [1.04, d]	1.04, d (7.1) [1.03, d]	1.00, d (5.9) [0.99, d]
34	5.00, dd (14.1, 9.4)	4.98, td (13.6, 9.4)	4.96, dt (14., 9.6)
35	6.50, d (14.3)	6.49, d (14.0)	6.50, d (14.9)
35-NMe	3.02, s [3.06, s]	3.02, s [3.07, s]	3.02, s [3.06, s]
35-NCHO	8.29, s [8.07, s]	8.28, s [8.07, s]	8.29, s [8.07, s]
37			3.81, t (4.8)
37-OMe			3.45, s
38			3.86, br s

[a]500 MHz. [b]Proton signals in brackets are for the minor rotamer.

Table 2.2. ^{13}C NMR Chemical Shifts of Ulapualides A-E (2.1-2.5) in $CDCl_3$

	1		2		3		4		5	
position	δ_C[a,b]	type	δ_C[a,b]	type	δ_C[a,b]	type	δ_C[a,c]	type	δ_C[a,c]	type
1	172.5	C	172.5	C	172.5	C	172.6	C	172.4	C
2	43.0	CH_2	43.0	CH_2	43.0	CH_2	43.4	CH_2	42.8	CH_2
3	68.1	CH	68.1	CH	68.0	CH	69.0	CH	68.3	CH
4	37.1	CH_2	37.1	CH_2	37.1	CH_2	37.5	CH_2	37.0	CH_2
5	20.8	CH_2	20.7	CH_2	20.8	CH_2	29.8	CH_2	20.5	CH_2
6	43.8	CH_2	43.7	CH_2	43.8	CH_2	36.8	CH_2	43.7	CH_2
7	210.5	C	210.4	C	210.5	C	71.2	CH	210.0	C
8	47.8	CH_2	47.7	CH_2	47.7	CH_2	45.4	CH_2	47.8	CH_2
9	27.4	CH	27.3	CH	27.3	CH	31.1	CH	27.4	CH
9-Me	19.6	CH_3	19.6	CH_3	19.7	CH_3	19.3	CH_3	19.4	CH_3
10	146.3	C	146.3	C	146.3	C	146.8	C	146.1	C
11	133.5	CH	133.5	CH	133.5	CH	133.8	CH	133.2	CH
12	154.1	C	154.1	C	154.1	C	154.4	C	153.8	C
13	130.1	C	130.0	C	129.8	C	ND[d]		ND[d]	
14	137.3	CH	137.3	CH	137.3	CH	137.0	CH	ND[d]	
15	156.1	C	156.0	C	156.1	C	156.2	C	155.8	C
16	131.5	C	131.4	C	131.5	C	ND[d]		ND[d]	
17	137.7	CH	137.7	CH	137.7	CH	137.3	CH	ND[d]	
18	162.7	C	162.7	C	162.7	C	162.9	C	162.4	C
19	116.9	CH	116.8	CH	116.8	CH	115.9	CH	116.9	CH
20	139.9	CH	140.0	CH	140.1	CH	141.4	CH	139.7	CH
21	33.8	CH_2	33.9	CH_2	34.0	CH_2	35.0	CH_2	33.4	CH_2
22	79.9	CH	79.9	CH	79.9	CH	78.3	CH	79.6	CH
22-OMe	57.7	CH_3	57.7	CH_3	57.8	CH_3	58.1	CH_3	57.6	CH_3
23	40.3	CH	40.3	CH	40.4	CH	41.0	CH	40.1	CH
23-Me	9.0	CH_3	8.9	CH_3	9.0	CH_3	9.0	CH_3	9.0	CH_3
24	72.8	CH	72.9	CH	72.9	CH	72.6	CH	72.6	CH
25	31.9	CH_2	31.8	CH_2	32.1	CH_2	33.6	CH_2	31.6	CH_2
26	81.7	CH	81.6	CH	81.1	CH	81.6	CH	81.4	CH
26-OMe	58.0	CH_3	57.9	CH_3	58.1	CH_3	58.0	CH_3	57.8	CH_3
27	34.4	CH	34.7	CH	35.5	CH	34.5	CH	34.4	CH
27-Me	15.4	CH_3	15.5	CH_3	15.4	CH_3	15.7	CH_3	15.6	CH_3
28	25.0	CH_2	27.0	CH_2	28.4	CH_2	25.2	CH_2	26.6	CH_2
29	39.8	CH_2	30.4	CH_2	29.7	CH_2	39.8	CH_2	30.3	CH_2
30	211.6	C	73.03	CH	70.0	CH	211.6	C	72.7	CH
31	48.6	CH	37.5	CH	39.7	CH	48.6	CH	37.2	CH
31-Me	13.3	CH_3	9.7	CH_3	8.5	CH_3	13.6	CH_3	9.1	CH_3
32	77.2	CH	79.8	CH	79.3	CH	77.2	CH	76.4	CH
32-OAc	170.0	C	170.6	C	172.5	C	170.0	C	171.1	C
32''	20.8	CH_3	20.9	CH_3	20.9	CH_3	20.9	CH_3	20.8	CH_3
33	36.8	CH	36.9	CH	36.5	CH	36.9	CH	36.7	CH
33-Me	18.8	CH_3	19.3	CH_3	19.4	CH_3	19.0	CH_3	19.4	CH_3
34	110.4	CH	110.2	CH	110.0	CH	110.5	CH	109.5	CH
35	129.4	CH	129.4	CH	129.4	CH	129.4	CH	129.4	CH
35-NMe	27.5	CH_3	27.5	CH_3	27.5	CH_3	27.5	CH_3	27.5	CH_3
35-NCHO	162.1	CH	162.1	CH	162.1	CH	162.1	CH	161.9	CH
36			170.2	C					170.3	C
37			80.6	CH					81.4	CH
37-OMe			58.6	CH_3					58.2	CH_3
38			72.98	CH_2					62.9	CH_2
38-OMe			59.3	CH_3						

[a]Carbon spectra recorded at 125 MHz. [b]Resonances for minor rotamers can be found in the supporting information. [c]Carbon resonances extrapolated from HSQC and HMBC experiments. [d]Not detected.

All new compounds provided ^{1}H NMR spectra consistent with tris-oxazole macrolides. These characteristic signals included the presence of a minor rotamer in an approximate 2:1 ratio evidenced by doubling of the signals for the *N*-methyl group (δ_H 3.02 and 3.06; 35-NMe) and formamide proton (δ_H 8.29 and 8.07; 35-NCHO). This doubling arises from the slow interconversion of the *s-cis*- and *s-trans*- rotamers of the tertiary amide and has been documented in molecules containing similar tail regions including tolytoxin,[45] scytophycins,[46] luminaolide,[47] and rhizapodin.[48] Additionally, for compounds **2.3-2.5**, the deshielded ^{1}H NMR signals for H-11, H-14, and H-17 (Table 1) were consistent with the three contiguous 2,4-disubstituted oxazole rings. Co-isolation of **2.1**-**2.2** from this egg mass supported the conclusion that **2.3**-**2.5** were ulapualide analogs. In addition, **2.1**-**2.5** contained the same UV chromophore with a maximum at 249 nm and produced a consistent pattern of ESI-MS cations including $[M+H-H_2O]^+$, $[M+H]^+$, $[M+NH_4]^+$, and $[M+Na]^+$ where the $[M+H]^+$ were the least abundant.

High resolution mass spectrometry of **2.3** produced a protonated molecule at *m*/*z* 883.4700 $[M+H]^+$. This datum is consistent with a molecular formula of $C_{46}H_{66}N_4O_{13}$ for the parent molecule. Comparison to the ^{1}H NMR spectrum of **2.1** indicated **2.3** contained two more protons, while the ^{13}C NMR spectrum of **2.3** contained an additional sp^3 oxygenated carbon δ_C 70.0 (C-30; **2.3**) at the expense of a keto group at δ_C 211.6 (C-30; **2.1**). HMBC correlations from the methyl group at position 31 to C-30 confirm the keto group on the aliphatic tail of **2.1** was reduced rather than the one in the macrolide ring.

High resolution mass spectrometry of **2.4** provided a protonated molecule at *m*/*z* 883.4662 $[M+H]^+$ as well. Comparison between the NMR data of **2.4** and **2.1** showed an additional oxygenated sp^3 carbon δ_C 71.2 (C-7; **2.4**) and a corresponding proton signal at δ_H 4.07 (H-7; **2.4**)

again at the expense of a carbonyl resonance δ_C 210.5 (C-7; **2.1**). COSY correlations from the methyl group at position 9 to H-9 and from H_2-8 to both H-9 and H-7 support the conclusion that C-7 was a secondary alcohol in **2.4**.

High resolution mass spectrometry of **2.5** gave a protonated molecule at *m*/*z* 985.4976 $[M+H]^+$ consistent with the molecular formula ($C_{50}H_{72}N_4O_{16}$) 14 amu smaller than **2.2**. Comparison of the ^{13}C and ^1H NMR spectra of **2.5** with **2.2** indicated that **2.5** contained one less methoxy group. Taken together, the data suggested **2.5** contained a hydroxy rather than methoxy group. HMBC correlations from the existing OMe groups in **2.5** pinpoint the placement of the methoxy groups and through deduction that C-38 was a primary alcohol.

2.1.2. Relative and Absolute Configurations of Ulapualides A-E

The relative and absolute configurations of **2.3**-**2.5** could not be determined due to the limited amount of material available. In mass limited cases, configurational assignment based on carbon chemical shift comparisons with known analogs is a common tactic. In this case, synthetic studies have demonstrated that this approach is unreliable for distinguishing diasteromers within to this family of natural products.[49] However, all of the tris-oxazole compounds characterized by X-ray crystallography have the same absolute configuration (with the omission of position 9).[50] This suggests that those stereocenters are conserved via a shared biogenesis. In addition, the two other stereocenters in **2.5** are most likely 30*R*,37*R* consistent with **2.2** and the structurally-related mycalolides.[51]

2.2. Bioactivity of Ulapualides A-C

Compounds **2.1-2.3** were tested against select cancer cell lines within the NCI 60-cell panel. These included human renal cell adenocarcinoma (768-0), prostate carcinoma (DU-145), mammary gland adenocarcinoma (MDA-MB-231) and lung carcinoma (A549) cell lines. Samples were tested in triplicate in two independent trials. For the second independent experiment, the concentration was determined through colorimetry using a standard curve made from the more abundant **2.2**. As expected, low to sub-micromolar IC_{50} values were observed for all samples (Table 3). The activities of **2.1-2.2** were similar in all cell-lines tested, while **2.3** was two to four times less potent. Removal of methyl or methoxy groups from the tail region or the introduction of charged groups is predicted to decrease binding affinity to G-actin which is dominated by hydrophobic interactions in the cleft between actin subdomains 1 and 3.[42] The observed decrease in activity could be attributed to replacement of the modified glycerate or keto group with a more polar hydroxy group.

Table 2.3. IC_{50} Values of Ulapualides A-C (2.1-2.3) Against Select NCI Cell Lines (μM)

	768-0		DU-145		MDA-MB-231		A549	
	Trial 1	Trial 2	Trial 1	Trial 2	Trial 1	Trial 2	Trial 1	Trial 2
Ulapualide A (**2.1**)	0.28	0.26	0.26	0.25	0.25	0.23	0.28	0.29
Ulapualide B (**2.2**)	0.26	0.66	0.28	0.34	0.29	0.29	0.33	0.26
Ulapualide C (**2.3**)	1.1	1.4	0.76	0.85	0.58	0.76	0.68	0.60

2.3. Comments on Ulapualides

With the exception of the kabiramides, also isolated from nudibranch eggs, all other tris-oxazole containing molecules were isolated from sponges suggesting that these molecules may be sequestered through predation. The support for this hypothesis includes observed predation of

Halichondria sp. by *Hexabranchus sanguineus*, isolation of dihydrohalichondramide from both species, and sequestration of dihydrohalichondramide in the mantle and the digestive system/gonad of the nudibranch.[52] That similar tris-oxazole compounds have been isolated from sponges of dissimilar phylogeny suggests the ultimate source may be microbial as was found with the bryostatins, metabolites originally isolated from the bryozoan *Bugula neritina*[53] and later discovered to be a product of the symbiont *Endobugula sertula.*[54] The symbiont *E. sertula* is vertically transmitted from bryozoan adult to embryo[55] and provides chemical defenses for the otherwise unprotected larvae.

Compound **2.3** could be an artifact as hydrolysis of the *O*-methylated glycerate in **2.2** would yield the free alcohol **2.3**. That significant amounts of **2.3** can be observed via LCMS in the original MeOH:CH_2Cl_2 extract, before buffers were used suggests this is not the case. Furthermore, treatment of **2.2** in a 2:1 mixture of MeOH:H_2O with 0.1% formic acid for seven days yielded no hydrolysis product detectable by LCMS.

CHAPTER 3

3. Bioactivity Guided Isolation of Metabolites Isolated From *Callyspongia*

3.1. Overview of Polyacetylenes

As part of our search for beta secretase (BACE1) inhibitors, the crude fractionation of a sponge extract collected from Maui displayed potent activity (98% inhibition at 30 μg/mL). Interestingly, no activity was observed by morphologically similar sponges collected from other locations on Maui. Only those samples collected at Black Rock, Maui consistently inhibited BACE1. A bio-assay guided fractionation led to the isolation of a pair of long chain polyacetylenes, known compound **3.1** (callyspongynic acid) and new compound **3.2** (decarboxycallyspongynic acid).

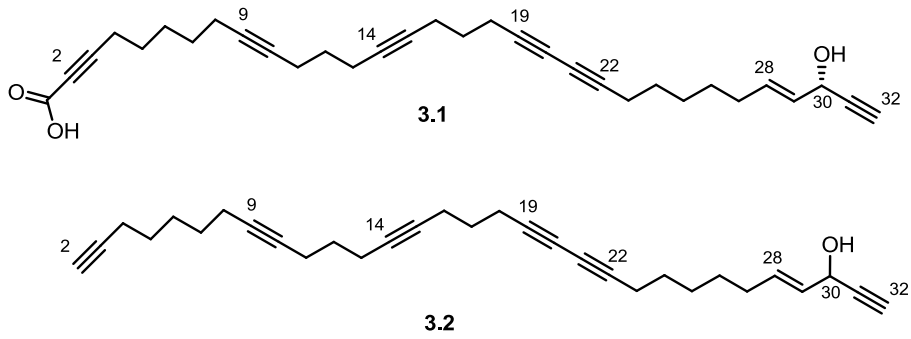

Figure 3.1 Polyacetylenes Isolated from *Callyspongia* sp.

Long chain polyacetylenes are polyketides of varying chain length, from C_{16}-C_{46}, that differ from each other by varying numbers of hydroxy groups and cyclizations. Many of these long chain polyacetylenes are axisymmetric or exhibit central symmetry, and these compounds are considered characteristic chemical markers of *Petrosia* sponges.[56] Others are asymmetric and although there have been a few cases of this type of metabolite isolated from different plants[57] and animals,[58] the order *Haplosclerida* are the main source of these molecules. As such,

asymmetric long chain polyacetylenes are considered a chemotaxonomic markers for some genera within this order including *Petrosia*, *Xestospongia*, and *Callyspongia*.[56]

A recent review compiled more than 600 polyacetylenes isolated from marine algae and invertebrates throughout the past five decades.[56] This simple structural class of compounds displays a variety of biological activities including antifungal,[59] antimicrobial,[60] HIV reverse transcriptase inhibition,[61] and cytotoxicity.[62] Additionally, polyacetylenes have many ecological roles, including inhibiting starfish gametes,[63] preventing fouling by barnacle larvae and inducing metamorphosis of ascidian larvae.[64]

A subtype of marine polyacetylenes contains a 1-yne-3-ol moiety, [65] very similar to callyspongynic acid (**3.1**) and decarboxycallyspongynic acid (**3.2**). The terminal propargylic alcohol is responsible for the strong cytotoxicity observed from extracts containing these molecules. [66] SAR studies established that the flanking unsaturation and the absolute configuration of the carbinol play a significant role, as the (3*R*,4*E*)-en-1-yn-3-ol pharmacophore displayed the more potent submicromolar activity against HTC116 cells. [67 , 68] Various antiproliferative mechanisms were demonstrated by one member of this class, dideoxypetrosynol A,[69] including inhibition of DNA replication,[70] inhibition of cyclooxygenase-2 and telomerase activity,[71] and induction of cyclin-dependent kinase inhibitor p16 and down regulation of retinoblastoma protein phosphorylation.[72]

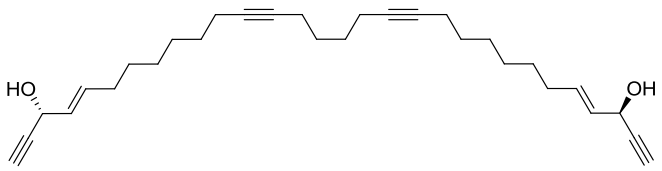

Figure 3.2 Dideoxypetrosynol A. Dideoxypetrosynol A exhibits two (3*R*,4*E*)-en-1-yn-3-ol moieties and displays submicromolar activities against HT116 cells.

3.1.1. Isolation and Structure Elucidation of 3.1 and 3.2

8.0 g of sponges were extracted with 1:1 MeOH:CH_2Cl_2 overnight three times. The resultant extract was subject to a modified Kupchan partitioning and the active CH_2Cl_2 layer was dry loaded on C8 silica gel before elution with a step gradient of increasing MeOH in H_2O. The most potent fraction, 75% MeOH, was then subjected to reversed-phase HPLC. The subsequent 14 fractions were again tested against BACE1. The most active fraction was comprised of one major compound (**3.1**), as determined by ^{1}H NMR, that had a weak UV chromophore and ionized poorly during positive mode ESI analysis. APCI-LCMS yielded a sodium adduct at *m/z* 493.2729 and a dehydrated protonated molecule with *m/z* 453.2820. Both ions are consistent with the molecular formula $C_{32}H_{38}O_3$ and 14 degrees of unsaturation. The large number of signals in the ^{13}C NMR between δ_C 62 and 84 (13) coupled with only a single oxygenated proton signal in the ^{1}H NMR, suggested **3.1** was a polyacetylene. Dereplication through Anti-Marin[73] using the LCMS, ^{1}H and ^{13}C NMR data established it was the known compound callyspongynic acid (**3.1**).[74]

In addition to **3.1**, **3.2** was isolated and characterized. High resolution mass spectrometry of **3.2** yielded a faint ion with *m/z* 427.3010 and a more abundant ion 409.2912 consistent with the protonated ions $[M+H]^+$ and $[M+H-H_2O].^+$ These data indicated a molecule with molecular formula of $C_{31}H_{38}O$ and 13 degrees of unsaturation. The NMR spectra of **3.2** contained many of the same chemical proton and carbon resonances as **3.1**, most notably those belonging to the propargylic alcohol (positions 27-32). With one fewer degree of unsaturation and being by 46 amu smaller than **3.1**,, **3.2** was hypothesized to be a decarboxy version. This is supported by the absence of a carboxyl carbon resonance at δ_C 163.1 (C-1; **3.1**, not shown). Also, **3.2** was

determined to have a second terminal alkyne based on the observed $^{1}J_{CH}$ and $^{2}J_{CH}$ from H-2 of 247.8 Hz and 48.9 Hz to C-2 and C-3, respectively.

Table 3.1. NMR Spectroscopic Data for **3.2** (CD_3OD)

	3.2				
Position	δ_C[a]	Type	δ_H[b] (*J* in Hz)	COSY	HMBC (^{1}H to ^{13}C)
2	69.5	CH	2.17, m		
3	85.0	qC			
4	19.0	CH_2	2.17, m		
5	29.1[c]	CH_2	1.51, m		
6	29.4[c]	CH_2	1.51, m		
7	29.3[c]	CH_2	1.51, m		
8	19.3	CH_2	2.14, m		
9	81.3	qC			
10	80.2	qC			
11	18.48	CH_2	2.24, m		
12	29.8	CH_2	1.60, p (6.9)	H-11/H-13[d]	C-10, C-11,[d] C-13,[d] C-14
13	18.51	CH_2	2.24, m		
14	81.1	qC			
15	80.1	qC			
16	18.6	CH_2	2.24, m		
17	29.0	CH_2	1.65, p (6.9)	H-16,[d] H-18	C-15, C-16,[d] C-18 C-19
18	18.8	CH_2	2.35, t (6.9)	H-17	
19	77.0	qC			
20	66.7	qC			
21	66.3	qC			
22	78.0	qC			
23	19.7	CH_2	2.25, m		
24	29.4	CH_2	1.51, m		
25	29.6	CH_2	1.42, p (3.3)		
26	29.7	CH_2	1.42, p (3.3)		
27	32.8	CH_2	2.08, br q (6.4)	H-26,[d] H-28	C-25, C-28, C-29
28	133.9	CH	5.85, dtd (15.1, 6.8, 1.3)	H-27, H-29	C-26, C-27, C-30
29	130.8	CH	5.56, ddt (15.1, 6.1, 1.3)	H-28, H-30	C-27, C-30, C-31
30	63.1	CH	4.74, br d (6.1)	H-29	C-28, C-29, C-31, C-32
31	84.7	qC			
32	74.6	CH	2.86, d (2.3)	H-30	C-29, C-30

[a]Carbon spectra recorded at 125 MHz. [b]Carbon spectra recorded at 125 MHz. [c]Positions cannot be conclusively determined. [d]Correlation is to a value that is overlapped.

3.1.2. Relative and Absolute Stereochemistry of 3.1-3.2

For new compound **3.2**, absolute chemistry of the lone stereocenter at position 30 was not conclusively determined due to insufficient material to perform a Mosher's analysis. Attempts to

assign the configuration based upon comparisons of optical rotations with known and proven structures were conducted.

Corticatic acid A (**3.3**) is a polyacetylene with only one stereocenter and structural features similar to **3.1**. Reported specific rotations of **3.3** are +28 in $CHCl_3$[75] and -18 in MeOH. The decarboxy version of **3.3**, corticatynol A (**3.4**), displayed a specific rotation of -12 in $CHCl_3$.[76] In all reports, the compounds were confirmed by Mosher's analysis to be the *R* enantiomer. The observation that the specific rotation of **3.3** changed sign in aprotic vs. protic solvents while **3.4** displayed a specific rotation of opposite sign in an aprotic solvent sparked the hypothesis that the sign of the specific rotation was an effect of hydrogen bonding. The hypothesis was that hydrogen bonding between the carboxylic acid and the lone alcohol may induce a secondary structure which creates a specific rotation opposite in sign to that when the hydrogen bonding is disrupted through interactions with the solvent, whereas the decaboxy congeners would not change sign. These interactions would presumably be intramolecular or through small aggregates.

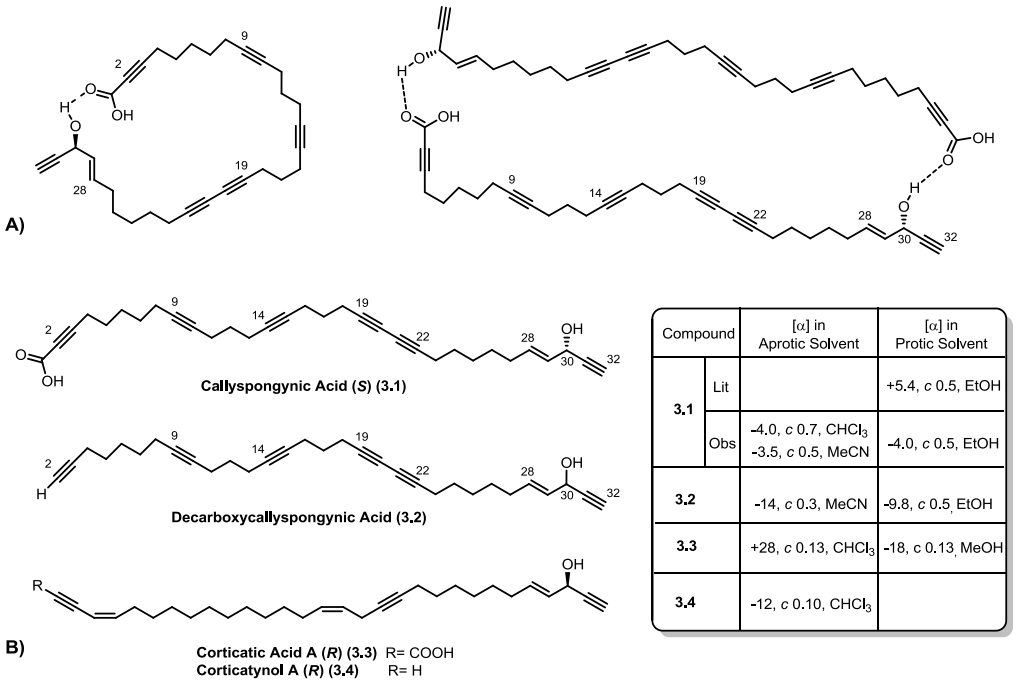

Compound		[α] in Aprotic Solvent	[α] in Protic Solvent
3.1	Lit		+5.4, *c* 0.5, EtOH
	Obs	-4.0, *c* 0.7, $CHCl_3$ -3.5, *c* 0.5, MeCN	-4.0, *c* 0.5, EtOH
3.2		-14, *c* 0.3, MeCN	-9.8, *c* 0.5, EtOH
3.3		+28, *c* 0.13, $CHCl_3$	-18, c 0.13, MeOH
3.4		-12, *c* 0.10, $CHCl_3$	

Figure 3.3 Optical Rotation Analysis of 3.1 and 3.2. A) Potential intramolecular or small aggregate hydrogen bonding in **3.1**. B) Observed and measured [α] of poly acetylenes and their decarboxy congeners in protic vs. aprotic solvents.

Initially, the data seemed to support this hypothesis. The specific rotation of **3.2** (-9.5, EtOH) was similar magnitude but opposite in sign to the reported optical rotation of **3.1** (+5.4, EtOH) in the protic solvent, suggesting that the lone stereocenter is epimeric to **3.1**. As a follow up, the observed optical rotations of both **3.1** and **3.2** displayed a negative sign in the aprotic solvent MeCN, supporting the observation that the sign will invert only for the carboxy analogue. However, in our collected sample, the optical rotation of **3.1** in EtOH displayed a negative sign (-4.0, EtOH). Thus, our hypothesis was disproved as **3.1** displayed the same sign optical activity in both protic and aprotic solvents. Instead, the negative sign suggested that the *R* enantiomer of **3.1** was isolated and highlights the importance of obtaining optical rotations of all pure compounds isolated.

To conclusively tell whether **3.1** isolated was the *R* or *S* enantiomer, the absolute configuration of **3.1** was to be determined. ^{1}H NMR data of both the *R* and *S* Mosher's esters of the saturated *S*-callyspongynic acid have been previously reported. Creating just the *R* Mosher's ester of the hydrogenated product of **3.1** would yield either the *R*-*S* compound (identical to reported) or the *R*-*R* compound (enantiomeric to the reported *S*-*S* stereoisomer). **3.1** was hydrogenated using Pd on carbon under an atmosphere of H_2, and the resultant saturated fatty acid was reacted with the *R*-Mosher's acid chloride to create the *S*-Mosher's ester. Unfortunately, the absolute configuration continues to be ambiguous as the reaction failed to produce the intended product.

3.2. Bioactivity of 3.1-3.2

Callyspongynic acid (**3.1**) previously was reported to be a potent selective inhibitor of α-glucosidase (IC_{50} 0.25 μg/mL) that was inactive against β-glucosidase and β-galactosidase.[74] An important distinction since the in-house BACE1 assay would result in a false positive if the

compound inhibited β-galactosidase. Callyspongynic acid (**3.1**) displayed 95.3% inhibition of BACE1 at 64 μM while the other compounds were inactive against BACE1 at 30 μg/mL. Unfortunately, no IC_{50} values were determined due to the discontinuation of our assay kit. Attempts at using an assay with an orthogonal mechanism (FRET vs. EFC) for BACE1 failed to provide meaningful results. Using two different batches of the kit, we were unable to demonstrate inhibition of BACE1 using either of two positive controls, both of which were commercial BACE1 inhibitors and one of which we had been using for years.

Additionally, **3.1** and **3.2** inhibited pancreatic cell growth with an IC_{50} of 15 and 1 μM, respectively. Both IC_{50} curves display Hill slopes of -10 indicating they are likely promiscuous aggregators.[118] However, these steep Hill slopes are due to a lack of data points in the IC_{50} range and are needed for more accurate assessments. The biological activity data obtained suggests that both ends of **3.1** contain a pharmacophore. The carboxylic acid in **3.1** was previously proven to be necessary for activity with α-glucosidase and is the case for BACE1. At the terminal end, the aforementioned 4-en-1-yn-3-ol moiety likely produces the observed cytotoxicity.

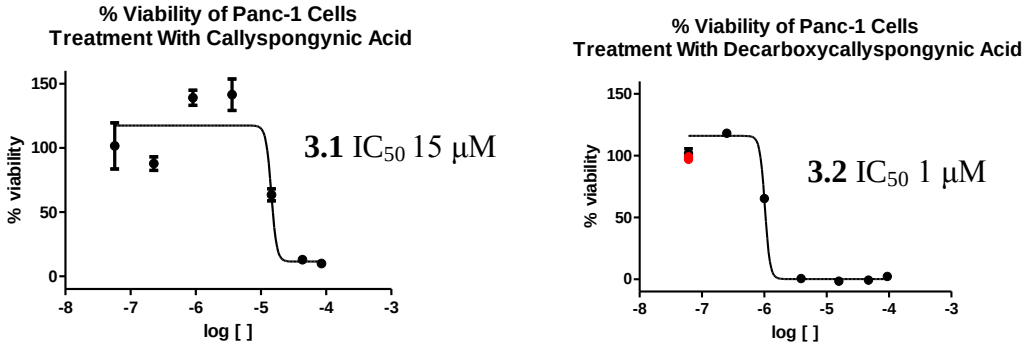

Figure 3.4 IC_{50} Curves for 3.1 and 3.2 With Panc-1 Cells.

3.3. Comments on 3.1-3.2

There are two biosynthetic proposals for the formation of acetylenic bonds. The first is through desaturation of an existing alkene through iron-catalyzed dehydrogenation with molecular oxygen. The second is the elimination of an activated enol carboxylate. Although most evidence to date comes from plants and supports the former, the latter was supported when Fleming demonstrated 3-hydroxy-2-alkene carboxylates eliminate to acetylenes under mild conditions.[77]

A biosynthetic route for marine polyacetylenes has been proposed involving an offshoot of mycolic acid biosynthesis and extension of the Fleming hypothesis.[78] The enol tautomer of the ketoacid could be converted into a good leaving group through phosphorylation. Decarboxylation can then eliminate the leaving group to create an acetylenic bond (Figure 3.5).

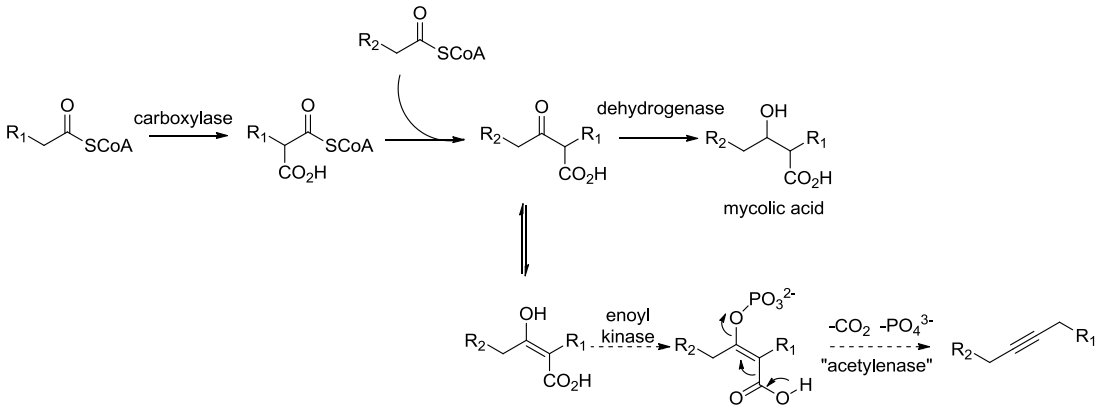

Figure 3.5 Viable Polyketide Biosynthesis for Marine Polyacetylenes. This figure is adapted from Minto, R. E.; Blacklock, B. *J. Prog. Lipid Res*. 2008, *47*, 233-306.

Callyspongynic acid (**3.1**) was isolated from both of the sponge samples which displayed potent BACE1 inhibition. The limited amount of other two morphologically similar sponges have been exhaustively extracted and fractionated, and the resulting fractions sent for screening. At this time, we only have biomass left for one of those samples, which was subjected to LCMS analysis. This resulting ion chromatogram lacked a significant peak with a *m/z* of $[M-H]^-$ 469 corresponding to **3.1**. This suggests **3.1** is the likely causative agent for BACE1 inhibition.

However, as this datum is dependent on the accurate storage of our extract and since the entireties of these sponges have already been used, taxonomical and/or metabolomic analyses are still necessary to confirm this hypothesis and is pending on collection and isolation of more sponge.

CHAPTER 4

4. New Diterpene Isolated From a Hawaiian Sponge of Genus *Myrmekioderma*

4.1. Overview of Metabolites Isolated from *Myrmekioderma*

Although a large diversity of terpenoid and steroidal compounds have been isolated from marine invertebrates, few derivatives of the pregnane class of compounds have been reported.[79,80,81,82] The most recent report being a set of pregnane-10,2-carbolactones isolated by our group.[83] Oxidation of the A ring into phenol pregnane derivatives are even rarer, and lead to bioactivities ranging from barnacle larvae lethality[84] to antimalarial.[85] Initial screening of an undescribed Hawaiian sponge belonging to the genus *Myrmekioderma* and collected off the southern coast of Lana‘i displayed moderate activity against HSV-1 and strong activity against VSV at 200 μg/mL. When extracted on a larger scale, all fractions failed to reproduce this activity. Therefore, a chemical investigation of the sponge was conducted, the fruits of which yielded myrmenaphthol A, **4.1,** and known compounds **4.2-4.4**. Cinanthrenol A (**4.2**) was previously isolated from the sponge *Cinachyrella* sp.[86] while 3,4-dihydroxypregna-5,17-diene-10,2-carbolactone (**4.3**) and 3,4-dihydroxypregna-5,20-diene-10,2-carbolactone (**4.4**) were previously isolated from *Strongylophora* sp. (Haplosclerida).[83]

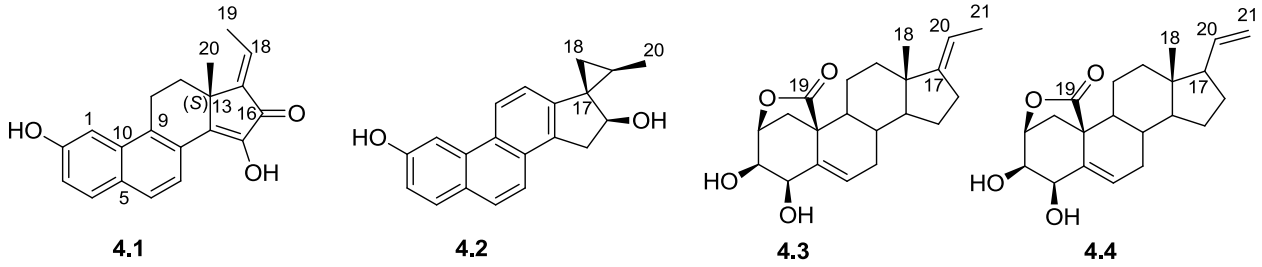

Figure 4.1 Pregnane Derivatives Isolated from the Marine Sponge *Myrmekioderma* sp.

4.1.1. Isolation and Structure Elucidation New Compound Myrmenaphthol A, 4.1

Myrmenaphthol A, **4.1**, was isolated as an amorphous yellow powder after multiple rounds of chromatography of the 75% MeOH fraction. High resolution mass spectrometry provided a protonated molecule with *m/z* 307.1135 $[M+H]^+$. This datum is consistent for a compound with the molecular formula $C_{20}H_{18}O_3$, indicating 12 degrees of unsaturation. The ^{13}C NMR spectrum displayed 14 sp^2 non-carbonyl carbons and the HMBC spectrum displayed an additional sp^2 with a chemical shift indicative of an α,β-unsaturated ketone ($\delta_{C\text{-}16}$ 190.9). Therefore, the molecule has seven double bonds, a ketone, and four rings to account for the degrees of unsaturation.

The structure of **4.1** was assembled by COSY and HMBC correlations. H-6 showed a COSY correlation to H-7 as well as HMBC correlations to C-4,-5,-7,-8, and -10 to help establish part of fragment 1. This fragment was completed with a COSY correlation from H-4 to H-3. A COSY correlation between H-11 and H-12, HMBC correlations from H-19 to C-13,-18,-17, and -16 and HMBC correlations from H-20 to C-12,-14, and -17 allowed the assembly of fragment 2.

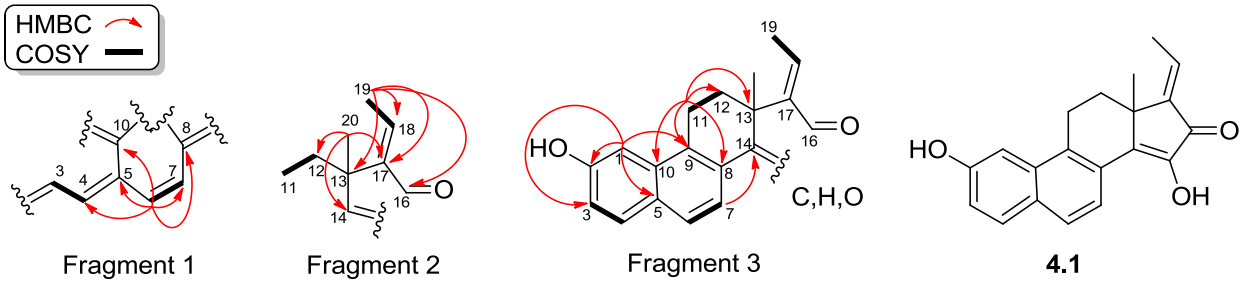

Figure 4.2 Key HMBC and COSY Correlations of 4.1. Key HMBC and COSY correlations leading to the construction of fragments 1-3 and the overall structure elucidation of **4.1**.

More HMBC correlations from H-1 to C-2,-3,-5 and -9 created the phenol A ring while correlations from H-11 to C-8,-9, and -10 connected fragments 1 and 2 to create the naphthyl nucleus. Correlations from H-7 to C-14 then extended the ring system to create fragment 3. At this point, the only remaining pieces in our chemical inventory were a quaternary carbon (δ_C 149.6, C-15), an oxygen, a hydrogen and one degree of unsaturation. Therefore, the only existing option was to create an α-hydroxyketone moiety by inserting the enol between carbons 14 and 16 while closing the ring to create structure **4.1**.

Table 4.2: NMR Spectroscopic Data for **4.1** (CD_3OD)

	4.1					
Position	δ_C[a]	Type	δ_H[b] (*J* in Hz)	COSY	HMBC (^1H to ^{13}C)	ROESY
1	106.8	CH	7.33 d (2.2)	H-3	2, 3, 5, 9	H_2-11
2	157.1	C				
3	119.5	CH	7.09 dd (8.8, 2.2)	H-1, H-4	2, 5	H-4
4	131.1	CH	7.70 d (8.8)	H-3	1, 2, 5, 6, 9, 10	H-3
5	129.6	C				
6	127.2	CH	7.64 d (8.6)	H-7	4, 5, 7 , 8, 10	H-7
7	124.6	CH	8.07 d (8.6)	H-6	5, 8, 9, 10, 14	H-6
8	128.3	C				
9	131.8	C				
10	134.7	C				
11a	24.8	CH_2	3.32 m	H-12 $_b$	8, 9, 10, 12, 13	H-1, H-11
11b			3.22 m	H_2-12	8, 9, 10, 12,	H-1, H-11, H-20
12a	33.0	CH_2	2.68 dd (13.0, 6.1)	H-11_b, H-12_b	9, 11, 13, 14	H-11_b, H-12, H-19, H-20
12b			1.82 td (12.5, 6.4)	H_2-11, H-12_a	11, 13, 20	H-12_a
13	40.7	C				
14	143.1	C				
15	149.6	C				
16	190.9[c]	C				
17	144.1	C				
18	130.7	CH	6.63 q (7.5)	H-19	13, 16, 17, 19	H-19
19	14.8	CH_3	2.05 d (7.5)	H-18	13, 16, 17, 18	H-12_a, H-18, H-20
20	22.3	CH_3	1.31 s		12, 13, 14	H-11_b, H-12_a, H-19

[a]Carbon acquired at 125 MHz. [b]Proton acquired at 500 MHz. [c]Carbon acquired by HMBC experiment

The relative configuration was determined through analysis of ROESY correlations. A ROESY correlation between H-20 and H-19 determined the geometry of the pregnene's C-17 double bond to be *E*. Further ROESY correlations from H-20 to H-11b suggested a cis orientation and correlations from H-20 to H-12a but not H-12b suggested that the methyl group adopts a conformation in which it is pseudo-axial. This is supported by the MM2 minimized energy conformer shown in Figure 4.3B.

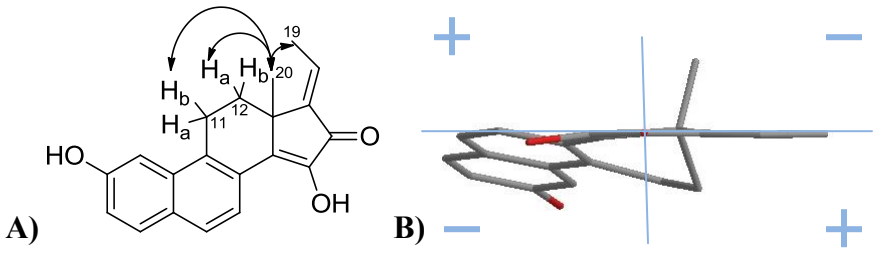

Figure 4.3 Absolute Configuration of 4.1. A) NOE correlations from H-20 to H-19 is evidence the geometry of C-17 olefin is *E*. B) MM2 minimized energy conformer of the *S* conformer of **4.1** as seen looking down the carbonyl bond.

The absolute configuration of **4.1** was determined through CD spectroscopy. Applying the octant rules[87] as described by Djerassi, Moffitt, Klyne, Moscowitz and Woodward to the MM2 minimized energy conformer of **4.1** suggests that **4.1** should yield a negative cotton effect for the *S* conformer and a positive cotton effect for the *R* conformer. Figure 4.3B shows the minimized energy conformer of the *S* enantiomer looking down the carbonyl bond. While the methyl (C-20) lies in the top right negative quadrant and the two opposing methylenes (C-11,-12) in the bottom-right positive quadrant, the bulk of the naphthyl substituent exists in the bottom-left negative quadrant. Additionally, time-dependent density functional theory (TDDFT)[88,89] calculations were performed using Gaussian09 to predict CD spectra for the *S* enantiomer. TDDFT calculations are becoming a more commonly used technique for determining absolute configuration of various natural products of different classes.[90] Conformational analysis of **4.1**, a rigid molecule, displayed four conformers which differed only in the direction of the two oxygen-hydrogen bonds. The two conformers with the α-hydroxy proton in position to hydrogen bond to the carbonyl accounted for 99.7% of the conformers. The predicted CD spectra of these two major conformers supported a negative cotton effect at 360 nm. Experimentally, a negative cotton effect was indeed observed confirming an *S* configuration for the molecule's lone stereocenter at position 13.

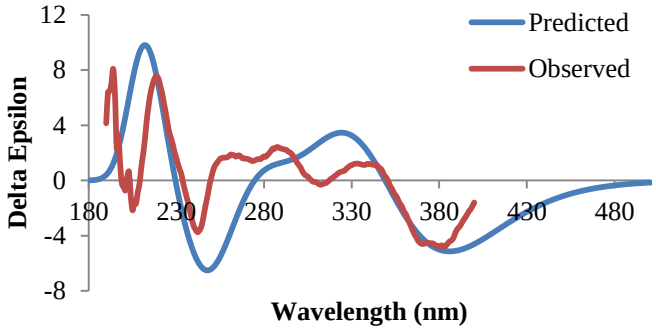

Figure 4.4 Predicted and Observed CD Spectra of 4.1.

4.1.2. Isolation of Known Compounds 4.2-4.4

In pursuit of obtaining more **4.1** from adjacent fractions, HPLC of the 50% MeOH fraction displayed multiple easy to isolate peaks when monitoring 280 nm. Collection of these peaks yielded **4.2** as a pure compound and both **4.3** and **4.4** as mixtures.

The first, **4.2**, shared many of the same proton resonances as **4.1**. Perhaps the biggest similarity was **4.2** displayed resonances consistent with the 2-napthol spin system. HRMS provided a protonated molecule with *m/z* of 291.1386 in agreement with the molecular formula of $C_{20}H_{18}O_2$ and 12 degrees of unsaturation. This coupled with two additional aromatic doublets facilitated our dereplication efforts to establish **4.2** as the known compound cinanthrenol A.

As they did not contain any aromatic signals, both **4.3** and **4.4** belonged to a different structural family. Having recently isolated multiple pregnanes from a similar sponge, the ^{1}H NMR spectrum of **4.3** and **4.4** were quickly determined to be consistent with 10-2-carbolactone pregnanes. Key characteristics in the ^{1}H NMR spectrum include three resolved, sharp doublets (δ_H 3.82, 4.36, and 4.65 ppm) correlating to the three contiguous oxygenated centers (positions 2-4) and a sharp doublet at δ_H 1.62 ppm corresponding to position 2. Both compounds produced a sodiated adduct $[M+Na]^+$ with *m/z* of 367.1885, consistent with the molecular formula $C_{21}H_{28}O_4$. Among other evidence, the ^{1}H NMR of **4.4** displayed only a single methyl signal (δ_H 0.81 ppm, s), i.e. it contained a terminal exocyclic vinyl group not the methyl-substituted exocyclic vinyl group. As such, it was determined to be to be 3,4-dihydroxypregna-5,20-diene-10,2-carbolactone. In contrast, the ^{1}H NMR of **4.3** displayed two methyl signals (δ_H 0.98 ppm, s; δ_H 1.31, d) consistent with 3,4-dihydroxypregna-5,17-diene-10,2-carbolactone containing the methyl-substituted exocyclic double bond.

4.2. Biological Activity of 4.1-4.2

Previous studies have shown **4.2** to have affinity for estrogen receptors. Cinanthrenol A[86] was formerly isolated from a sponge dredged from the depths of the East China Sea, Japan. The phen-anthracene compound previously displayed strong cytotoxicity against P-388 and He-La cells with IC_{50} values of 4.5 and 0.4 μg/mL respectively. Its strongest affinity was to estrogen receptor (ER1) which displayed competitive binding against estradiol with an IC_{50} of 10 nM.[86] Ent-(+)-cinanthrenol A has recently been published, confirming natural cinanthrenol A's absolute stereochemistry and providing a pathway to synthesizing structural analogues.[91] Due to **4.1**'s similar framework to **4.2**, testing of **4.1** and **4.2** against ER1 was conducted in parallel. Unexpectedly, no significant inhibition was displayed for either compound, with only 30% inhibition at 100 μM.

4.3. Comments on Compounds 4.1-4.4

Compound **4.1** displays an uncommon naphthyl nucleus in a traditional steroid ring system, which to the author's knowledge, represents the first example from a marine source. One of the few terrestrial examples of this moiety appears in equilenin,[92] a potent estrogen receptor activator and minor component of the FDA approved drug Premarin. A major difference of **4.1** from nearly all similar natural products is the oxidation of the A ring. Equilenin, like many known biological hormones such as testosterone and estradiol, have oxidation on the 3 position whereas **4.1** has oxidation of the 2 position. This rare oxidation of a steroid nucleus is only known to occur in cinanthrenol A, which has been isolated simultaneously with **4.1**.

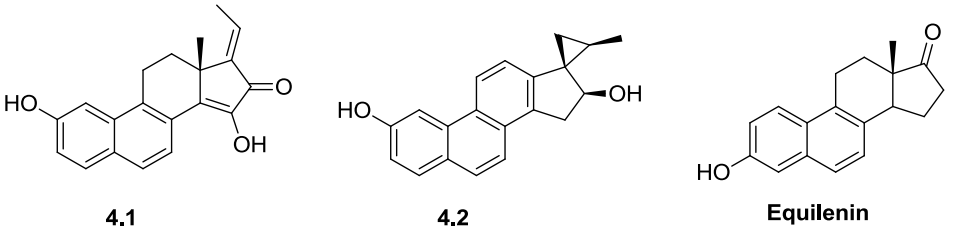

Figure 4.5 Structures of Equilenin, 4.1 and 4.2 for Comparison.

A hypothetical biosynthetic route is proposed for the conversion of **4.1** to **4.2**. The sp^3 methyl group (C-18) is oxidized off (**4.5-4.6**) and then a methylene unit added back on to create the cyclopropyl group through a SAM mechanism similar to fatty acid biosynthesis (**4.6-4.8**).[93] A base catalyzed dehydration of **4.8** yields **4.9** and a simple asymmetric reduction of **4.9** yields cinanthrenol A (**4.2**).

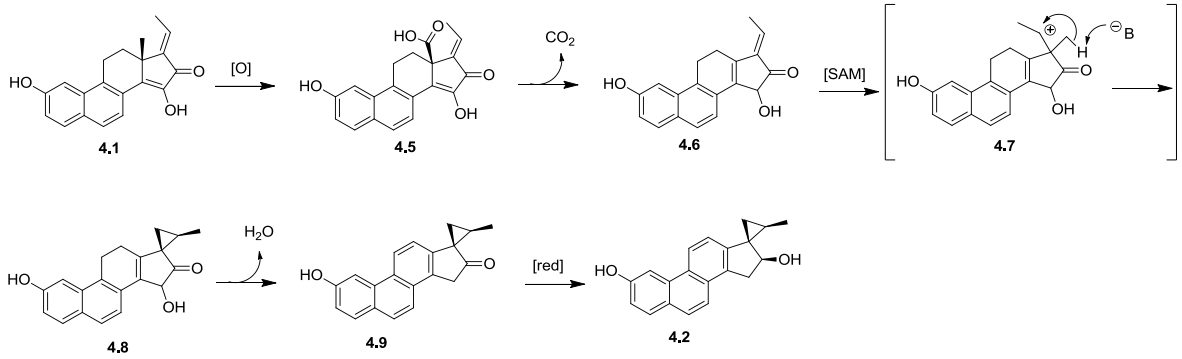

Figure 4.6 Plausible Biosynthetic Scheme of 4.1 to 4.2. New compound **4.1** is a potential precursor to Cinanthrenol A (**4.2**) which may arise after oxidation, SAM methylation, and a series of base catalyzed reactions.

CHAPTER 5

5. Bioactivity Guided Isolation of Metabolites Isolated From an Unidentified Hawaiian Sponge

5.1. Overview of Drimane and Friedodrimane Diterpenes

Friedodrimanes and other likely modified sesquiterpenoid ring units connected to a quinone or hydroquinone are a common moiety isolated from marine sponges and algae. Among the most well-known of these classes are avarol[94] and ilimaquinone.[95] A variety of biological activities have been reported for these compounds, including antileukemia activities, cytotoxicity (killing either coral polyps and/or fish), and possible anti-human immunodeficiency virus agent (HIV).[96] The bioactivity of terpenylquinones is likely due to the quinones' redox potential and/or ability to partake in Michael-type addition-elimination reactions.[97] The cytotoxicity may result from redox cycling and the production of reactive oxygen species (ROS) which could go on to damage tumor cells.[98,99] Support for the mechanism of antitumor action by ROS was previously obtained with avarone (**5.4**) and avarol (**5.1**),[100,101] although there was also evidence of the relevance of arylation of proteins.[97,102,103] Comprehensive reviews on these classes of compounds and their biological activity have been published by Gordaliza,[104] Sladić and Gašić,[105] and Marcos et al.[106]

Crude fractions of an extracted, unidentified Hawaiian sponge displayed moderate inhibition of BACE1. The fraction contained one major peak, a mixture of **5.1** and **5.2**. Further chemical investigation of the sponge yielded **5.3** and **5.4** as mixtures, along with two new pure compounds, **5.5-5.6**.

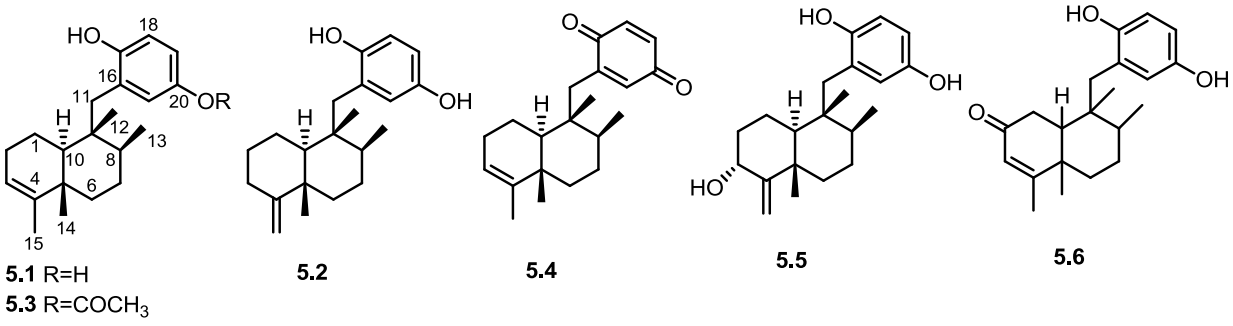

Figure 5.1 Compounds Isolated From Unidentified Hawaiian Sponge.

5.1.1. Isolation and Structure Elucidation of 5.5 and 5.6

Bioactivity guided isolation led to a 3:2 mixture of compounds which displayed moderate BACE1 inhibition. HRMS of this mixture only showed predominantly a single protonated molecule $[M+H]^+$ with *m/z* of 315.2325 consistent with the molecular formula $C_{21}H_{30}O_2$. Initial attempts to purify this mixture, including size exclusion, crystallization, and normal phase HPLC, ultimately failed. However, these attempts cleaned the mixture to a 4:1 ratio which allowed for the dereplication of the major compound, avarol (**5.1**). Only after a lengthy round of reversed-phase HPLC using a pentafluorophenyl column and multiple injections of microgram amounts allowed for the isolation of small quantities of pure **5.2**. With a pure sample in hand, dereplication quickly showed that **5.2** was the known compound isoavarol.

Preparative HPLC of the parent fraction was conducted to remove the major compounds in order to investigate the smaller components of the extract, yielding two more mixtures of compounds. The first, **5.3**, contained the same aromatic ^1H NMR corresponding to the 1,2,5 substituted benzene but displayed an additional methyl singlet. Furthermore, LCMS produced a deprotonated ion $[M-H]^-$ at *m/z* 355.2272 consistent with the molecular formula $C_{23}H_{32}O_3$, or C_2H_2O larger than **5.1**. It was then apparent **5.3** was avarol monoacetate. The second, **5.4**, displayed a protonated molecule with *m/z* of 313.2158, consistent with the molecular formula

$C_{21}H_{28}O_2$ and one degree of unsaturation more than **5.1**. Dereplication of ^{1}H NMR signals determined **5.4** was avarone. Minor compounds existed in both fractions of **5.3** and **5.4** as can be seen in the doubling of the two doublets (δ_H 2.59 and 2.73, H_2-11) in a similar way of **5.1** and **5.2**. These minor compounds are presumably their isomeric congeners with an exocyclic olefin. Further evidence for this assertion includes the appearance of minor carbon resonances at δ_C 159.9 and 105.7 in the ^{13}C NMR of **5.3** and proton resonances at δ_H 4.42 and δ_H 4.72. As known compounds, these were left impure due to the lengthy HPLC needed to separate these isomers.

Chemical exploration into a different fraction yielded a mixture of two more compounds, **5.5** and **5.6**. Similar aromatic and methyl signals suggested **5.5** to be an analogue of **5.1**. HRESIMS of **5.5** displayed a protonated molecule $[M+H]^+$ with *m/z* of 329.2095, consistent with the molecular formula $C_{21}H_{29}O_3$ and contained only an extra oxygen in comparison to known compound **5.1**. Comparison of the ^{1}H NMR spectrum of **5.5** to **5.1** indicated **5.5** contained an oxygenated methine (δ_H 4.27, H-3). COSY correlations from H-3 to H_2-2 coupled with HMBC correlations from H-3 to C-2, C-4, and C-15 suggested the oxygenation was at the 3 position.

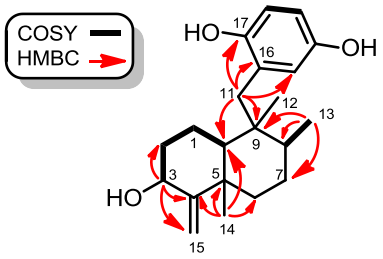

Figure 5.2 Key COSY and HMBC Correlations of 5.5

Table 5.1: NMR Spectroscopic Data (500 MHz, CD_3OD) for 3α-hydroxyisoavarol (**5.5**)

				3α-hydroxyisoavarol (5)	
position	δ_C[a]	type	δ_H, (*J* in Hz)[b]	COSY[b]	HMBC[b] (^1H to ^{13}C)
1a	22.9	CH_2	2.28, dq (13.5, 2.5)	H-10, H-2b, H-1b	C-5
1b			1.59, qd (13.3, 3.3)	H-10, H_2-2, H-1a	C-3, C-5, C-10
2a	38.16	CH_2	2.11, m	H-3, H-2b, H-1b	C-3, C-4
2b			1.28, m		
3	70.5	CH	4.27, ddt (12.0, 5.5, 1.7)	H_2-2, H_2-15	C-2, C-4, C-15
4	163.3	qC			
5	41.5	qC			
6	38.24	CH_2	1.47, m		
7a	28.7	CH_2	1.49, m		
7b			1.42, m		
8	37.3	CH	1.51, m		
9	43.0	qC			
10	49.2	CH	0.99, dd (12.1, 2.3)	H_2-1	C-9, C-12, C-15
11a	38.3	CH_2	2.67, d (13.9)	H-11b	C-8, C-9, C-10, C-12, C-16, C-17, C-21
11b			2.46, d (13.9)	H-11a	C-8, C-9, C-10, C-12, C-16, C-17, C-21
12	18.1	CH_3	0.84, s		C-8, C-9, C-10, C-11
13	18.0	CH_3	1.02, d (6.0)		C-7, C-8, C-9
14	21.5	CH_3	1.05. s		C-4, C-5, C-6, C-10,
15	100.1	CH_2	4.83, t (1.55)	H-15b, H-3	C-3, C-4, C-5
			4.55, brs		C-3, C-5
16	127.2	qC			
17	150.7	qC			
18	116.4	CH	6.53, d (8.6)		C-16, C-20
19	114.5	CH	6.43, dd (8.6, 3.0)		C-17, C-21
20	150.1	qC			
21	120.1	CH	6.48, d (3.0)		C-11, C-17, C-19

[a]Carbon spectra recorded at 125 MHz. [b]Proton spectra recorded at 500 MHz.

HRESIMS of **5.6** displayed a protonated molecule with *m/z* 327.1946 $[M+H]^+$ consistent with the molecular formula $C_{21}H_{27}O_3$, two protons short of **5.5**. HMBC correlations indicated **5.6** contained a keto group (δ_C 202.4, C-2), the only additional sp^2 carbon, and no resonances indicative of an sp^3 oxygenated carbon. This suggested the primary difference was the replacement of an alcohol with a keto group. HMBC correlations from H_3-15 to C-3,-4,-5 and H_3-14 to C-4,-5,-6,-10 helped determine the keto group to be on position 2 and α,β-unsaturated. At first glance, a carbon chemical shift of 176.7 ppm (C-4) is quite unusual for a beta carbon in an α,β-unsaturated system, with α,β-unsaturated cyclohexanone only reaching 150.6 ppm.[107] The deshielded resonance indicates ring strain in the trans-decalin structure. This is presumably

why in the first attempt at structure elucidation, it was noticed that the compound was decomposing. The solvent, MeOH, could undergo a Michael addition to the α,β-unsaturated ketone.

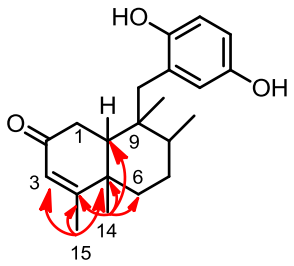

Figure 5.3 Key HMBC Correlations of 5.6

Table 5.2: NMR Spectroscopic Data (500 MHz, $CDCl_3$) for 2-oxoavarol (**5.6**)

			2-oxoavarol (6)		
position	δ_C[a]	type	δ_H, (*J* in Hz)[b]	COSY[b]	HMBC[b] (^{1}H to ^{13}C)
1a	36.6	CH	2.39, d (12.1)	H-10	C-2, C-10
2	202.4[c]	qC			
3	125.5	CH	5.63, d (1.2)	H-15	C-5, C-15
4	173.0[c]	qC			
5	40.2[c]	qC			
6	34.7	CH_2	1.69, m		C-10
7a	27.0	CH_2	1.45, m		
7b			1.45, m		
8	35.3	CH	1.57, m	H-13	
9	41.3[c]	qC			
10	45.9	CH	1.71, d (12.1)	H-1	C-1, C-5, C-9, C-12,
11a	37.0	CH_2	2.77, d (14.3)	H-11b	C-8, C-9, C-16, C-17, C-21
11b			2.43, d (14.3)	H-11a	C-9, C-10, C-16, C-17, C-21
12	17.6	CH_3	0.91, s		C-8, C-9, C-10, C-11,
13	17.2	CH_3	1.04, d (6.8)	H-8	C-7, C-8, C-9
14	18.1	CH_3	1.15, s		C-4, C-5, C-6, C10
15	19.0	CH_3	1.79, d (1.2)	H-3	C-3, C-4, C-5
16	125.6[c]	qC			
17	148.6[c]	qC			
18	116.2	CH	6.56, m		C-16, C-20
19	113.9	CH	6.55, m		C-21
20	148.7[c]	qC			
21	119.4	CH	6.53, br d (1.5)		C-11, C-17, C-19

[a]Carbon spectra recorded at 125 MHz. [b]Proton spectra recorded at 500 MHz. [c]Carbons acquired through HMBC correlations.

5.1.2. Relative and Absolute Configuration of 5.5-5.6

Relative configuration of **5.5** was determined through *J* based analyses and NOE correlations.

Both methines H-3 and H-10 displayed a large *J* of 12 Hz which placed them both axial in a cyclohexane system. An NOE between H-14 and H-3 indicated they were *cis*. Additional NOE was observed between H-12 to H-13 and H-14 placed these methyl groups *cis* to H-3. Absolute configuration could not be determined due to insufficient material. Absolute or relative configuration of **5.6** could not be determined due to degradation of the material when conducting 2D NMR experiments.

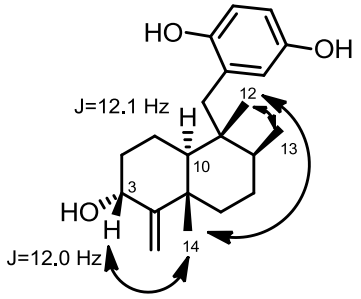

Figure 5.4 Relative Configuration of 5.5. Key NOE (Black arrows) and coupling constant values used in the determination of **5.5**'s relative configuration.

5.2. Bioactivity of 5.5-5.6

Although preliminary data on this family of compounds displayed weak inhibition of BACE1, IC_{50}'s on these compounds could not be determined due to the in-house assay system being discontinued and the eventual degradation of material. However, a very similar compound, ilimaquinone, was determined to inhibit BACE1 with an IC_{50} of 65 µM. Therefore, it is likely that new compounds **5.5** and **5.6** would also show a low degree of BACE1 inhibition.

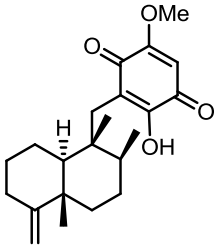

Figure 5.5 Ilimaquinone.

5.3. Comments on 5.5-5.6

Biosynthetically, farnesyl pyrophosphate is presumed to be the precursor for the decalin ring.[108] Electrophilic attack at the head position of the farnesyl derivative initiates a cyclization to create a bicyclic carbocation intermediate. A series of 1,2-hydride and alkyl shifts result in the rearranged friedodrimane structure while removal of a proton quenches the cation, generating the resultant olefin. Alternatively, intramolecular nucleophilic attack can also occur on the rearranged cation to yield many other previously isolated drimanes including puupehenol,[109] *ent*-chromazonarol,[110] and aureol.[111] This suggests it is likely that the hydroquinone or quinone is added before the decalin ring gets assembled.

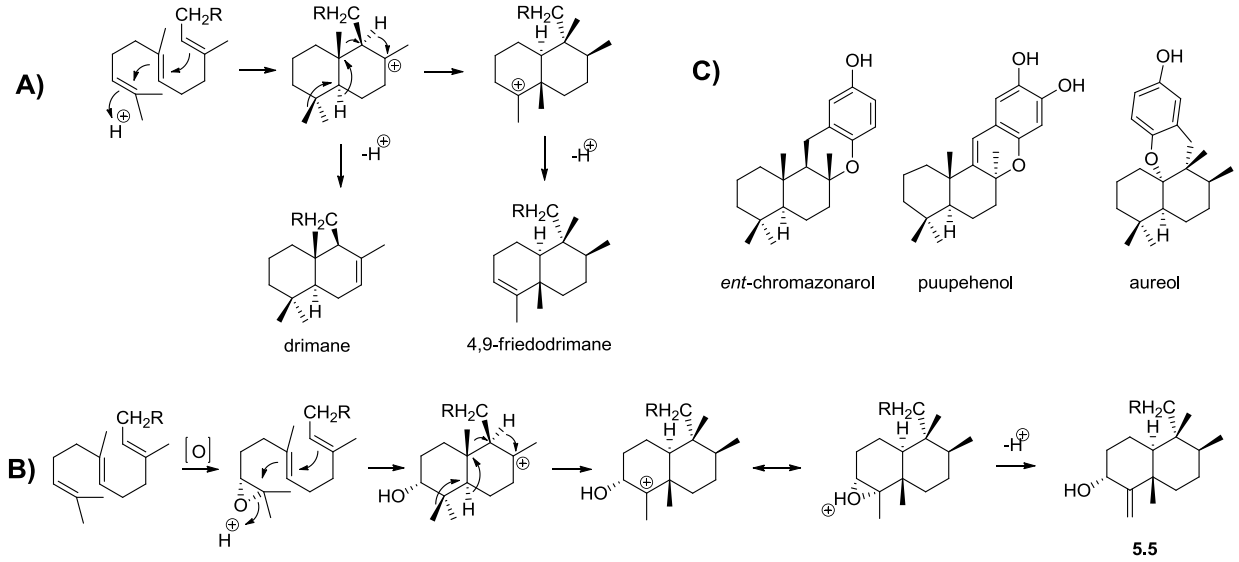

Figure 5.6 Likely Formation of Drimane and Friedodrimane Compounds. A) General formation of drimanes and rearranged friedodrimane skeletons. B) Plausaible biosynthesis of **5.5**. C) Known compounds arising from the intramolecular quenching via attack of the hydroquinone.

Compound **5.5**, could arise through the same steps if the olefin at the head position was first subjected to an epoxidation before electrophilic attack and cyclization. To the author's knowledge, **5.5** is the first friedodrimane and only the third drimane to be oxygenated on the A ring (the other two being 3-ketotauranin and 3α-hydroxytauranin). Compound **5.6** is unusual due to its oxidation at position 2 and has no obvious biogenesis.

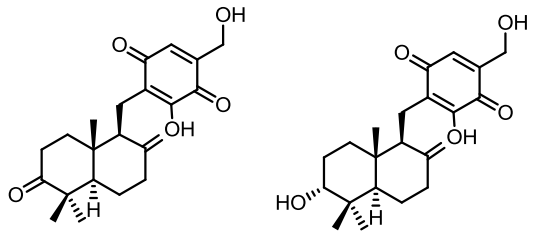

Figure 5.7 3-Ketotautanin and 3*α*-Hydroxytauranin.

CHAPTER 6

6. Experimental

6.1. General Experimental Conditions

6.1.1. NMR

^{1}H, ^{13}C NMR and 2D NMR experiments on the natural products were carried out on Varian Unity Inova 500 MHz spectrometer. NMR spectra were referenced to the appropriate residual solvent signal (δ_H 7.26, δ_C 77.2 for $CDCl_3$; δ_H 3.30, δ_C 49.0 for MeOH-d_4) with chemical shifts reported in δ units (ppm). Multiplicities are as indicated in the list of abbreviations. The HSQC experiments were optimized for $^{1}J_{C,H}$ = 140 Hz and HMBC experiments for $^{3}J_{C,H}$ = 7 Hz. Mixing times for ROESY and NOESY experiments were 500 ms and generally 80 ms for the 1D TOCSY experiments.

6.1.2. Mass Spectrometry

High-resolution ESI mass spectra were recorded in the positive or negative mode on an Agilent 1100 LC coupled to an Agilent 6210 MSD-TOF. The gas temperature was held at 325 °C, sheath nitrogen flow rate was set at 10 L/min, and the nebulizer at 30 psig. The ESI source needle voltage was set at 3.5 kV. For compounds **3.1** and **3.2**, the APCI source was used with the voltage set at 3.5 kV. Low-resolution ESI mass spectra were recorded in the positive/negative mode by an Agilent 1200 LC coupled to an Agilent 6410 Triple Quad MS. In these cases, the gas temperature was held at 325 °C, sheath nitrogen flow rate was set at 10 L/min, and the nebulizer at 30 psig. The ESI source needle voltage was set at 3.5 kV.

6.1.3. IR, UV, CD, and Optical Rotations

The UV spectra were determined on a Varian Cary 50 Bio series spectrophotometer and the IR spectra were recorded on a Shimadzu IRAffinity-1 series FTIR instrument as a thin solid on either CaF_2 or NaCl disks. CD spectrum was measured on a Jasco J-815 CD spectrometer with the sample dissolved in MeOH. The optical rotations were measured on a Jasco-DIP-700 polarimeter at the sodium D line (589 nm).

6.1.4. Computational Analysis

Conformers within 5 kcal/mol of the lowest energy conformer were searched using the Monte Carlo multiple minimum (MCMM) method and the OPLS-2005 force field in MacroModel (Schrodinger Inc.). Each conformer within 5 kcal/mol of the lowest energy conformer was optimized in Gaussian09[112] at the M06-2X/6-31+G level and the geometries of all conformers with similar energies were checked for redundancy. Density functional theory (DFT) was used to perform calculations, which were carried out in Gaussian 09. All ground-state geometries were optimized at the B3LYP/6-31+G level. The same DFT level was employed to evaluate the effects of solvation in methanol using the SCRF/PCM method.[113,114] TDDFT[88,89] calculations at the B3LYP/6-31+G and the B3LYP/aug-cc-pVDZ levels were conducted to calculate the electronic excitation energies and rotational strengths in methanol.

6.2. Biological Material

6.2.1. Extraction and Isolation of Metabolites from *Hexabranchus sanguineus*

The egg masses of *Hexabranchus sanguineus* were collected via SCUBA off the west shore of O'ahu at Electric Beach (21°21'14.3"N 158°07'49.7"W) at a depth of 20 feet on September 23rd, 2011. The two egg masses collected were bright pink and were immediately extracted with 1:1 MeOH:CH_2Cl_2 three times overnight to yield 2.7 g of extract. The combined extract was then dry loaded on C8 silica gel and was subjected to a solid phase extraction procedure consisting of five steps of increasing MeOH:H_2O content (0%, 25%, 50%, 75%, 100%, and an isopropanol wash). The 75% MeOH fraction was subjected to reversed-phase HPLC on a Phenomenex column (Luna C8; 250x10 mm, 5 µ) using a flow rate of 2.8 mL/min and a concentration gradient of 50%-70% (CH_3CN:H_2O) over 30 min. Detection was by UV, using a PDA and monitoring at 249 nm. This afforded pure compounds ulapualide B (**2.2**, t_R = 24 min, 8 mg, 0.32% yield), ulapualide A (**2.1**, t_R = 21 min, 6 mg, 0.24% yield; $[\alpha]^{22}_D$ -39, *c* 0.20, MeOH), ulapualide C (**2.3**, t_R = 18.5 min, 1.6 mg, 0.064% yield) and a mixture of ulapualides D and E. This mixture was further purified using a C18 column (Luna; 100x4.6 mm, 5 µ) at a flow of 1.0 mL/min and using an isocratic system of 65% MeOH-H_2O to yield ulapualide D (**2.4**, t_R =20 min, 0.5 mg, 0.02% yield) and ulapualide E (**2.5**, t_R =24 min, 0.5 mg, 0.02% yield). Purity was assessed at 210 nm and determined to be 95.3%, 94.5%, and 95.6% for **2.1**, **2.2** and **2.3** respectively, prior to biological testing. **2.4** and **2.5** were 91% and 85% pure by NMR respectively.

6.2.2. Extraction and Isolation of Metabolites from *Callyspongia* sp.

The pink and lavender sponge belonging to the genus *Callyspongia* (class Demospongiae,

order Haplosclerida, family Callyspongiidae) was collected at Black Rock, Maui (20°55'36.8"N, 156°41'47.8"W) at a depth of 28 ft. The sponges turned brown above water and were extracted with 1:1 MeOH:CH_2Cl_2 three times overnight to yield 1.7 g of extract. The combined extract was dissolved in MeOH and subject to a modified Kupchan partitioning with Hex, CH_2Cl_2, and H_2O. The CH_2Cl_2 partition (451 mg) was dry loaded on C8 silica gel and underwent a solid phase extraction procedure consisting of five steps of increasing MeOH:H_2O content (0%, 25%, 50%, 75%, 100%, and an isopropanol wash). The 75% MeOH fraction (62 mg) was subjected to reversed-phase HPLC on a Phenomenex column (Luna C18; 150x4.6 mm, 5 µ) using a flow rate of 1.0 mL/min and a concentration gradient of 50%-100% (MeCN:H_2O) over 20 min and then holding at 100% MeCN for an additional 10 min. This afforded known callyspongynic acid (**3.1**, t_R = 4.5 min, 6 mg, 0.4% yield), and small quantities of decarboxycallyspongynic acid. HPLC of the 100% MeOH fraction using the same method afforded larger quantities of decarboxycallyspongynic acid (**3.2**, t_R = 23.7 min, 0.6 mg, 0.04% yield). Purity was assessed by NMR and **3.1** and **3.2** were deemed to be 92% and 94% pure respectively.

6.2.3. Extraction and Isolation of Metabolites from *Myrmekioderma*.

450 grams of an undescribed species of *Myrmekioderma* (class Demospongiae, order Axinellida, family Heteroxyiidae) was collected 40-60 ft. deep off the southern shore of Lana'i at second cathedral (roughly 20°44'05.0"N, 156°55'25.7"W). The encrusting sponge has fingery projections and a smooth surface, produces clear mucus, cream colored in life and in spirit, and the interior has a pulpy consistency. The ectosomal skeleton is parchment-like and readily detachable, it consists of a tangential layer of a smaller category of strongyles (~265 x 9.8 µm). The choanosomal skeleton is largely confused with ascending tracts of larger strongyles (~555 x 9.5µm) among disorganized spicules including fine oxea/strongyles (~325 x 2.5µm) and

abundant rhaphides in 2 sizes of trichodragmata (~52.5 and 80µm). All megascleres are smooth, centrally curved or occasionally flexuous.

100 g of lyophilized sponge was extracted with 1:1 MeOH:CH_2Cl_2 three times overnight to yield 5.77 g of crude extract. The combined extract was then subjected to a modified Kupchan partitioning using only MeOH, Hex, and CH_2Cl_2. The CH_2Cl_2 partition (177.5 mg) was dry loaded on C8 silica gel and was subjected to a solid phase extraction procedure consisting of five steps of increasing MeOH:H_2O content (0%, 25%, 50%, 75%, 100%, and an isopropanol wash). Both the 50% MeOH and the 75% MeOH fractions contained our compounds of interest. The 50% was subjected to reversed phase HPLC on a Phenomenex column (Luna C18; 250x10 mm, 5 µ) using a flow rate of 2.8 mL/min and a concentration gradient of 40%-80% (ACN:H_2O) over 20 min. This afforded pure compounds **4.1** (t_R = 15.8 min, 0.6 mg, 0.01% yield) and **4.2** (t_R = 16.1 min, 1 mg, 0.02% yield), and mixtures **4.3** (t_R = 8 min, 2.3 mg, 0.04% yield) and **4.4** (t_R = 9 min, 2.2 mg, 0.04% yield). Purity was assessed by NMR and determined to be 95%, 88%, 85% and 77% for **4.1**, **4.2**, **4.3**, and **4.4**, respectively.

6.2.4. Extraction and Isolation of Metabolites from an Unidentified Hawaiian Sponge

The white, cobweb-like sponge was collected at Kewalo pipe, Oahu (21°17'25.6"N 157°51'47.3"W) at a depth of 15 ft. 60 g of lyopholized sponge was extracted with 1:1 MeOH:DCM three times overnight to yield 5.98 g of crude extract. The combined extract was then subjected to a solid phase extraction over 180 g of C8 silica gel with the eluents 25% MeOH:H_2O, MeCN, 100% MeOH, and CH_2Cl_2. The MeCN fraction, 876 mg, was subjected to reversed phase, flash column chromatography with a gradient of 50% MeOH:H2O to 100% MeOH to yield 4 fractions (pink, orange, green, and purple). The second (orange) fraction was

subjected to preparative HPLC of on a Phenomenex column (Gemini C18; 250x21.2 mm, 5 µ) with a gradient of 80%-100% (ACN:H_2O) over 20 min at flow rate of 10 mL/min. This afforded a mixture of **5.1** and **5.2** (t_R = 14.0 min), **5.3** (t_R = 19.5 min), and impure **5.4** (t_R = 23.7 min). **5.1** and **5.2** were further separated on a Sepulco column (Pentaflourophenyl; 250x4.6 mm, 5 µ) using a flow rate of 1.0 mL/min and a concentration gradient of 70%-75% (MeOH:H_2O) over 20 min and injecting 50 µg. The pink fraction was subjected to reversed phase HPLC on a Phenomenex column (Luna C18; 250x10 mm, 5 µ) using a flow rate of 2.8 mL/min and a concentration gradient of 30%-100% (ACN:H_2O) over 20 min to yield a mixture of **5.5** and **5.6** (t_R = 20.7 min). Further HPLC on a Phenomenex column (Luna Si; 150x4.6 mm, 5 µ) using a flow rate of 2.0 mL/min isocratically at 35% EtOAC:Hex to afford pure **5.5** (t_R = 6.6 min, 1 mg, 0.02% yield) and **5.6** (t_R = 4.4 min, 0.8 mg, 0.01% yield). Purity was assessed by NMR and were deemed 81%, 83%, 85%, 70% pure for known compounds **5.1**, **5.2**, **5.3** and **5.4**, respectively. Compounds **5.5** and **5.6** were both determined to be 95% pure by NMR.

6.3. Assay Protocols

6.3.1. BACE1 Assays

The HitHunter BACE1 EFC chemiluminescence assay was purchased from DiscoveRx and was run in house. The proteolytic cleavage of amyloid precursor protein was assayed as described by Naqvi[115]. Test compounds were solubilized in DMSO at the desired concentration and incubated in triplicate with the enzyme for 16 h in 96-well plates. A DMSO control (1.5 μL) and an inhibitor standard were also tested in triplicate. The chemiluminescence signal was read using a Fluostar Optima spectrophotometer. Data were analyzed using GraphPad Prism. BACE1

activity was calculated as a percent of the positive control using a nonlinear regression analysis function that corresponded to a best one-fit model.

The BACE1 Affinity assay was run in house. 50 µL of a 0.1 µg/µL BACE1 enzyme solution in a buffer consisting of 80% 10mm NH_4HCO_3 and 20% LC-MS grade MeOH was incubated overnight with 10 µL of a 5 µg/µL MeOH solution of extract and 10 µL of a 0.005 µg/µL MeOH solution of BACE1 inhibitor IV (Calbiochem). Bio-Gel P-6 Gel (150mg) was placed in a plastic Bio-Spin column and was equilibrated with 1:4 MeOH:buffer solution. Enzyme-extract-inhibitor solution (20 µL) was added to the column and centrifuged for 1 min at 4°C and 1000 rcf. The solution in the receiving vessel was transferred to the insert in the LC-MS vial and LC-ESI-TOFMS was performed separating over a Luna C18 150 x 4.6 mm column with particle size 3 microns. A positive control of just the extract, a negative control of the extract spun down on the SEC only, and the experiment of the above described process was run for every sample.

6.3.2. Cytotoxicity Assays

Human renal cell adenocarcinoma (768-0), prostate carcinoma (DU-145), mammary gland adenocarcinoma (MDA-MB-231) and lung carcinoma (A549) cell lines were maintained in RPME 1640 Medium (Gibco, REF: 11875-093) supplemented with 10% premium fetal bovine serum (Atlanta biological, Cat. No.: S11150) and 100 U/mL penicillin and 100 µg/mL streptomycin (Gibco, REF: 15140-122). The day before treatment, cancer cells were seeded with 4,000 cells per well into a 96-well tissue culture plate. Twenty hours post seeding, the serial diluted compounds were added to the cells for the cytotoxicity assay, and co-incubated at 37 ^oC with 5% CO_2 for 72 h. Then the medium with compounds were replaced with 1 × dye binding solution prepared according to the manufacturer's instruction (CyQuant NF Cell Proliferation Assay Kit [C35006, Invitrogen]) and incubated at 37 ^oC with 5% CO_2 for 60 minutes. After that,

cell viability data were collected with a PerkinElmer Multimode Plate Reader according to the manufacturer's instruction. IC_{50} curves were generated using GraphPad Prism 5.

Human panc-1 cell lines were maintained in DMEM media supplemented with 10% premium fetal bovine serum and 50 U/mL penicillin and 50 µg/mL streptomycin. The day before treatment, cancer cells were seeded with 5,000 cells per well into a 96-well tissue culture plate. Twenty-four hours post seeding, the serial diluted compounds were added to the cells making total volume of the cell mixture to 200 uL for the cytotoxicity assay, and incubated at 37 ^{o}C with 5% CO_2 for 72 h. Then 40 uL MTS dye (CellTiter aqueous One Solution Cell Proliferation Assay) was added to each well and incubated at 37 ^{o}C with 5% CO_2 for 90 minutes. After that, cell viability data were collected with a Modulus Microplate Reader. IC_{50} curves were generated using GraphPad Prism 5.

6.3.3. ER-alpha Assay

Assay was conducted through ThermoFischer Scientific's SelectScreen™ biochemical nuclear receptor profiling service employing the LanthaScreen™ TR-FRET Coregulator assay and using 17-β-estradiol as the stimulant.

6.4. Physical Data

Ulapualide A (**2.1**): $[\alpha]^{22}_{D}$ -39, *c* 0.20, MeOH; all other spectroscopy data was found to be identical to literature values.[38] Notebook SP-I-89

Ulapualide B (**2.2**): spectroscopy data was found to be identical to literature values.[38] Notebook SP-I-89

Ulapualide C (**2.3**): white amorphous powder; $[\alpha]^{22}_{D}$ -17 (*c* 0.32, MeOH); UV (MeOH) λ_{max} (log ε) 249 (4.5), 237 (4.6), 202 (4.5); IR ν_{max} 3600-3200 (br), 3162, 2964, 2934, 1720, 1691, 1655, 1597, 1458, 1241, 1086, 916 cm^{-1}. Tables 2.1 and 2.2 for NMR data; HRESI-TOFMS *m/z* 883.4700 $[M+H]^+$ (calcd for $C_{46}H_{67}N_4O_{13}$, 883.4705). Notebook SP-I-89

Ulapualide D (**2.4**): white amorphous powder; $[\alpha]^{22}_{D}$ -10 (*c* 0.08, MeOH); UV (MeOH) λ_{max} (log ε) 249 (4), 213 (5), 202 (5); Tables 2.1 and 2.2 for NMR data; HRESI-TOFMS *m/z* 883.4662 $[M+H]^+$ (calcd for $C_{46}H_{67}N_4O_{13}$, 883.4705). Notebook SP-I-89

Ulapualide E (**2.5**): white amorphous powder; $[\alpha]^{22}_{D}$ -23 (*c* 0.10, MeOH); UV (MeOH) λ_{max} (log ε) 249 (4), 213 (5), 202 (5); Tables 2.1 and 2.2 for NMR data; HRESI-TOFMS *m/z* 985.4976 $[M+H]^+$ (calcd for $C_{50}H_{73}N_4O_{16}$, 985.5022). Notebook SP-I-89

Callyspongynic Acid (**3.1**): $[\alpha]^{22}_{D}$ -4.0, *c* 0.50, EtOH; all other spectroscopy data was found to be identical to literature values.[74] Notebook SP-II-58

Decarboxycallyspongynic acid (**3.2**): white amorphous powder; $[\alpha]^{22}_{D}$ -9.8 (*c* 0.5, EtOH); UV (MeOH) λ_{max} (log ε) 202 (4.3), 214 (4.1); IR ν_{max} (CaF_2) 3413, 3295, 2115, 1589; See Table 1 For NMR Data; HRESI-TOFMS *m/z* 427.3010 $[M+H]^+$ (calcd for $C_{31}H_{39}O$, 427.2995). Notebook SP-II-58

Myrmenaphthol A (**4.1**): yellow amorphous powder; $[\alpha]^{22}_{D}$ -79 (*c* 0.2, MeOH); UV (MeOH) λ_{max} (log ε) 362 (3.8), 240 (4.1), 203 (4.2) nm; IR (CaF_2) ν_{max} 3396, 1667, 1597, 1218 cm^{-1}; See Table 4.1 for NMR data; HRESI-TOFMS *m/z* 307.1335 $[M+H]^+$ (calcd for $C_{20}H_{19}O_3$, 307.1329). Notebook SP-II-75

Cinanthrenol A (**4.2**): spectroscopy data was found to be identical to literature values.[86] Notebook SP-II-75

3,4-Dihydroxypregna-5,17-diene-10,2-carbolactone (**4.3**): spectroscopy data was found to be identical to literature values.[83] Notebook SP-II-75

3,4-dihydroxypregna-5,20-diene-10,2-carbolactone (**4.4**): spectroscopy data was found to be identical to literature values.[83] Notebook SP-II-75

Avarol **(5.1)**: spectroscopy data was found to be identical to literature values.[94] Notebook SP-II-27-31

Isoavarol (**5.2**)**:** spectroscopy data was found to be identical to literature values.[116] Notebook SP-II-27-31

Avarol monoacetate (**5.3**): all spectroscopy data was found to be identical to literature values.[117] Notebook SP-II-27-31

Avarone (**5.4**): Compound was collected as a mixture, ^{1}H NMR and HRMS data was found to be identical to literature values.[94] Notebook SP-II-27-31

3α-Hydroxyisoavarol (**5.5**): white amorphous powder; $[\alpha]^{22}_{D}$ 0.8 (*c* 0.2, $CHCl_3$); UV (MeOH) λ_{max} (log ε) 243 (3.06); See Tables 5.1 for NMR data; HRESI-TOFMS *m/z* 329.2095 $[M+H]^+$ (calcd for $C_{21}H_{29}O_3$, 329.2111). Notebook SP-II-27-31

2-Oxoavarol (**5.6**): white amorphous powder; optical rotation and UV data were not collected due to decomposition; See Table 5.2 for NMR data; HRESI-TOFMS *m/z* 327.1946 $[M+H]^+$ (calcd for $C_{21}H_{27}O_3$, 327.1955). Notebook SP-II-27-31

Table of Appendices

Appendix 1: ^{1}H NMR Spectrum of Ulapualide A (2.1) ($CDCl_3$, 500 MHz)

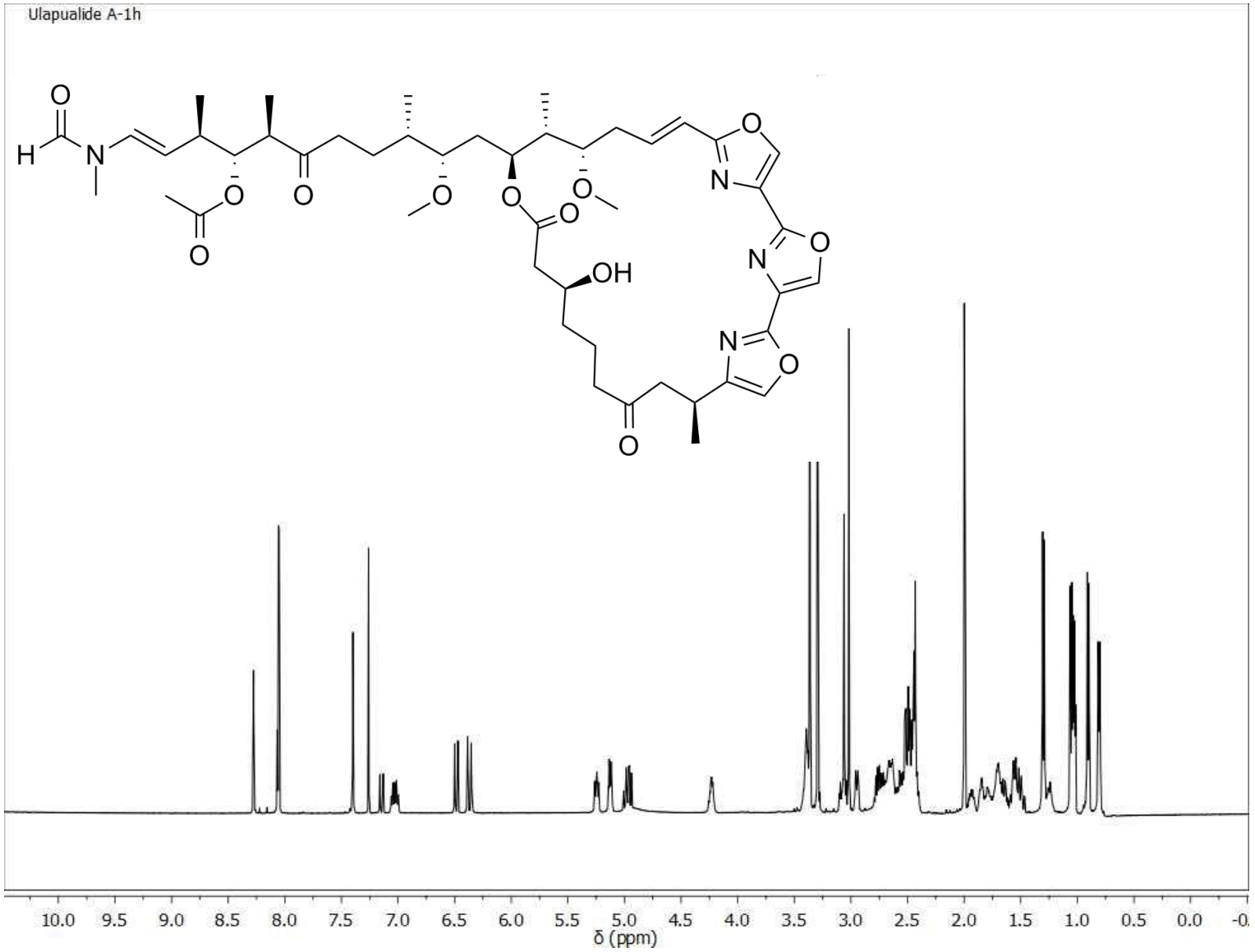

Appendix 2: ^{13}C NMR Spectrum of Ulapualide A (2.1) ($CDCl_3$, 125 MHz)

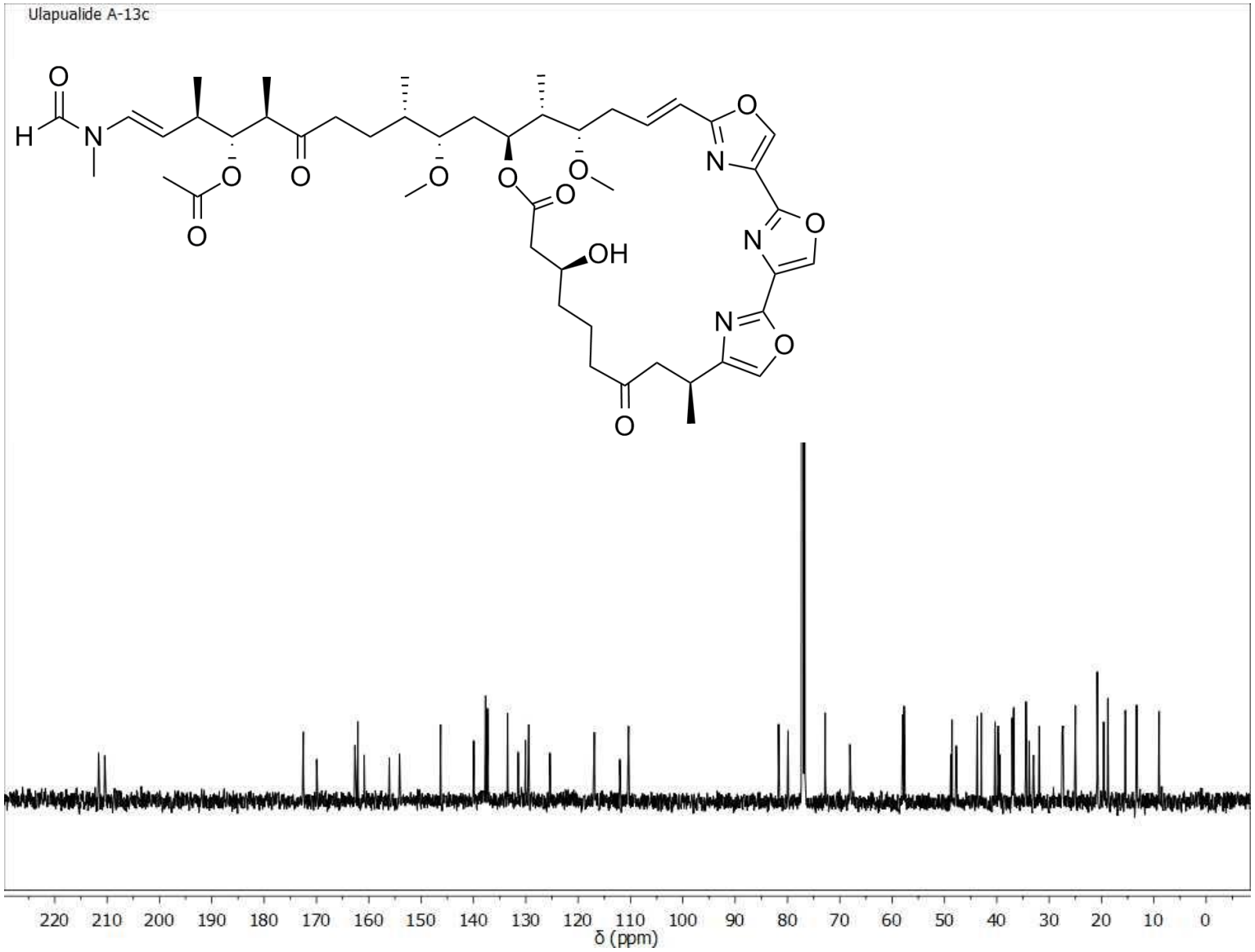

Appendix 3: ^{1}H NMR Spectrum of Ulapualide B (2.2) ($CDCl_3$, 500 MHz)

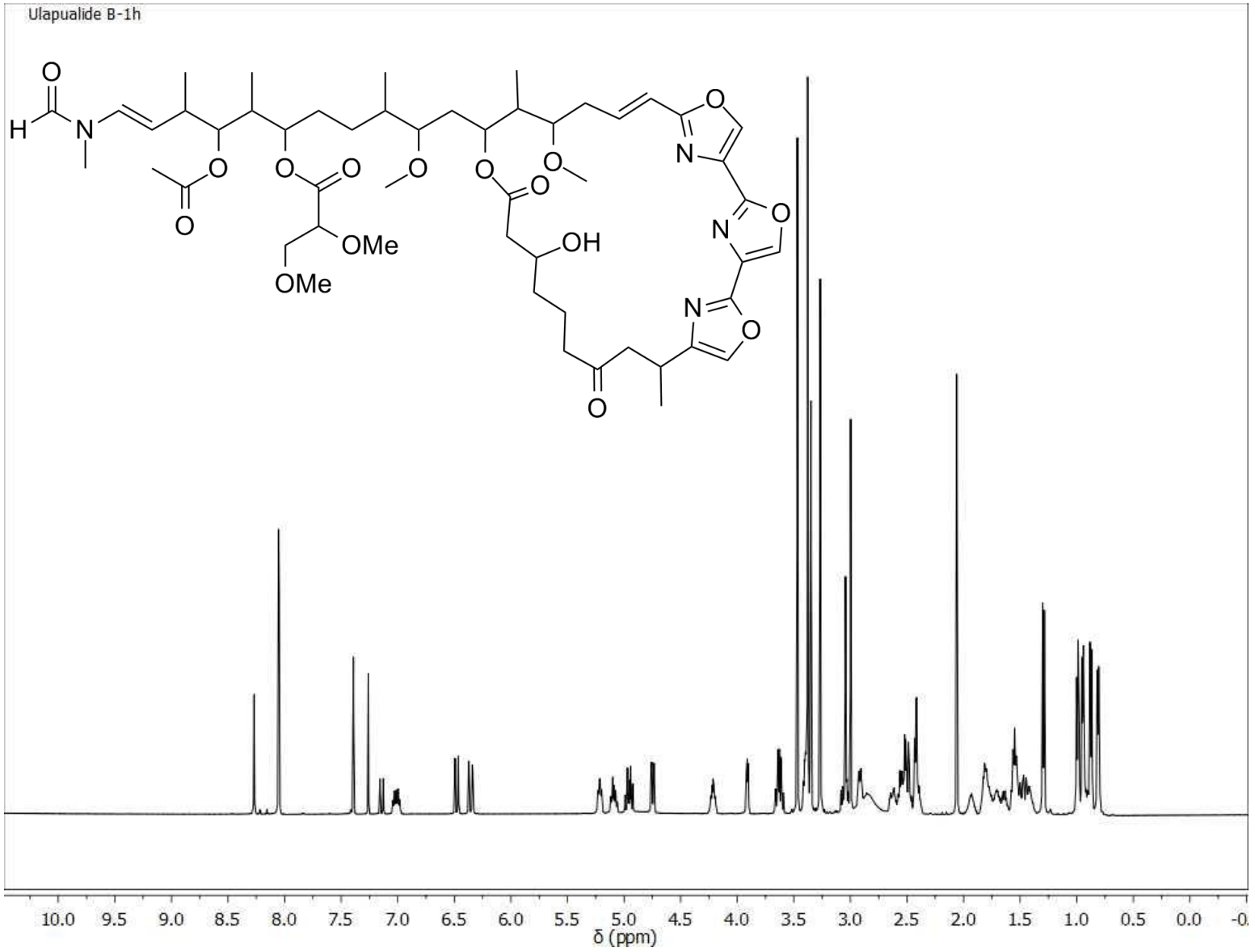

Appendix 4: ^{13}C NMR Spectrum of Ulapualide B (2.2) ($CDCl_3$, 125 MHz)

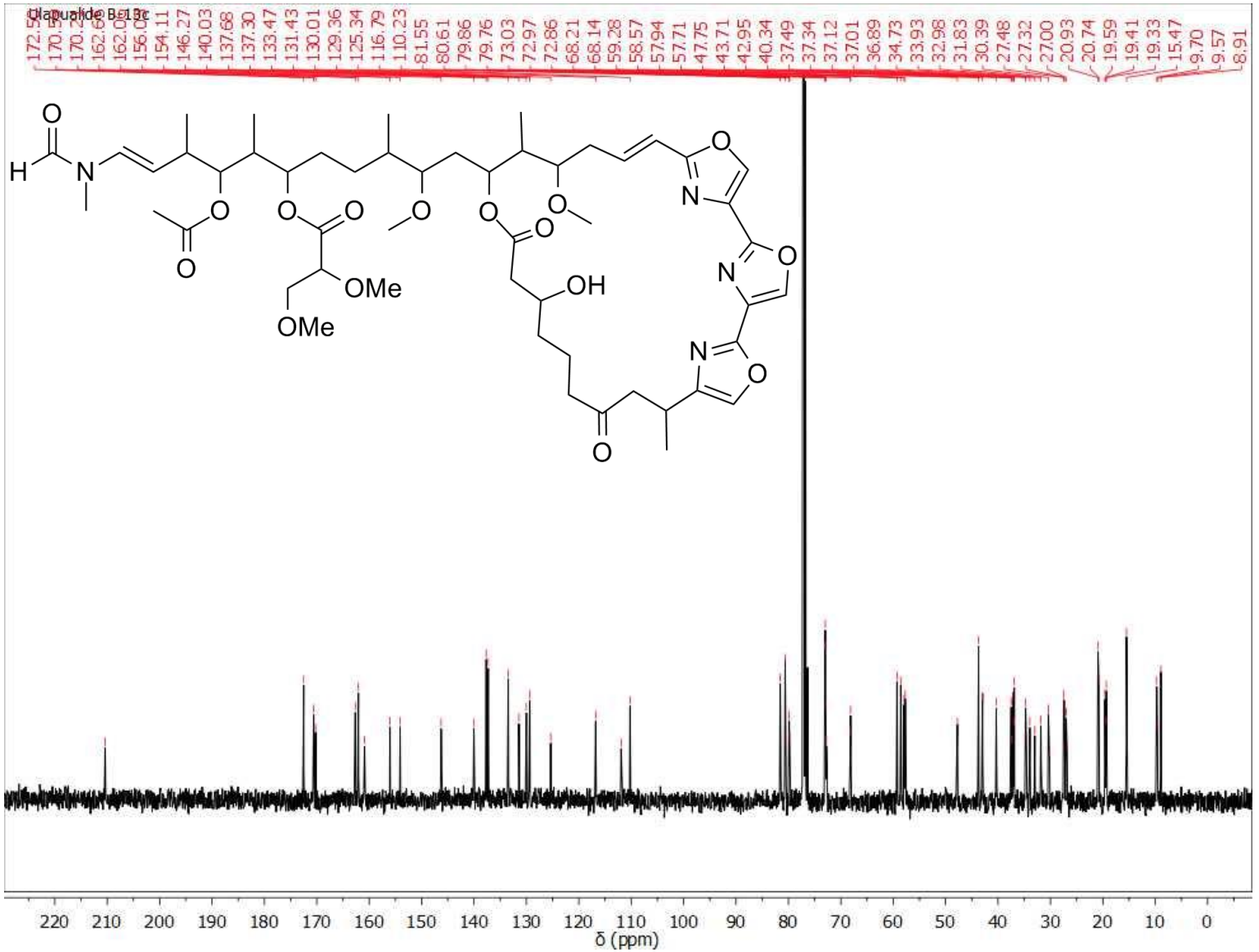

Appendix 5: ^{1}H NMR Spectrum of Ulapualide C (2.3) ($CDCl_3$, 500 MHz)

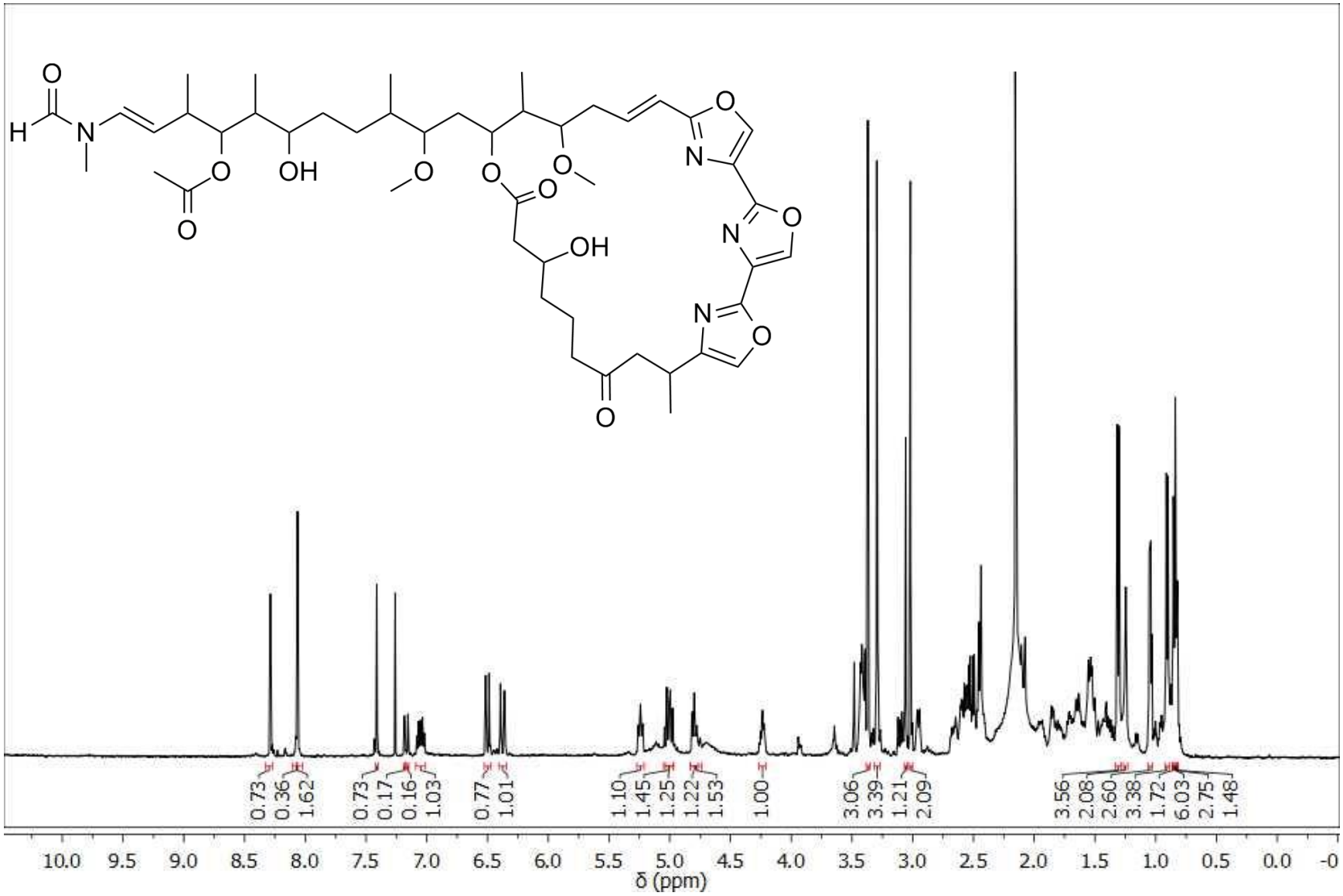

Appendix 6: ^{13}C NMR Spectrum of Ulapualide C (2.3) ($CDCl_3$, 125 MHz)

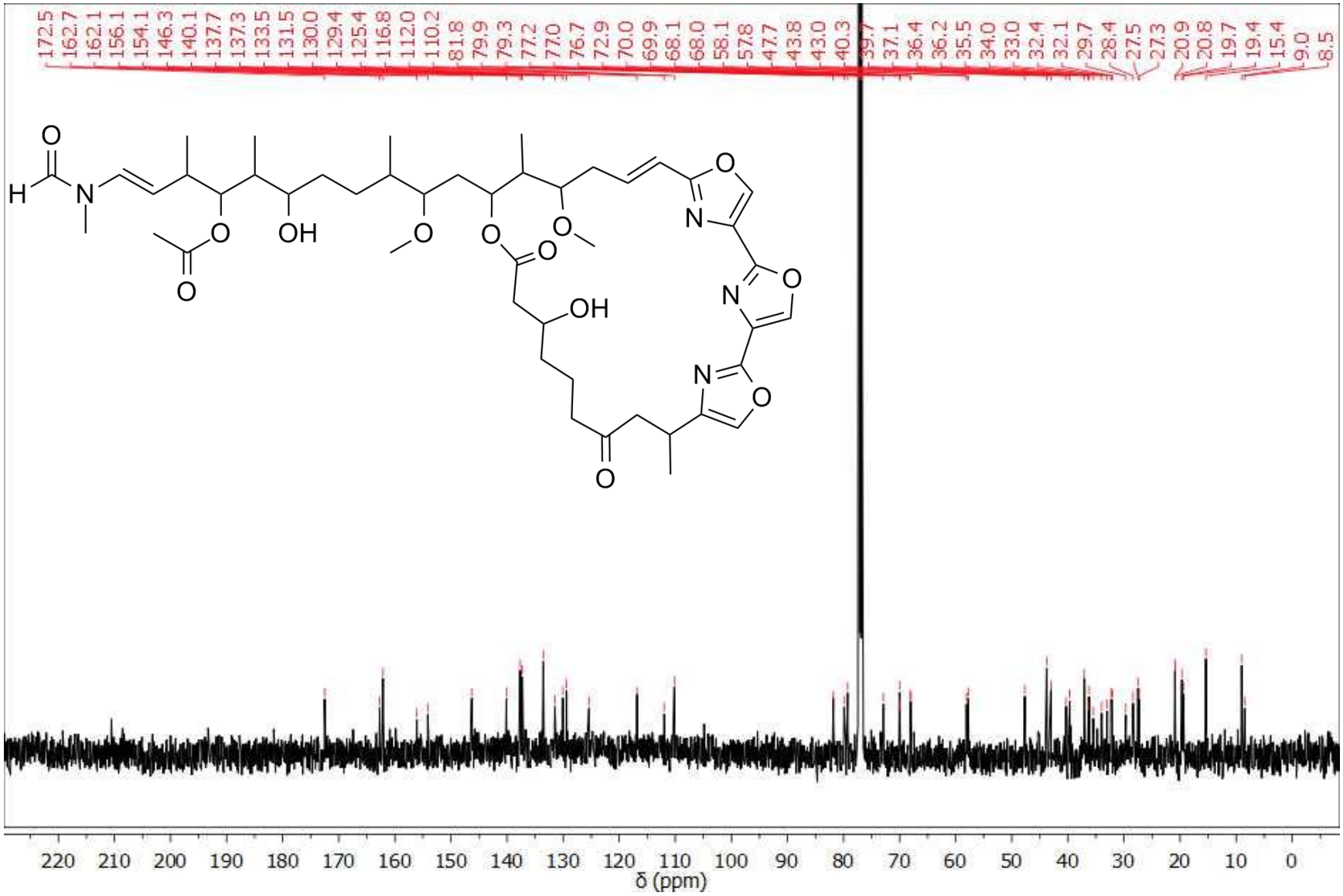

Appendix 7: gHSQC Spectrum of Ulapualide C (2.3) ($CDCl_3$, 500 MHz)

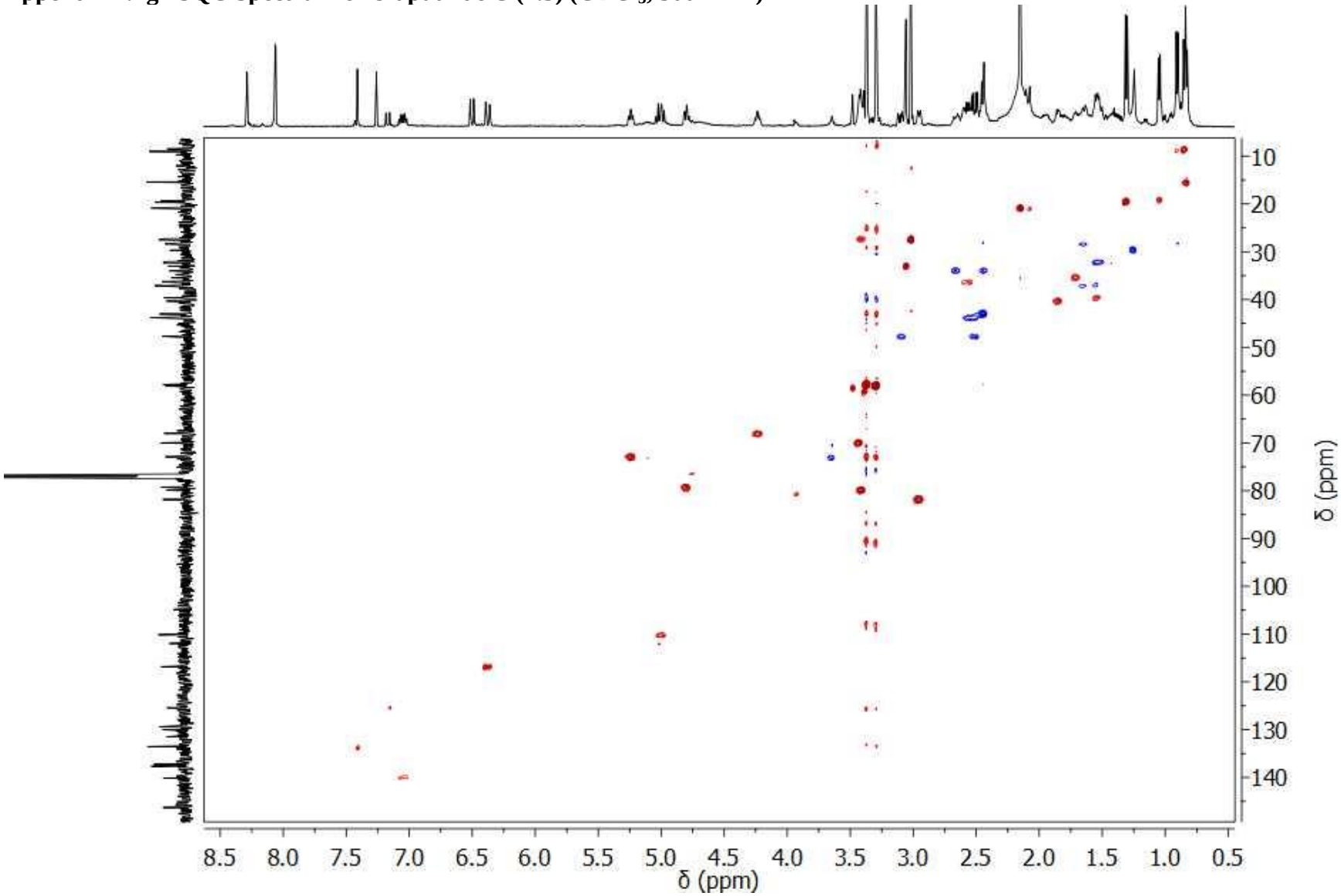

Appendix 8: gCOSY Spectrum of Ulapualide C (2.3) ($CDCl_3$, 500 MHz)

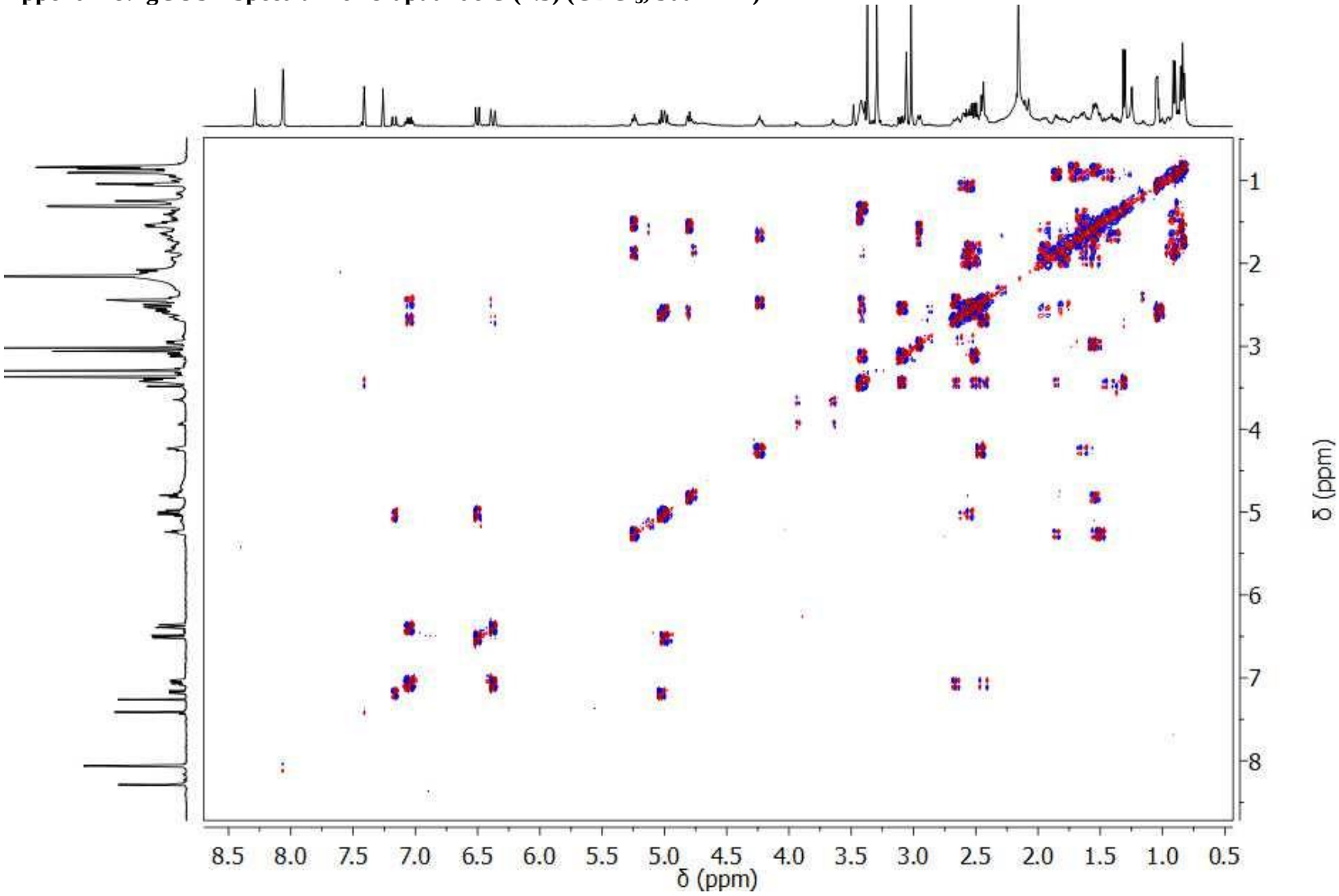

Appendix 9: gHMBC Spectrum of Ulapualide C (2.3) ($CDCl_3$, 500 MHz)

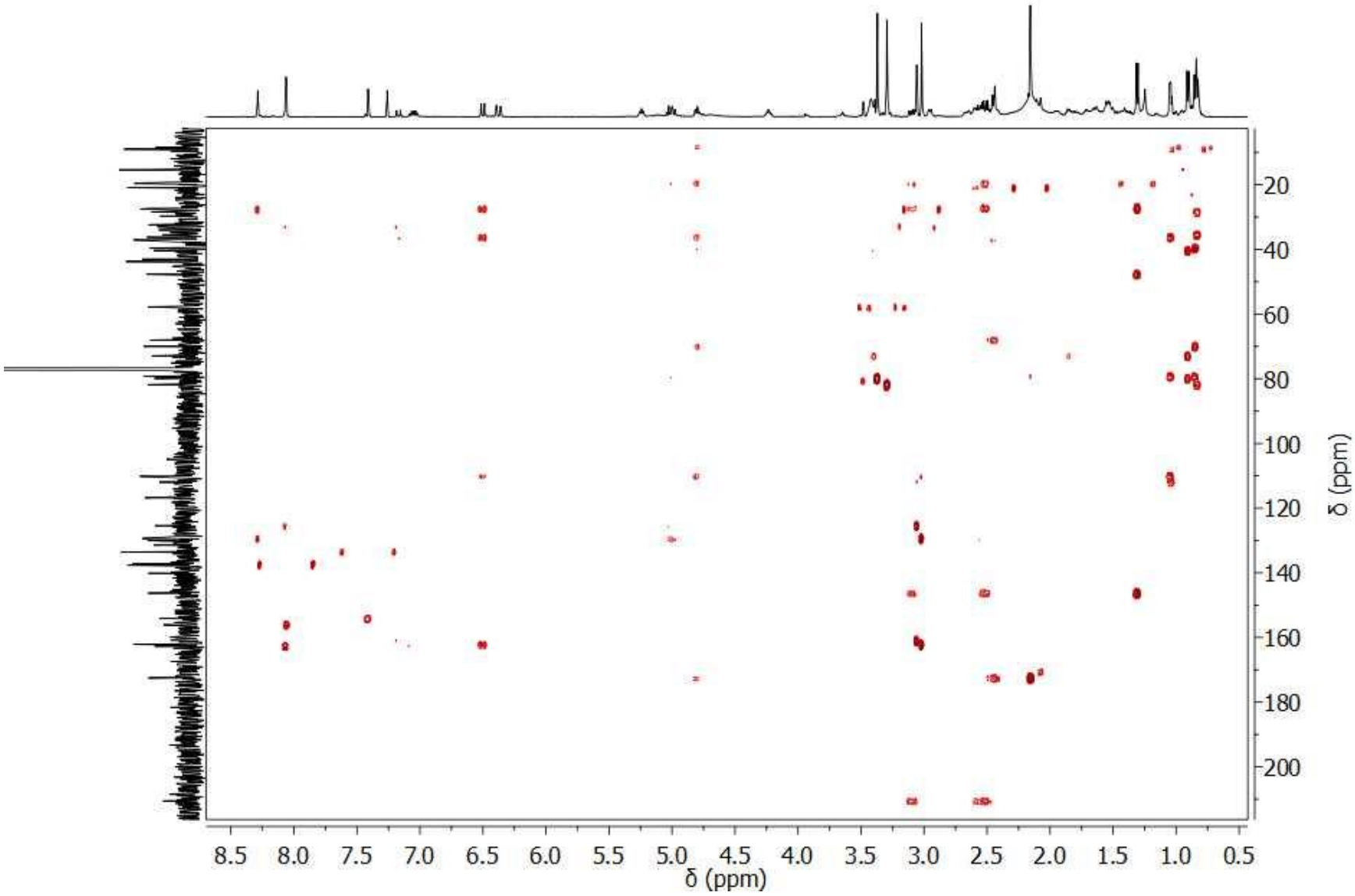

Appendix 10: ^{1}H NMR Spectrum of Ulapualide D (2.4) ($CDCl_3$, 500 MHz)

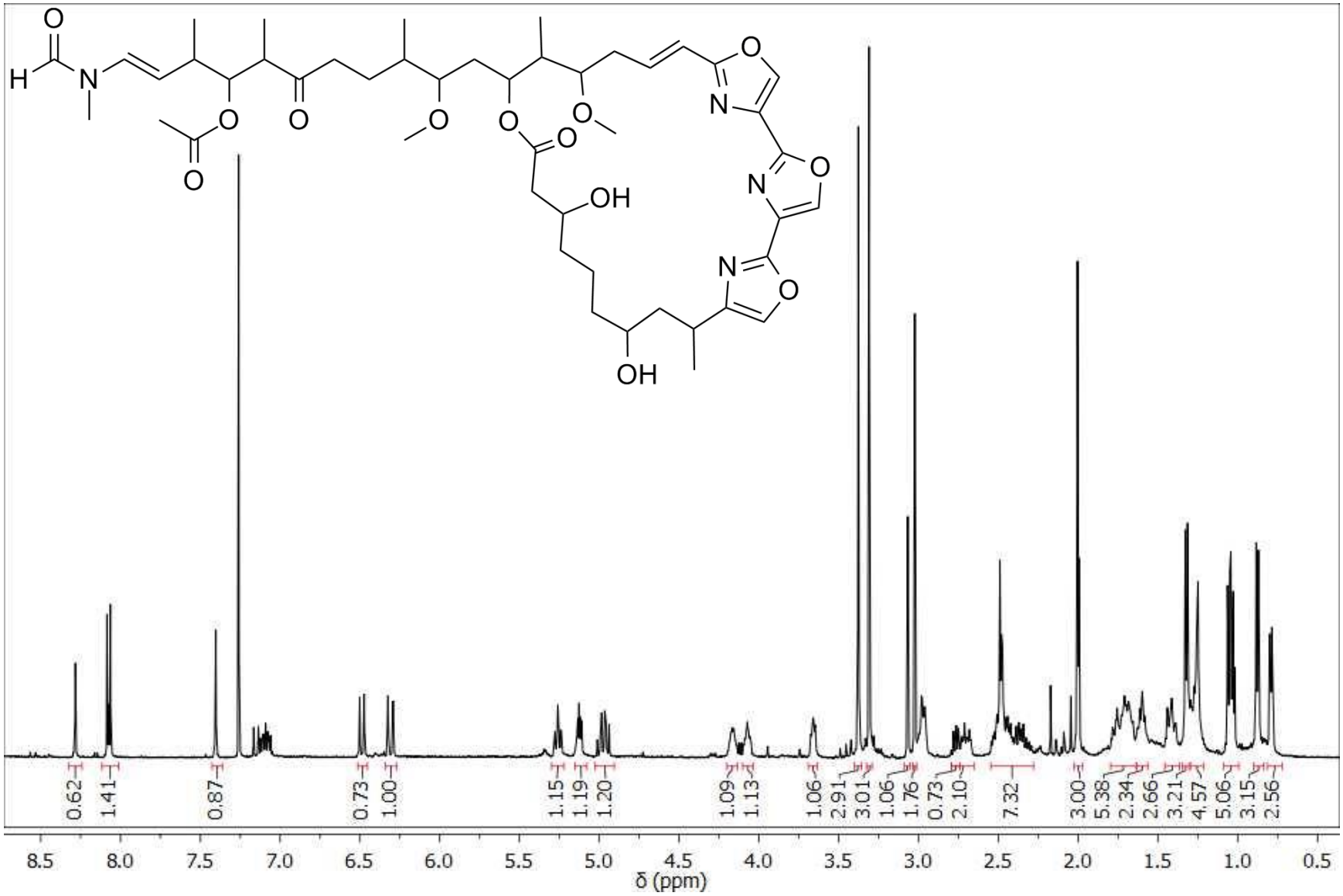

Appendix 11: ^{13}C NMR Spectrum of Ulapualide D (2.4) ($CDCl_3$, 125 MHz)

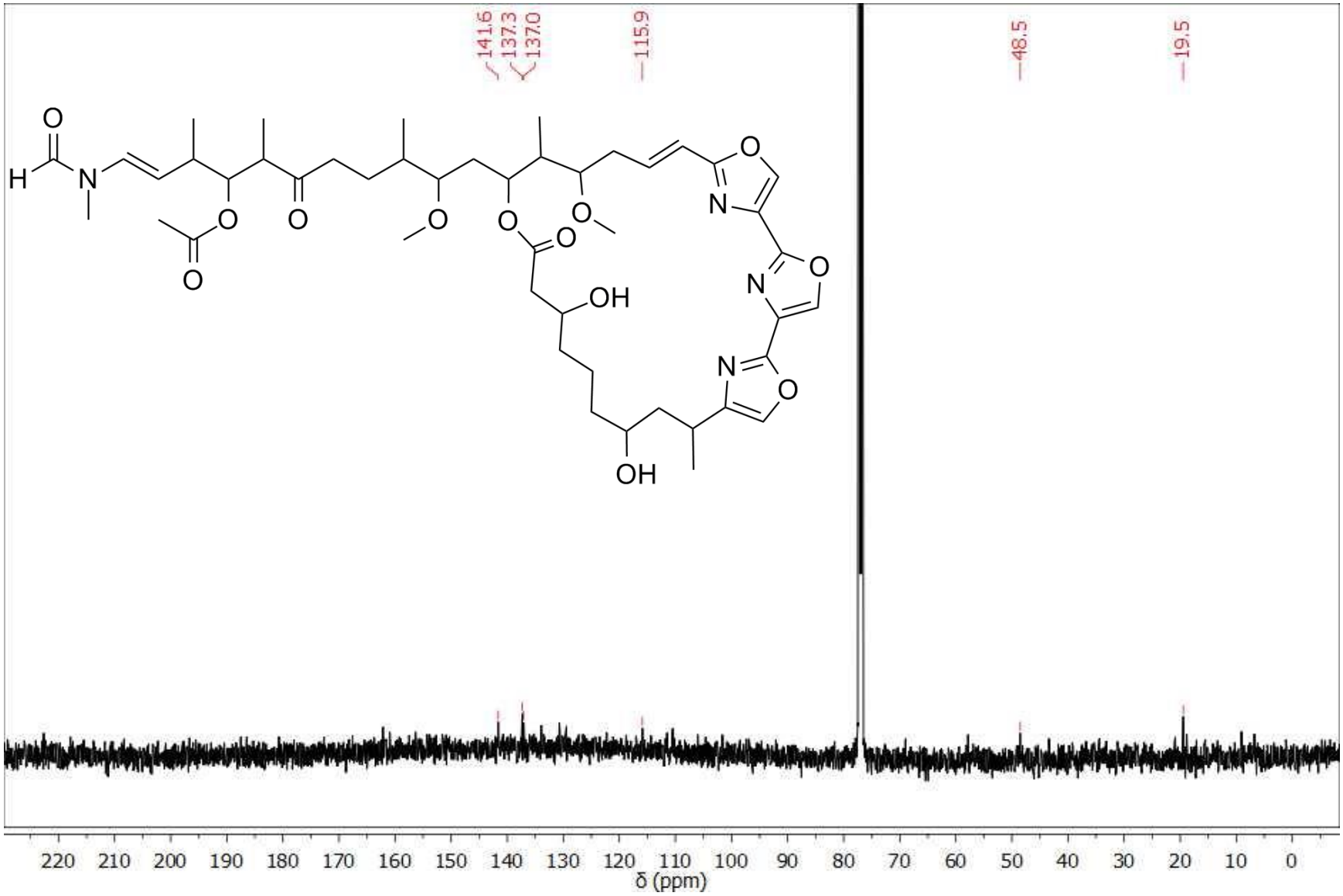

Appendix 12: gHSQC Spectrum of Ulapualide D (2.4) ($CDCl_3$, 500 MHz)

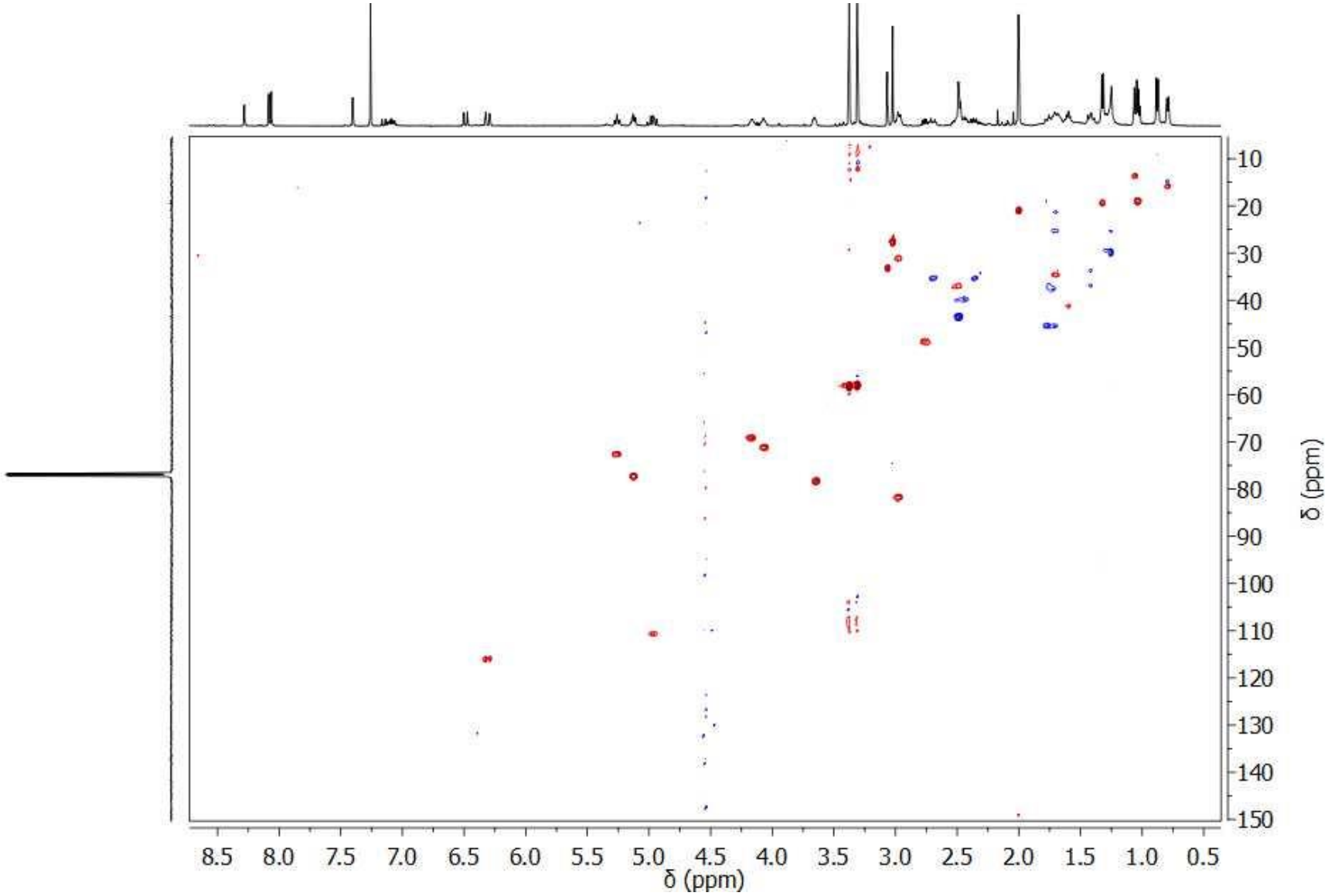

Appendix 13: gCOSY Spectrum of Ulapualide D (2.4) ($CDCl_3$, 500 MHz)

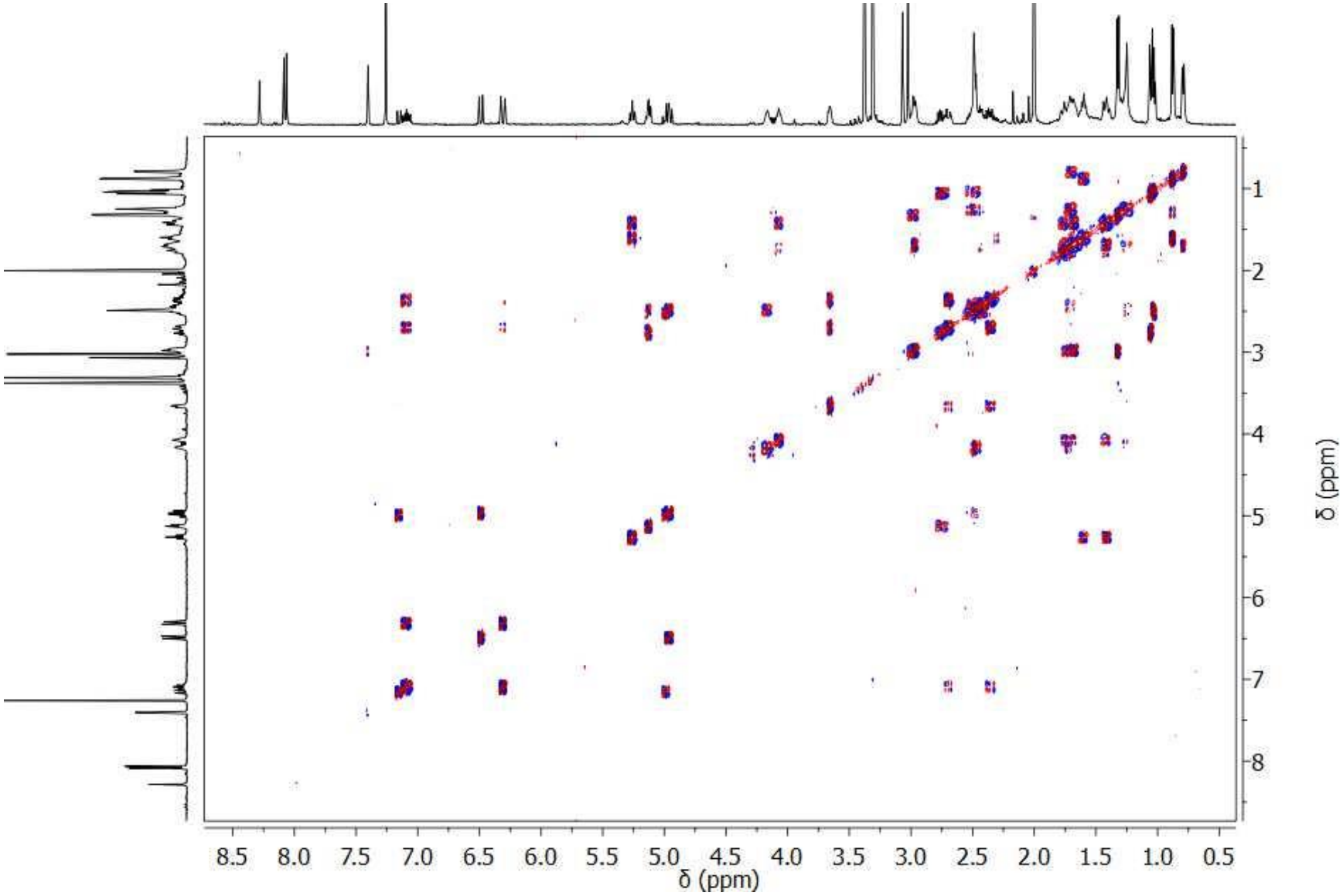

Appendix 14: HMBC Spectrum of Ulapualide D (2.4) ($CDCl_3$, 500 MHz)

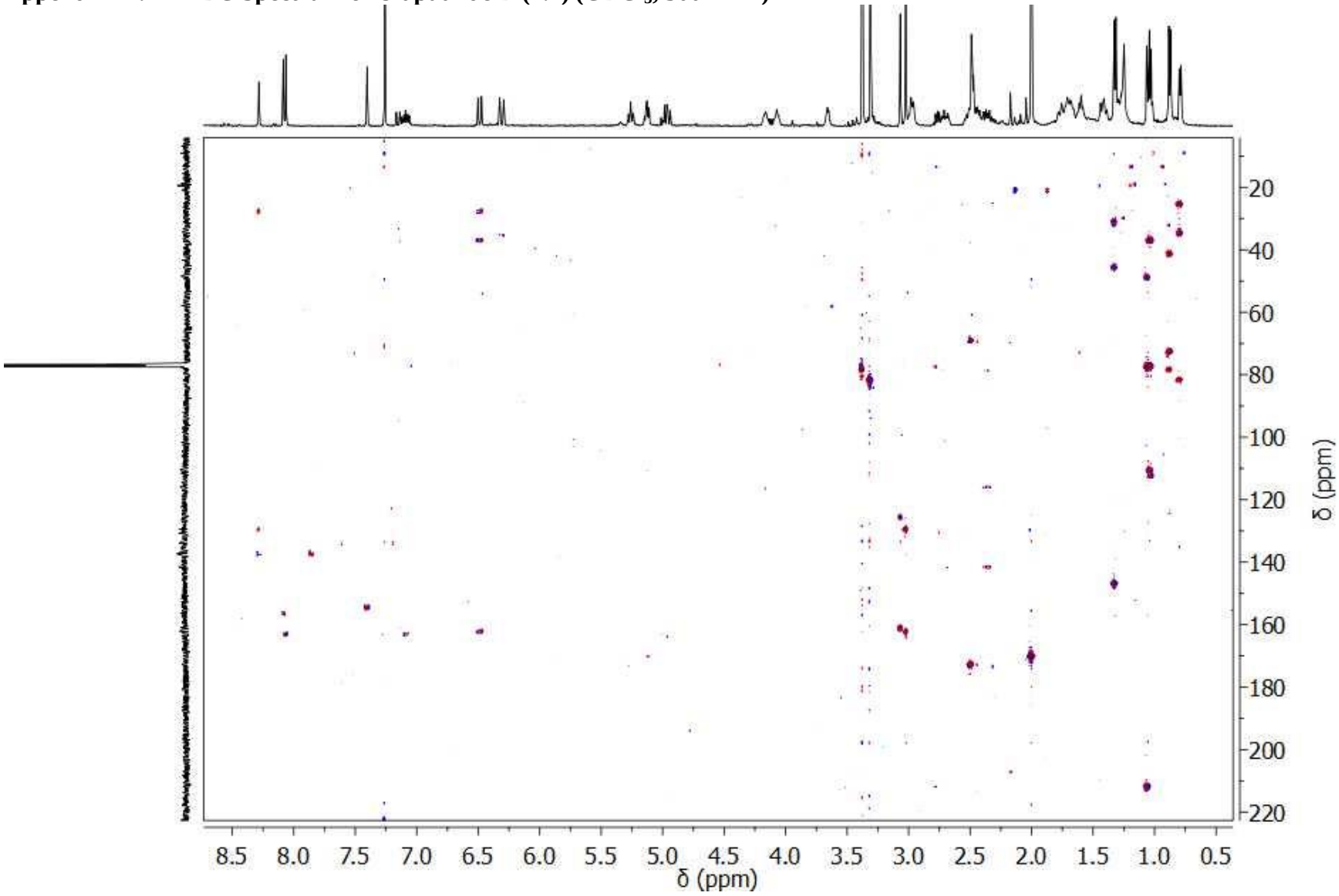

Appendix 15: ^{1}H NMR Spectrum of Ulapualide E (2.5) ($CDCl_3$, 500 MHz)

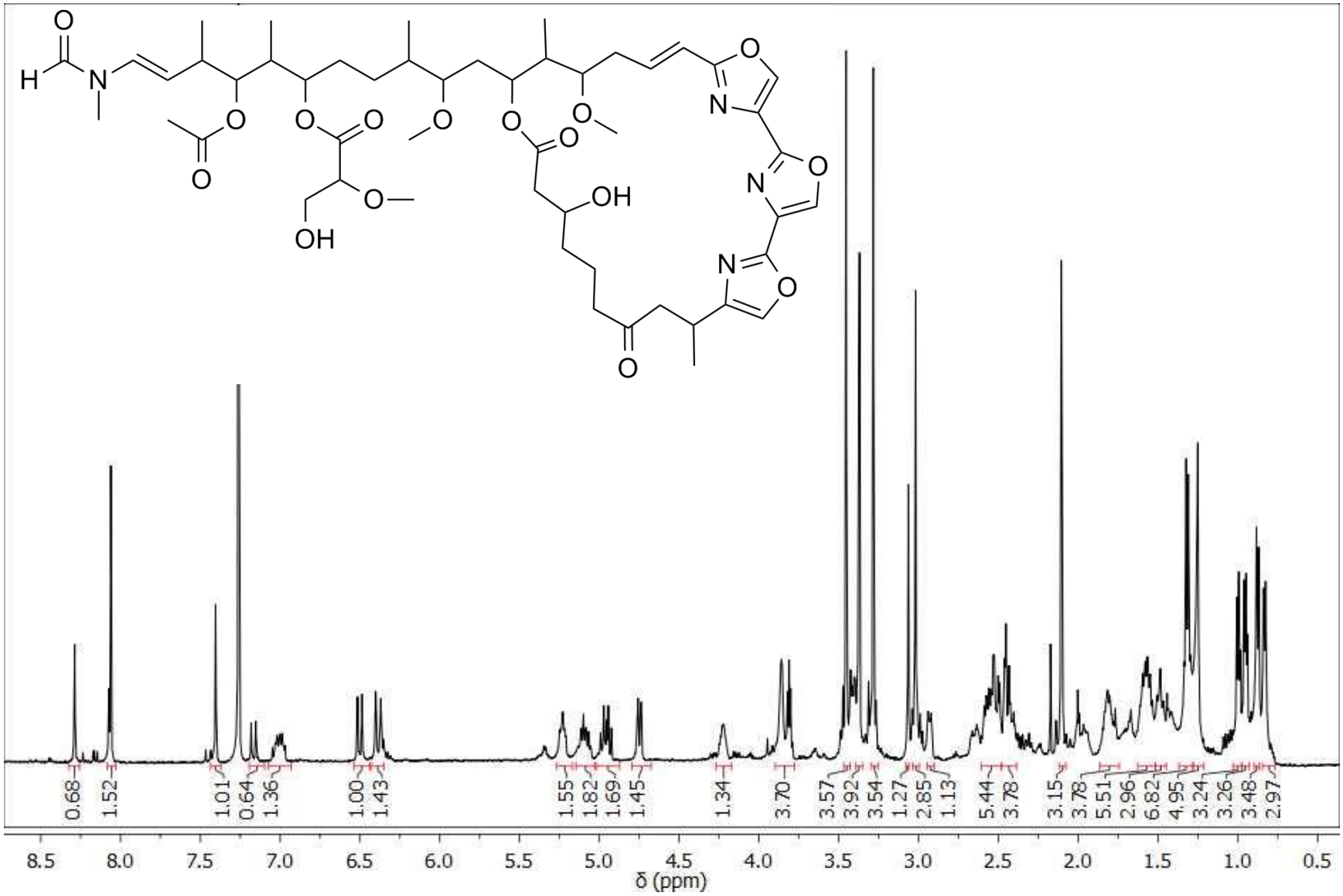

Appendix 16: ^{13}C NMR Spectrum of Ulapualide E (2.5) ($CDCl_3$, 125 MHz)

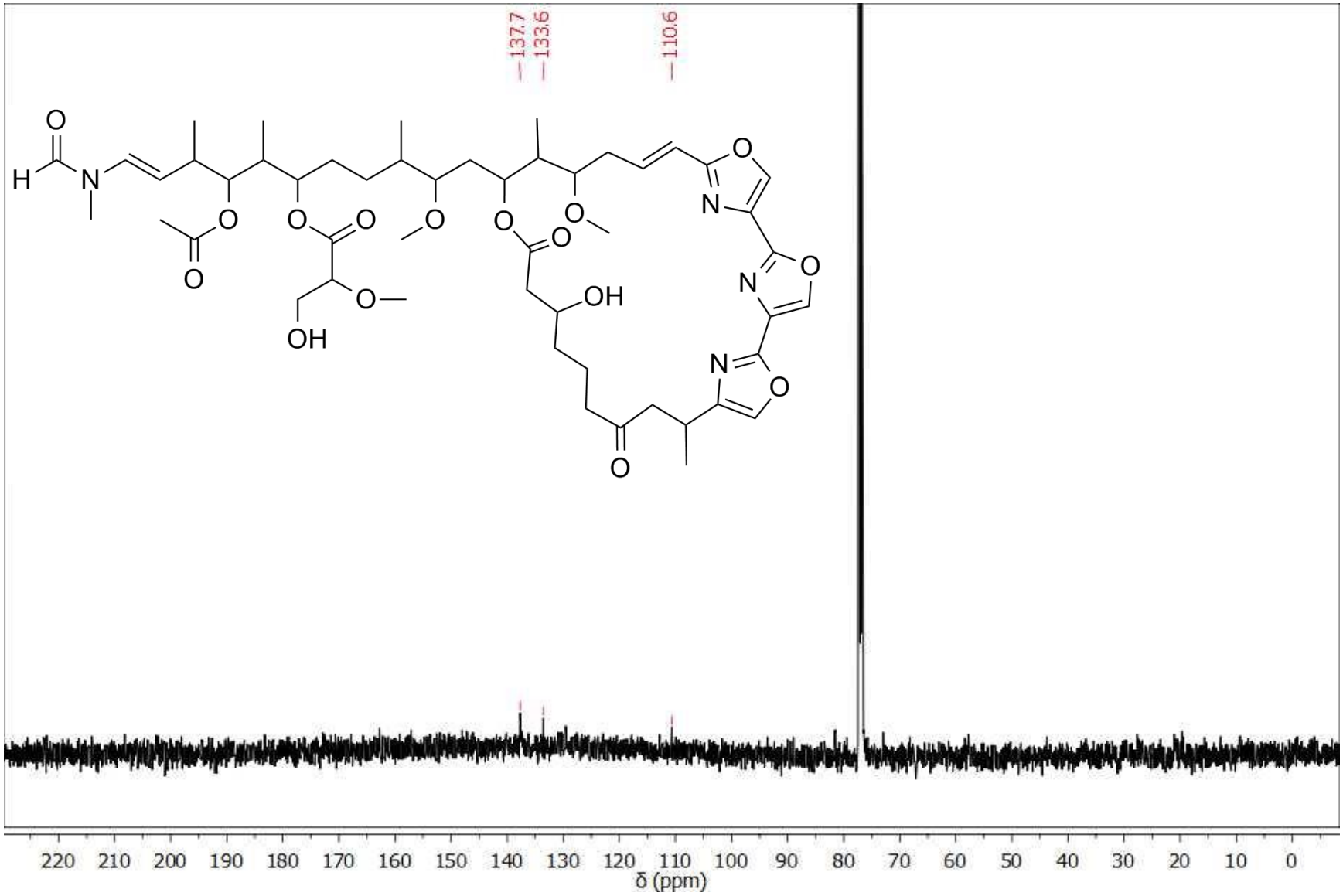

Appendix 17: gHSQC Spectrum of Ulapualide E (2.5) ($CDCl_3$, 500 MHz)

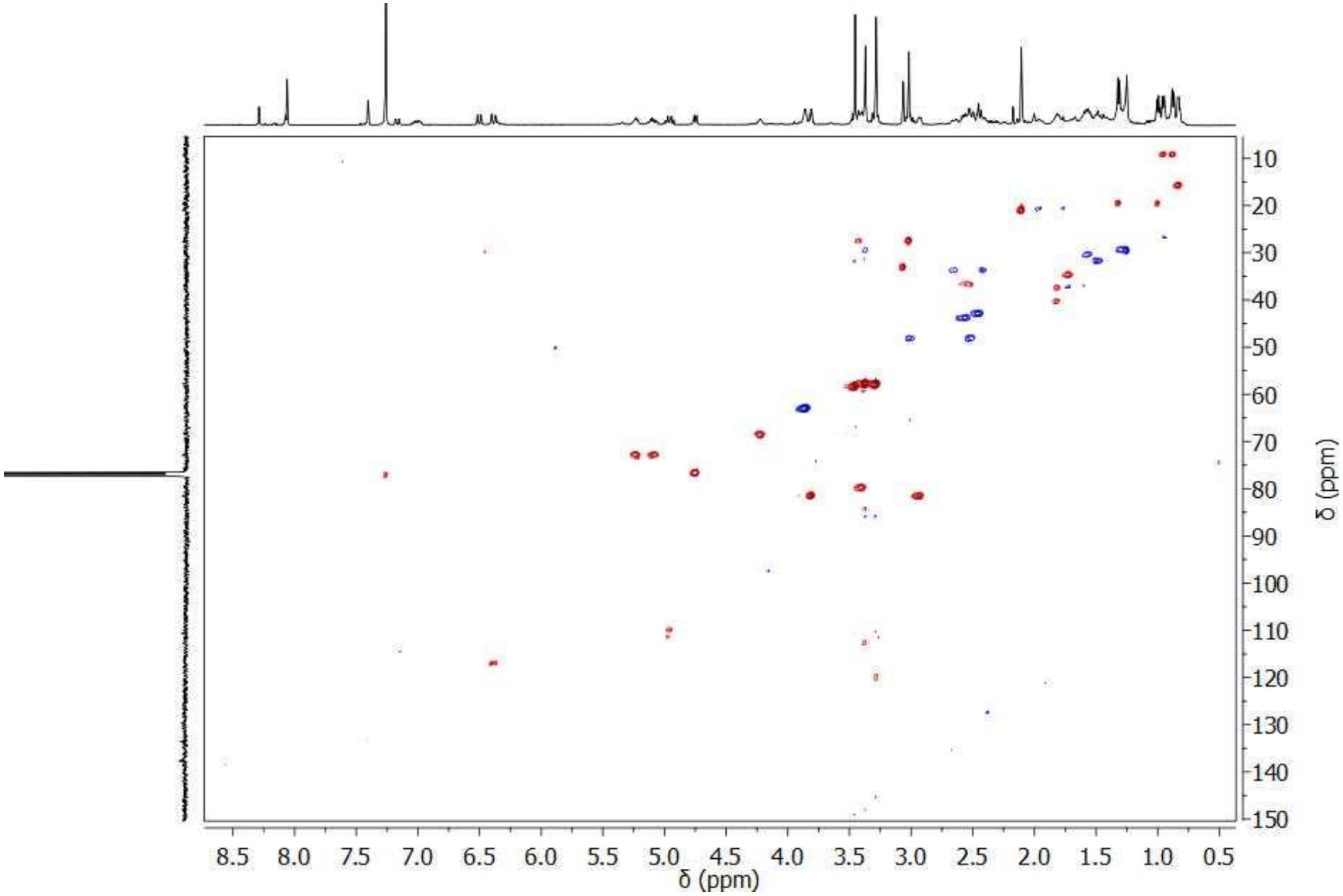

Appendix 18: gCOSY Spectrum of Ulapualide E (2.5) ($CDCl_3$, 500 MHz)

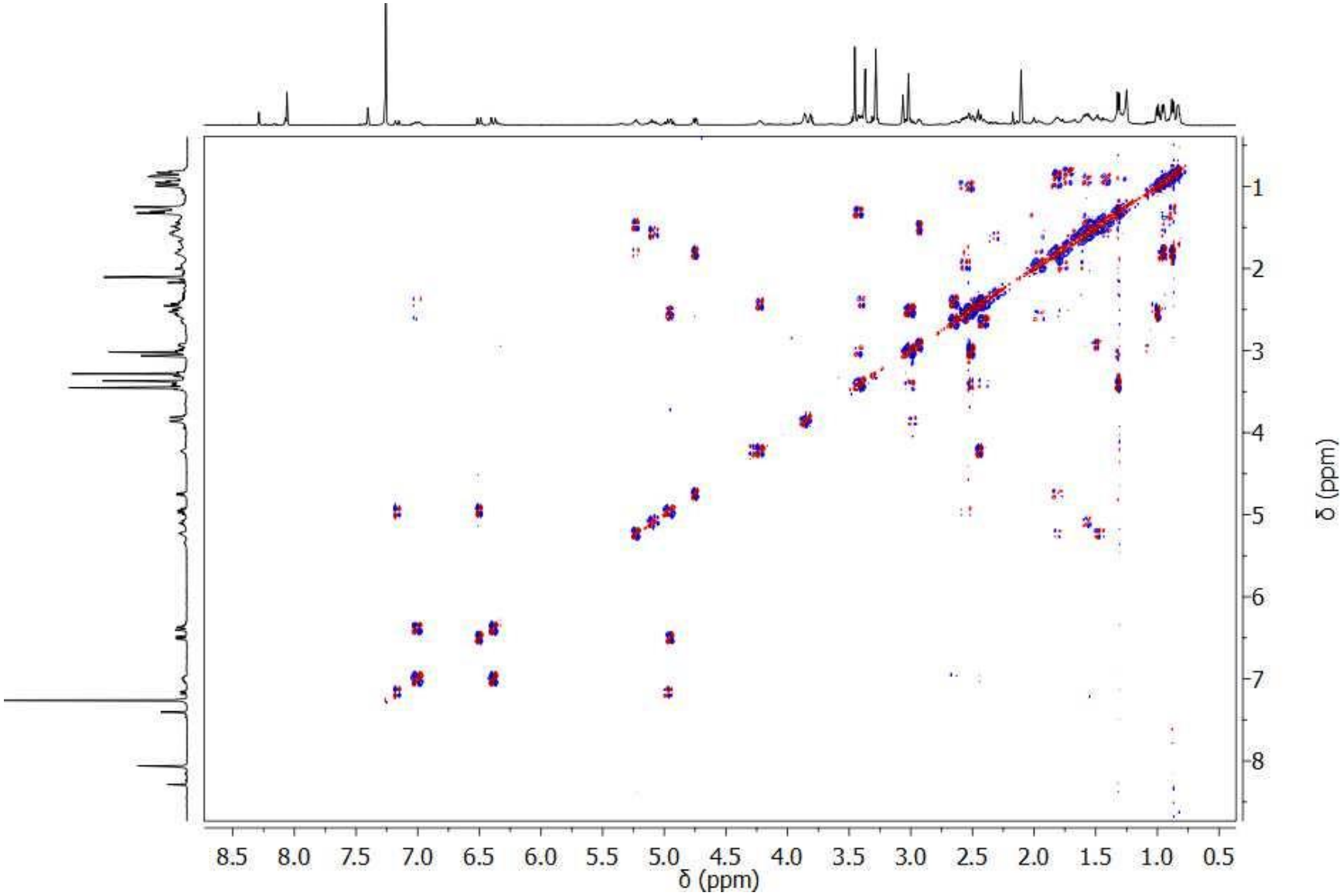

Appendix19: HMBC Spectrum of Ulapualide E (2.5) ($CDCl_3$, 500 MHz)

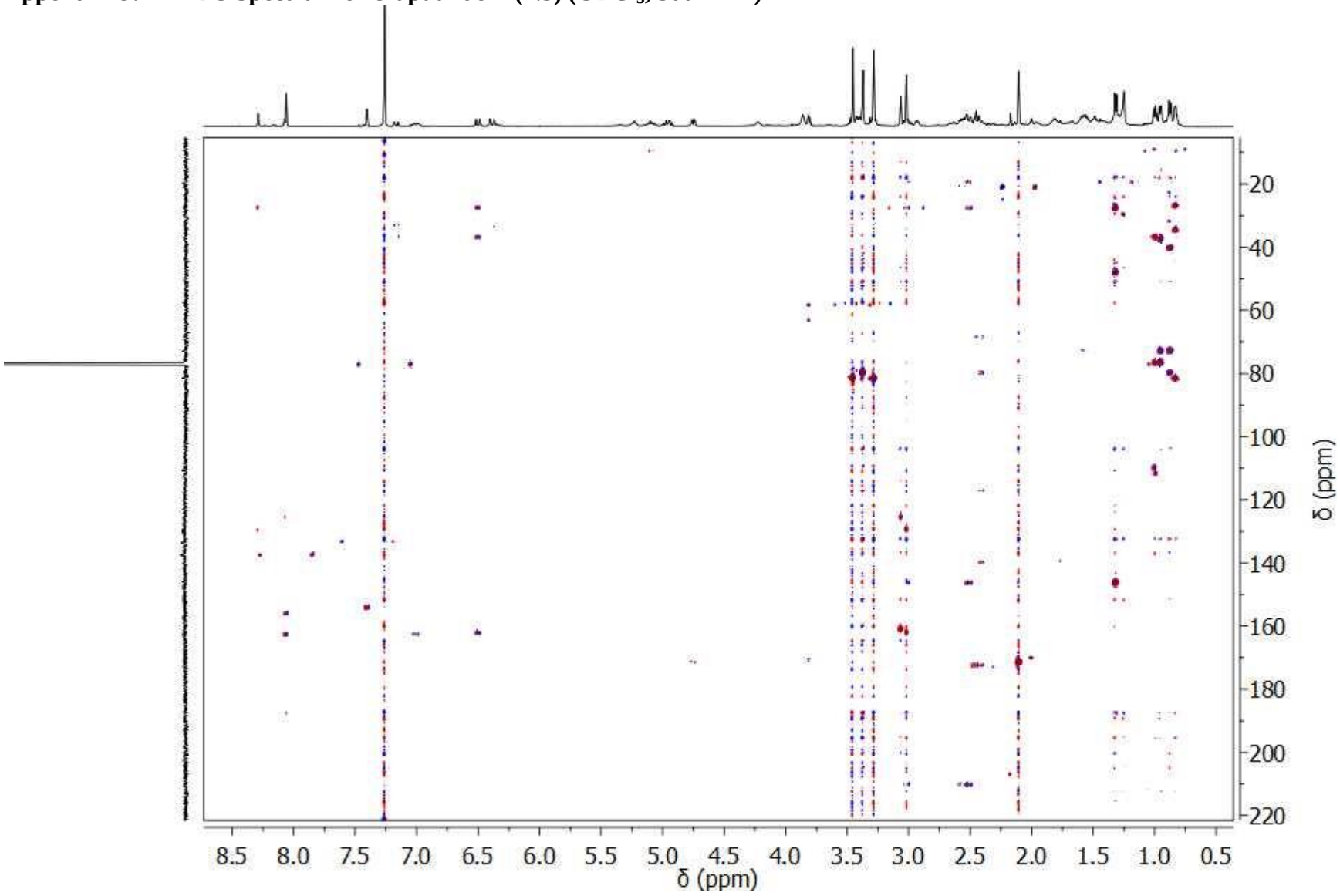

Appendix 20: IC_{50} Curves for Ulapualides A-C (2.1-2.3) Against Select Cell Lines

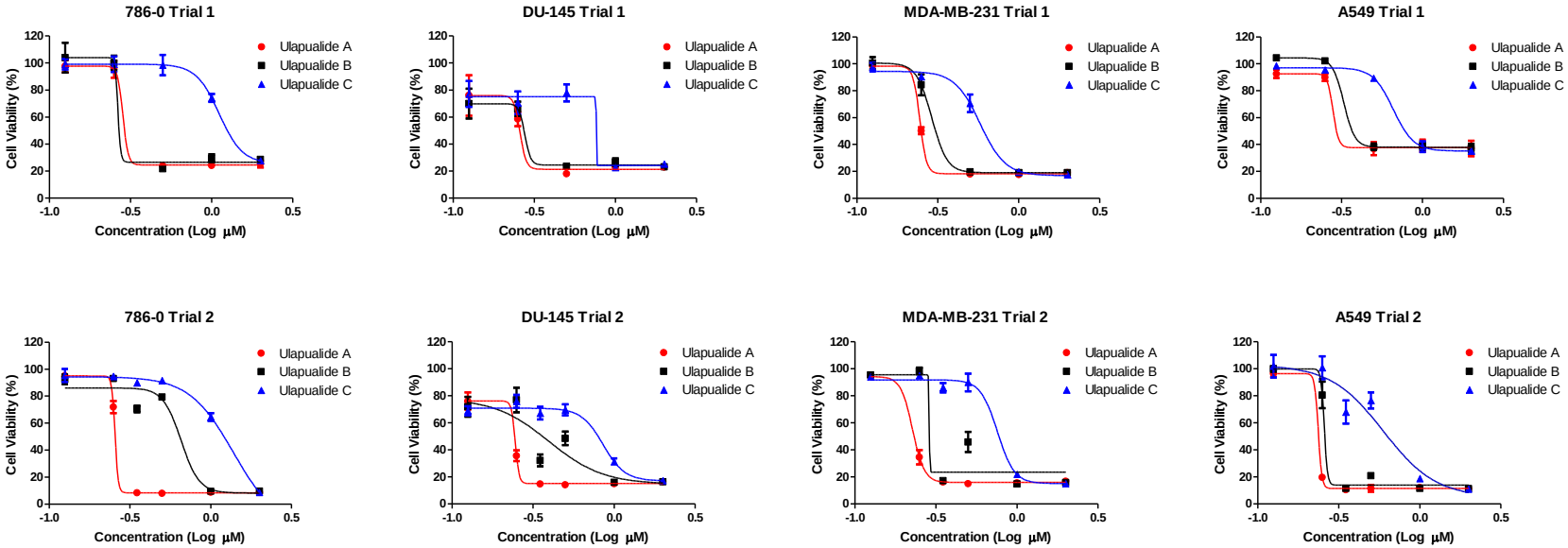

Appendix 21: Image of *Hexabranchus sanguineus* Egg Mass

Collected approximately 20 ft deep at Electric Beach, O'ahu (21°21'14.3"N 158°07'49.7"W).

Appendix 22: ^{13}C Chemical Shifts of Minor Rotamers of Ulapualides A-C (1-3) ($CDCl_3$, 125 MHz)

	1		**2**		**3**	
position	δ_C	type	δ_C	type	δ_C	type
26-OMe			57.8	CH_3		
27			34.5	CH		
29	39.5	CH_2	30.2	CH_2		
30	211.7	C			69.9	CH
31	48.8	CH	37.3	CH		
31-Me			9.6	CH_3	8.4	CH_3
32-OAc					172.47[a]	C
32-OAc					20.8	CH_3
33	36.9	CH	37.0	CH		
33-Me			19.4	CH_3		
34	112.1	CH	112.0	CH	112.0	CH
35	125.4	CH	125.4	CH	125.4	CH
35-NMe	33.0	CH_3	33.0	CH_3	33.0	CH_3
35-NCHO	160.9	CH	160.9	CH	160.8	CH
			170.3	C		

[a]The minor rotamer for 32-OAc is the more shielded of the two resonances at δ_C 172.5

Appendix 23: ^{1}H NMR Spectrum of Callyspongynic Acid (3.1) (CD_3OD, 500 MHz)

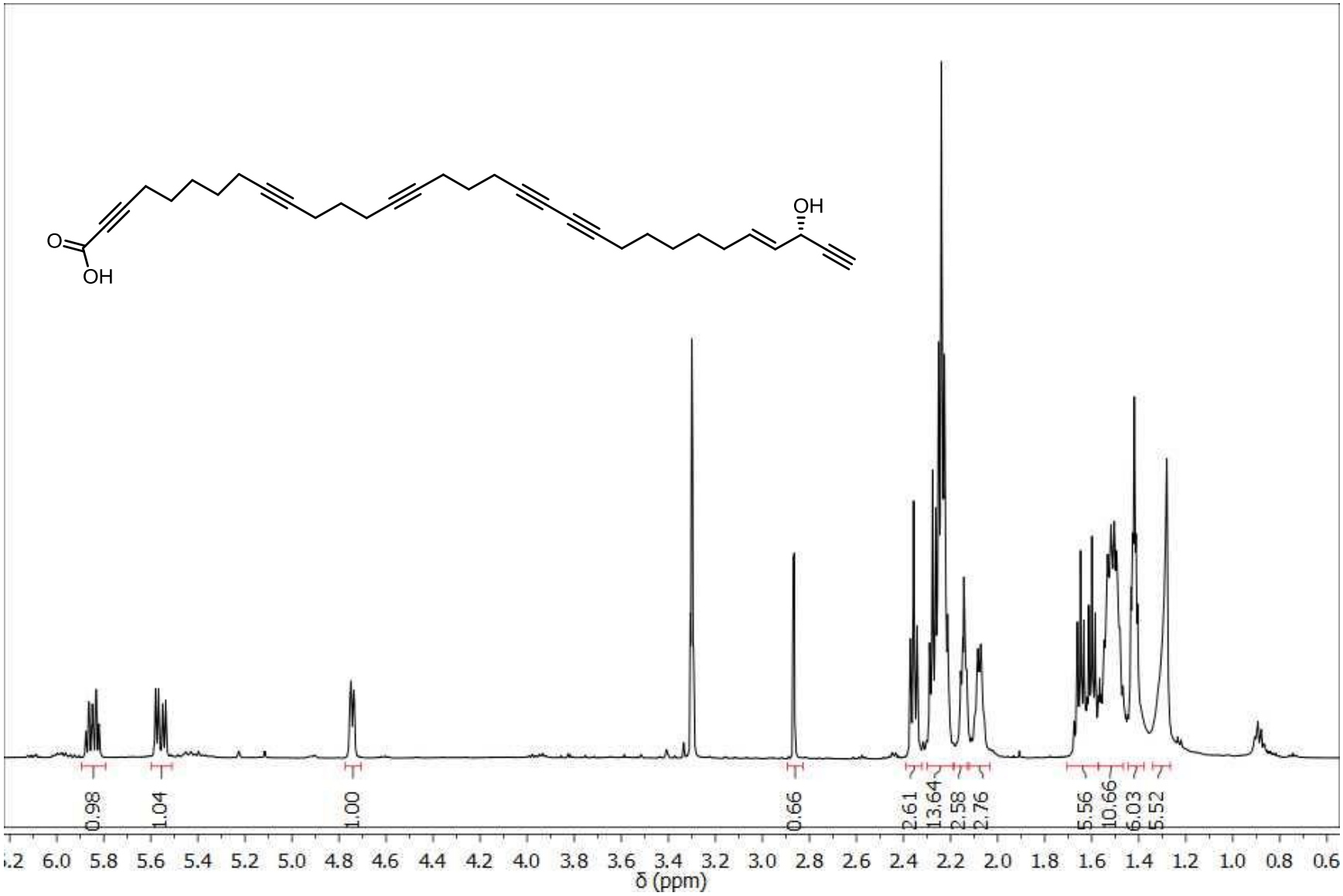

Appendix 24: ^{13}C NMR Spectrum of Callyspongynic Acid (3.1) ($CDCl_3$, 125 MHz)

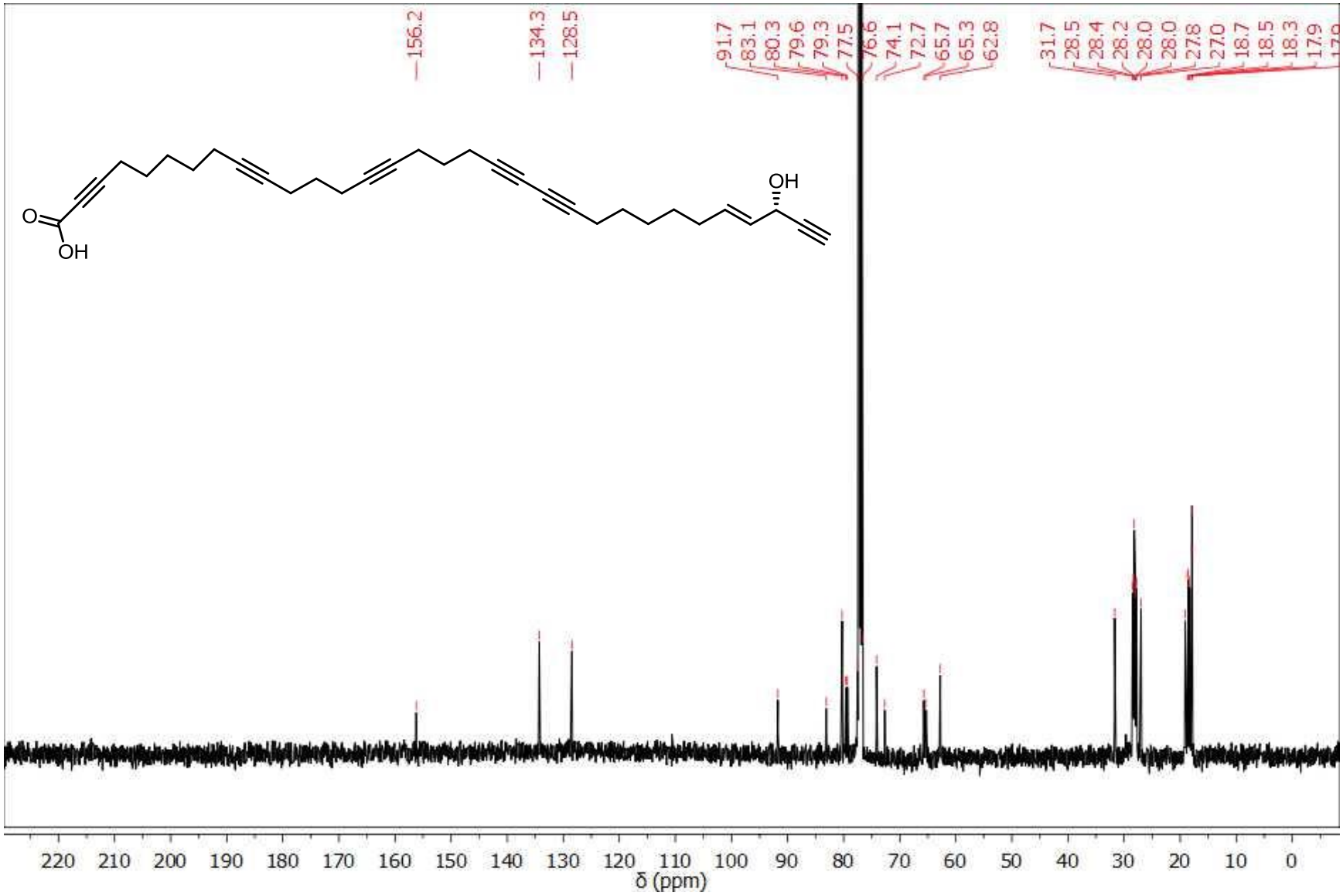

Appendix 25: ^{1}H NMR Spectrum of Decarboxycallyspongynic Acid (3.2) (CD_3OD, 500 MHz)

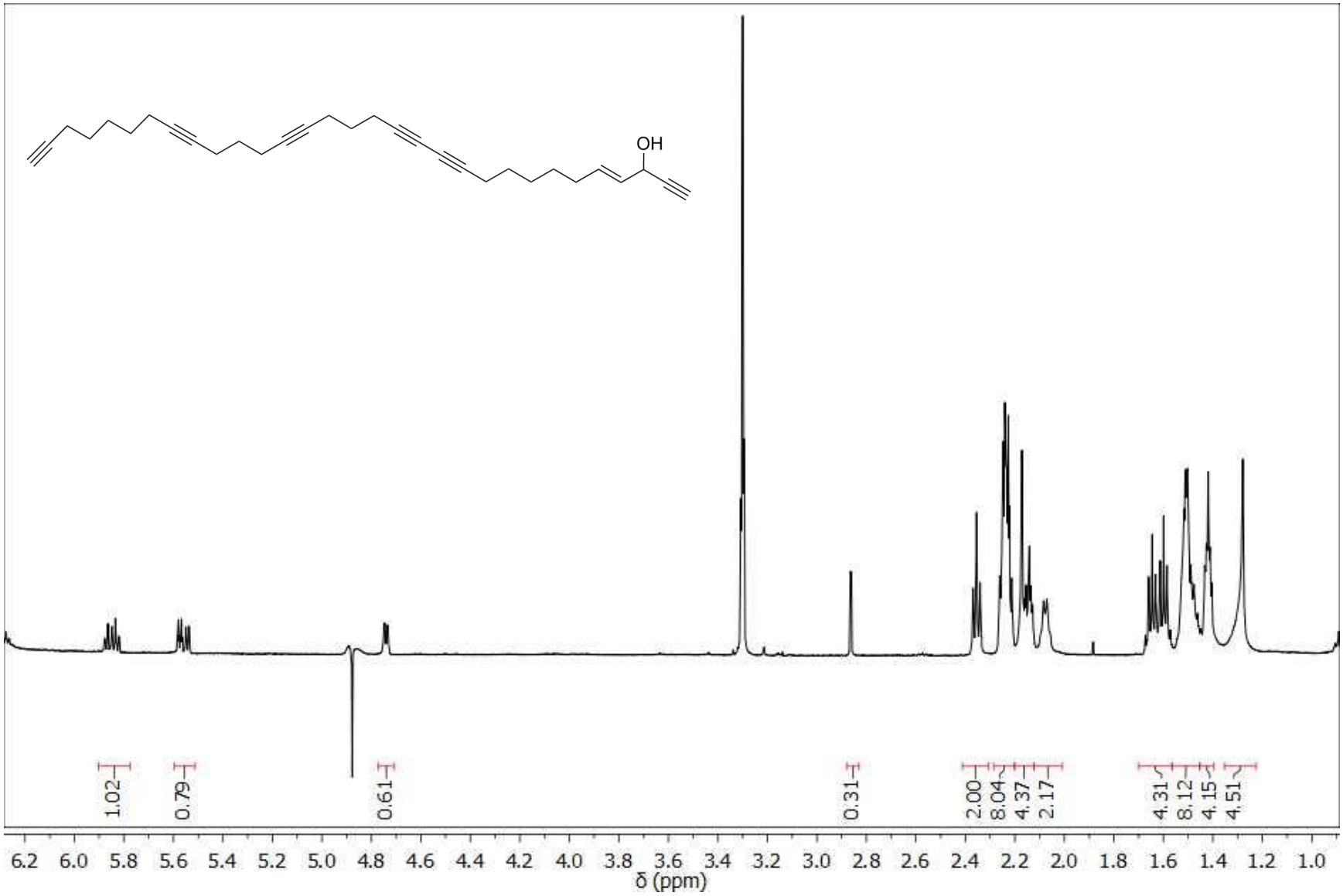

Appendix 26: ^{13}C NMR Spectrum of Decarboxycallyspongynic Acid (3.2) (CD_3OD, 125 MHz)

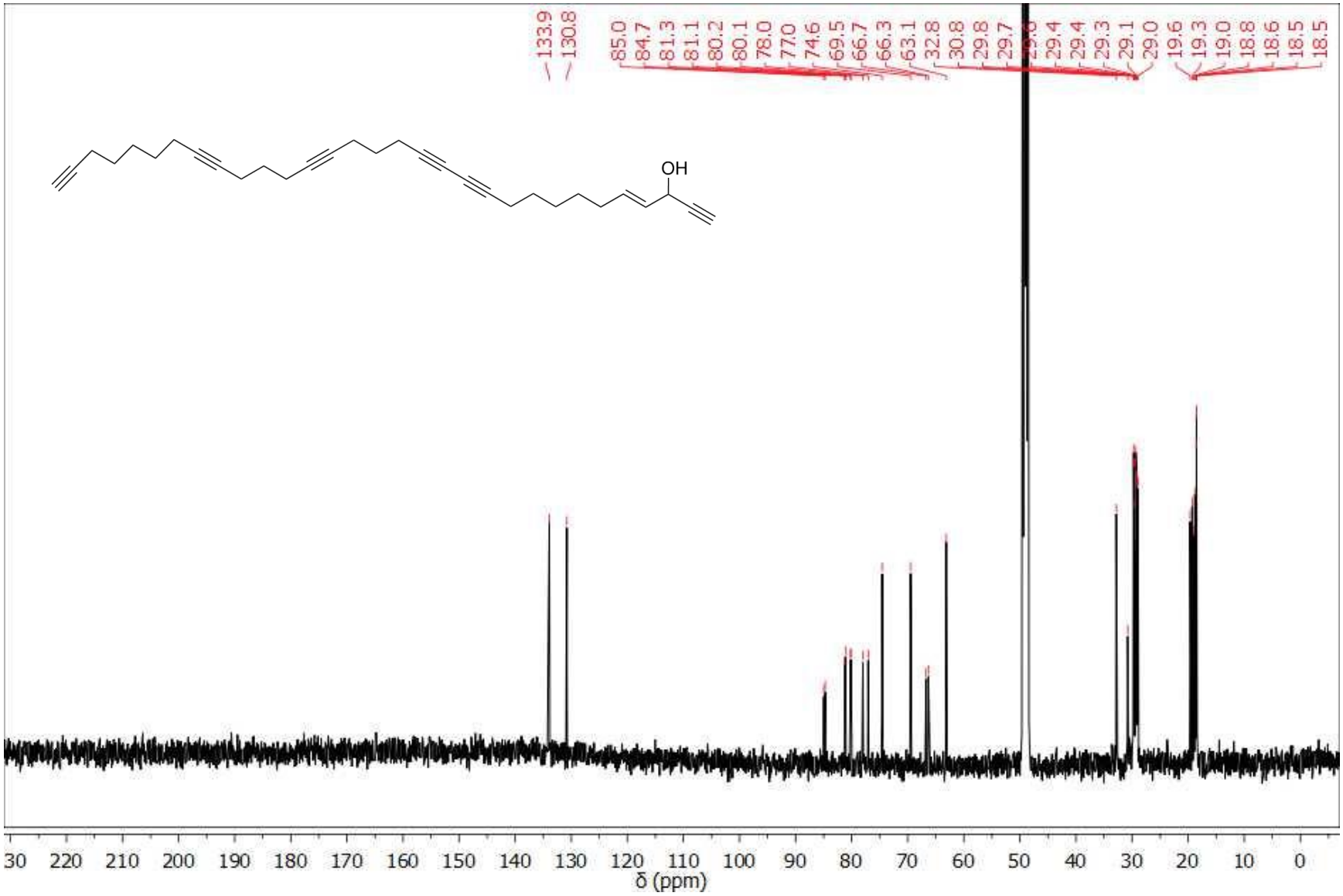

Appendix 27: gHSQC Spectrum of Decarboxycallyspongynic Acid (3.2) (CD_3OD, 500 MHz)

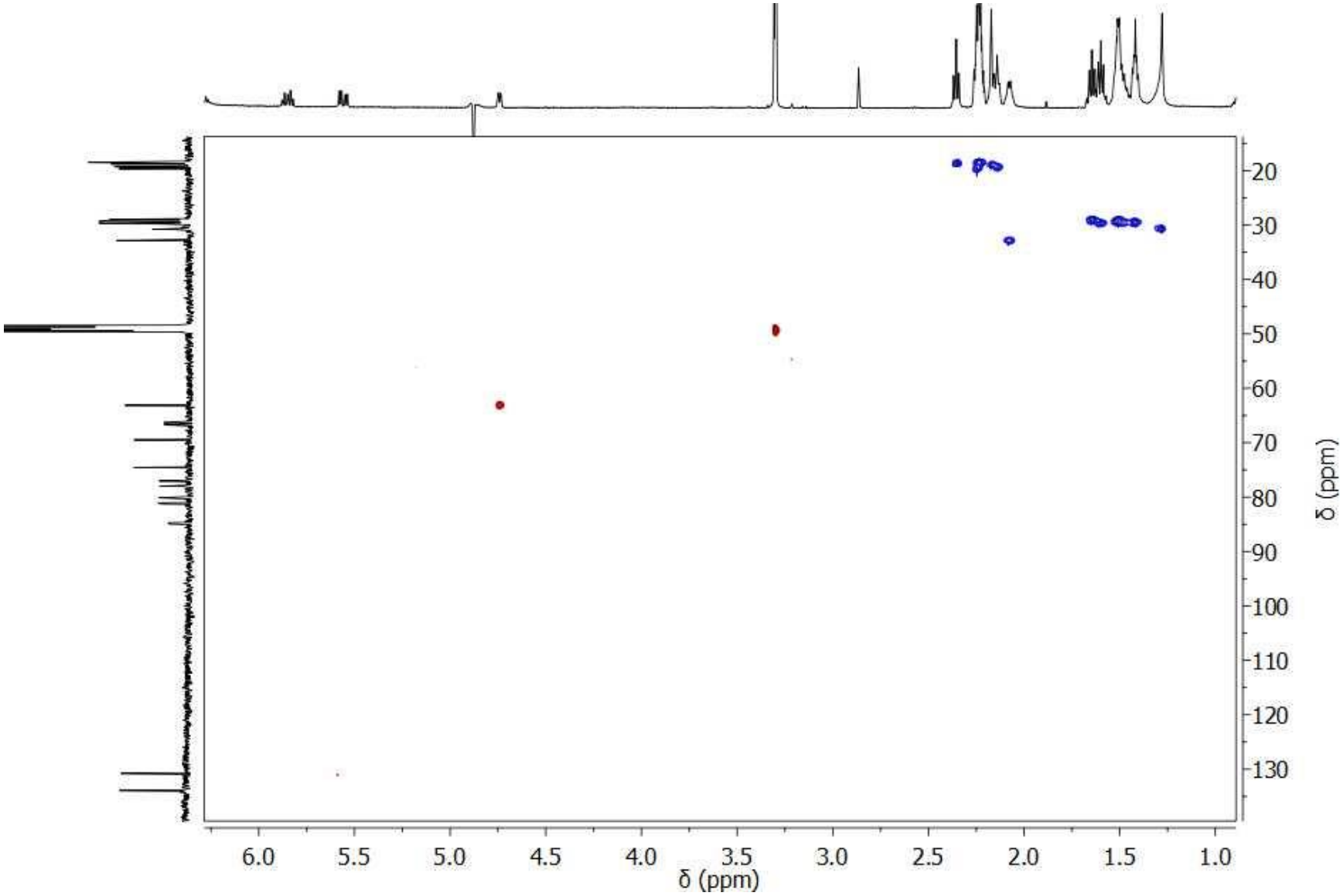

Appendix 28: gDQCOSY Spectrum of Decarboxycallyspongynic Acid (3.2) (CD_3OD, 500 MHz)

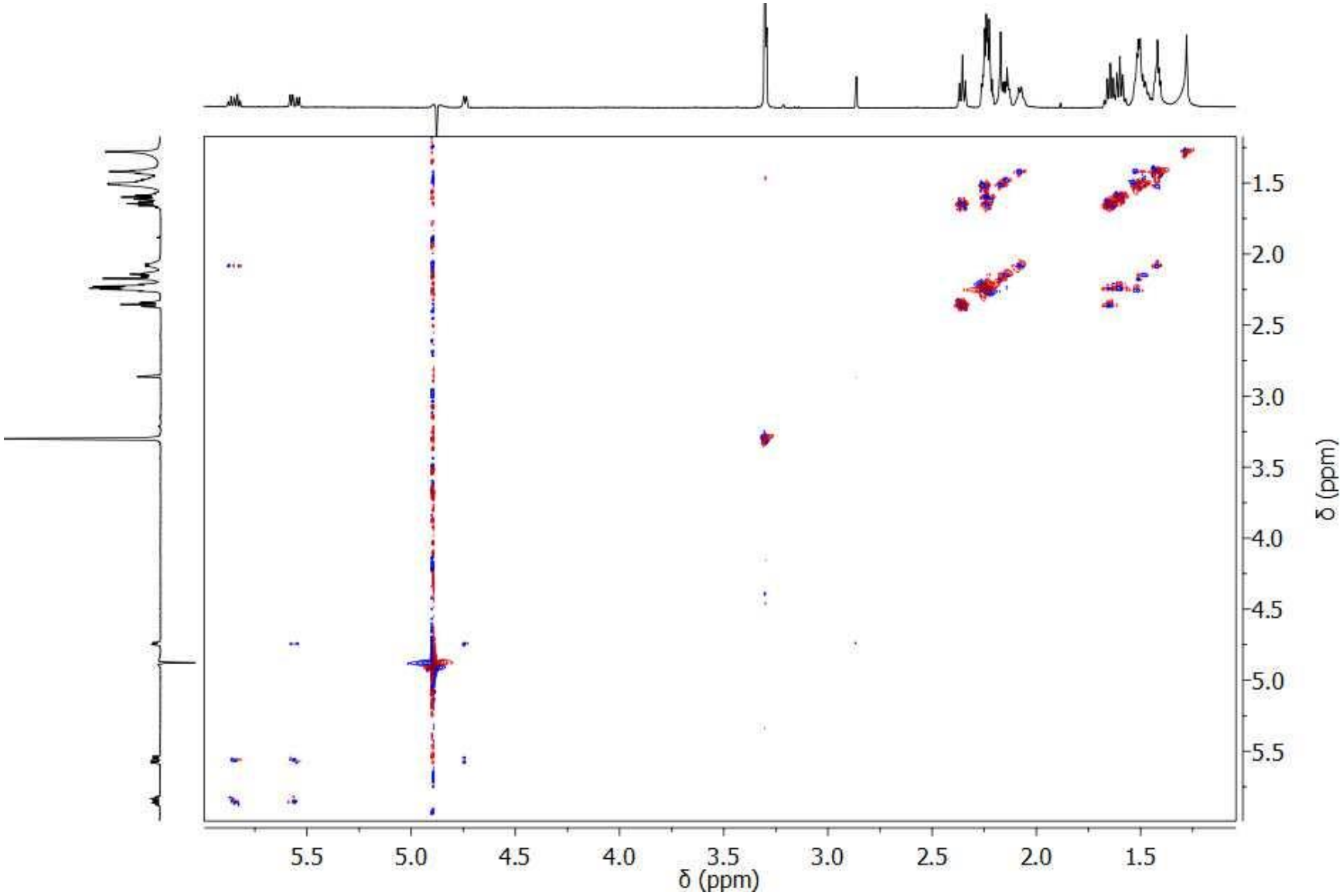

Appendix 29: gHMBC Spectrum of Decarboxycallyspongynic Acid (3.2) (CD_3OD, 500 MHz)

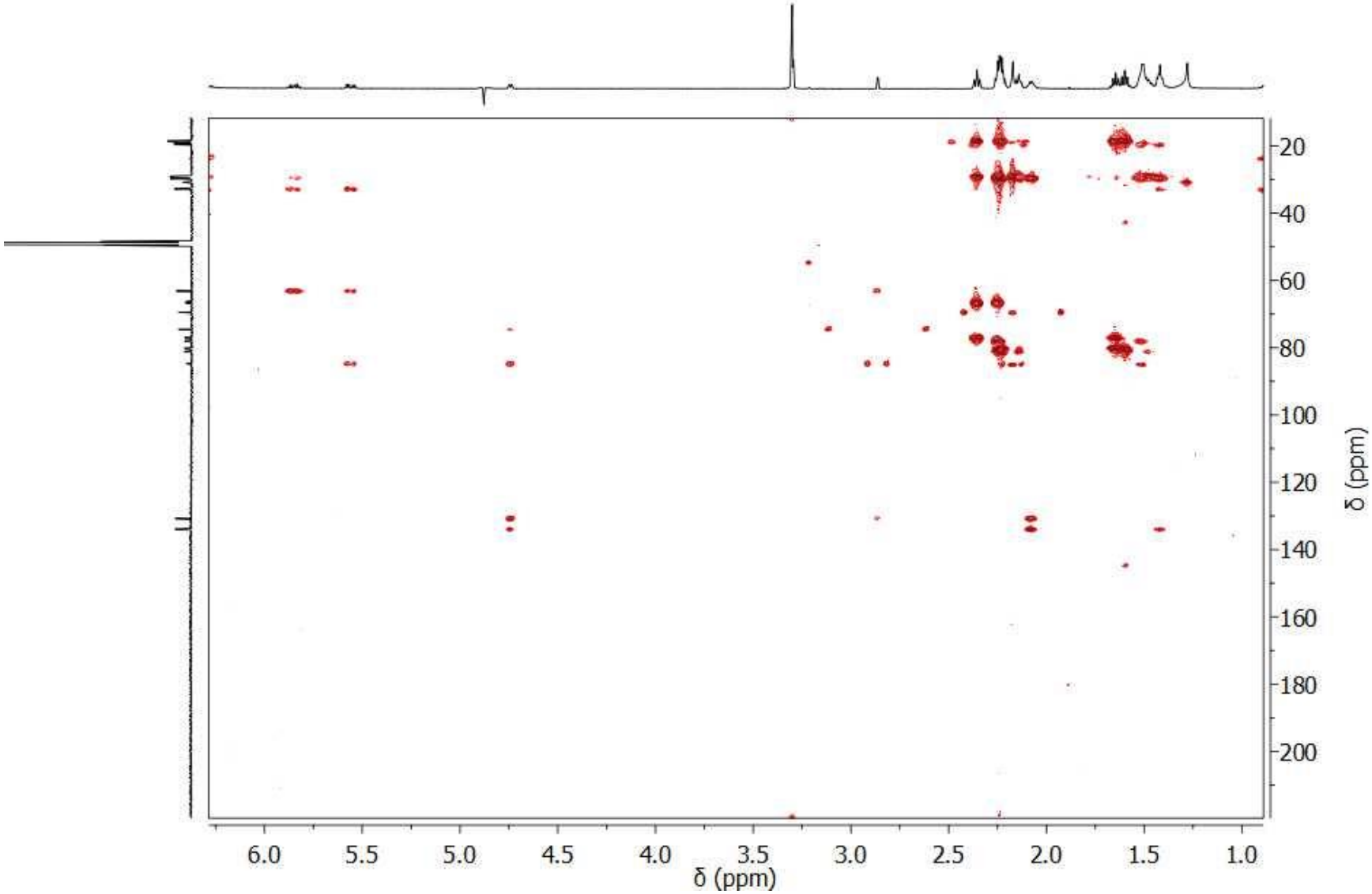

Appendix 30: Image of *Callyspongia* sp.

Appendix 31: ^{1}H NMR Spectrum of Myrmenaphthol A (4.1) (CD_3OD, 500 MHz)

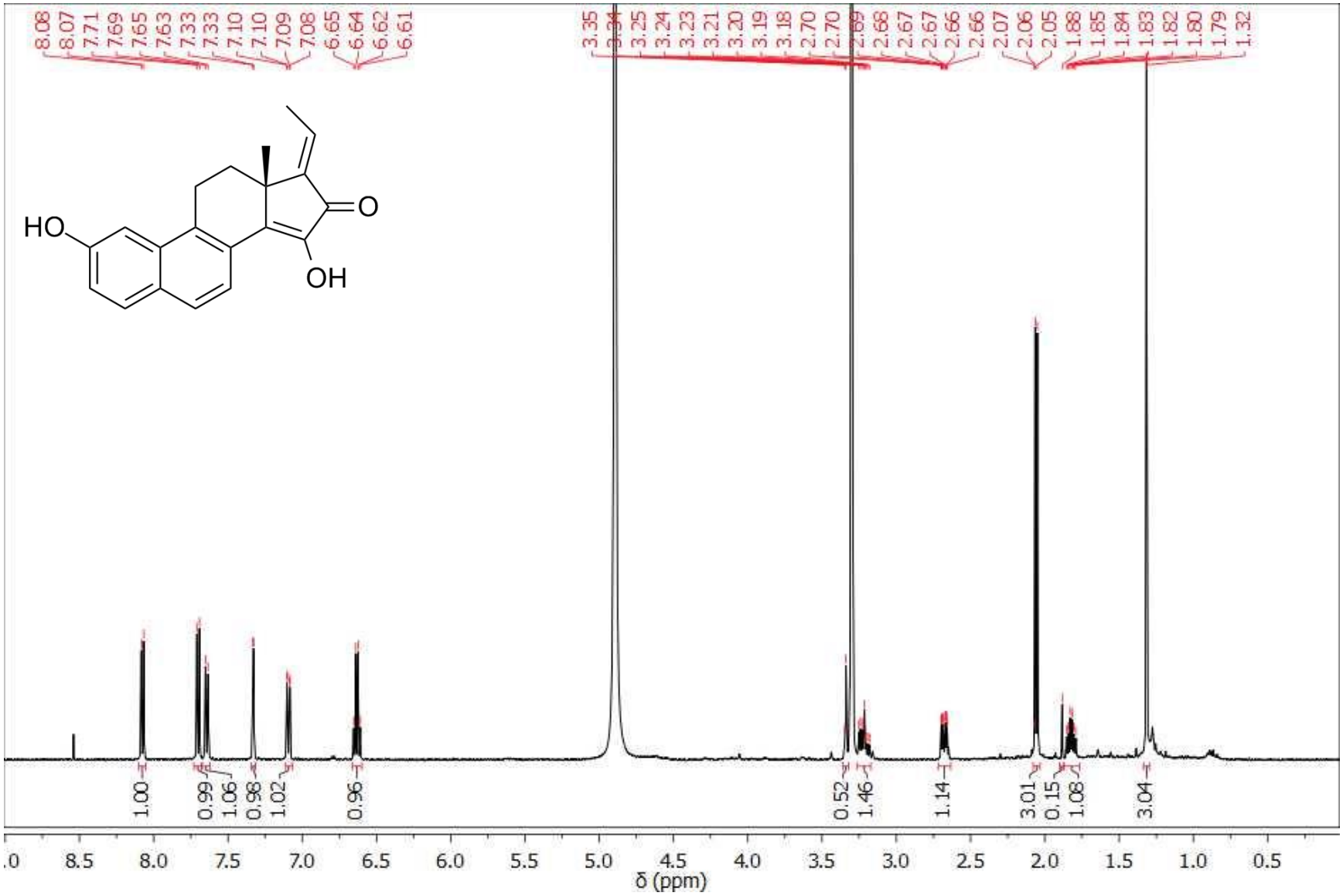

Appendix 32: ^{13}C NMR Spectrum of Myrmenaphthol A (4.1) (CD_3OD, 125 MHz)

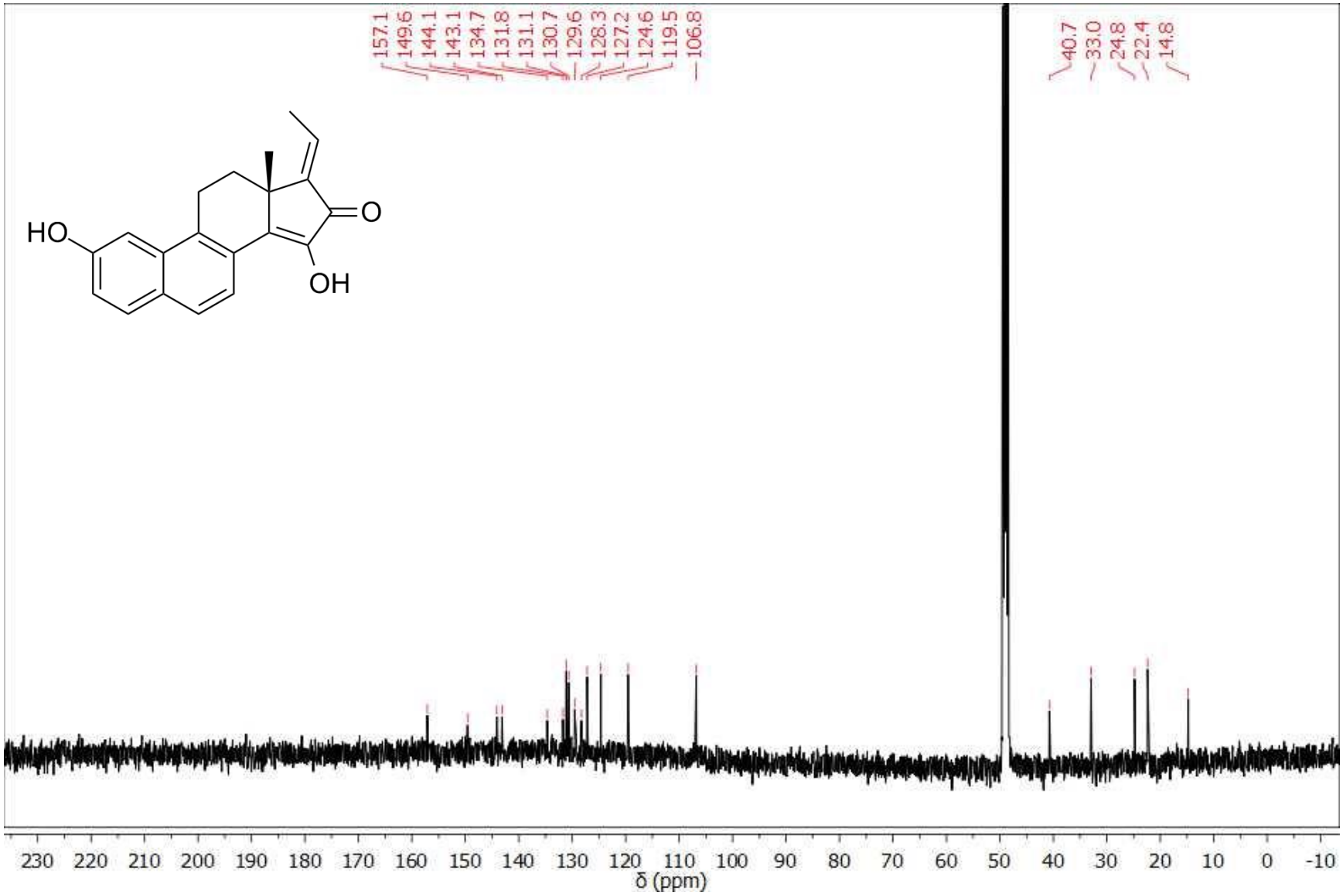

Appendix 33: gHSQC Spectrum of Myrmenaphthol A (4.1) (CD_3OD, 500 MHz)

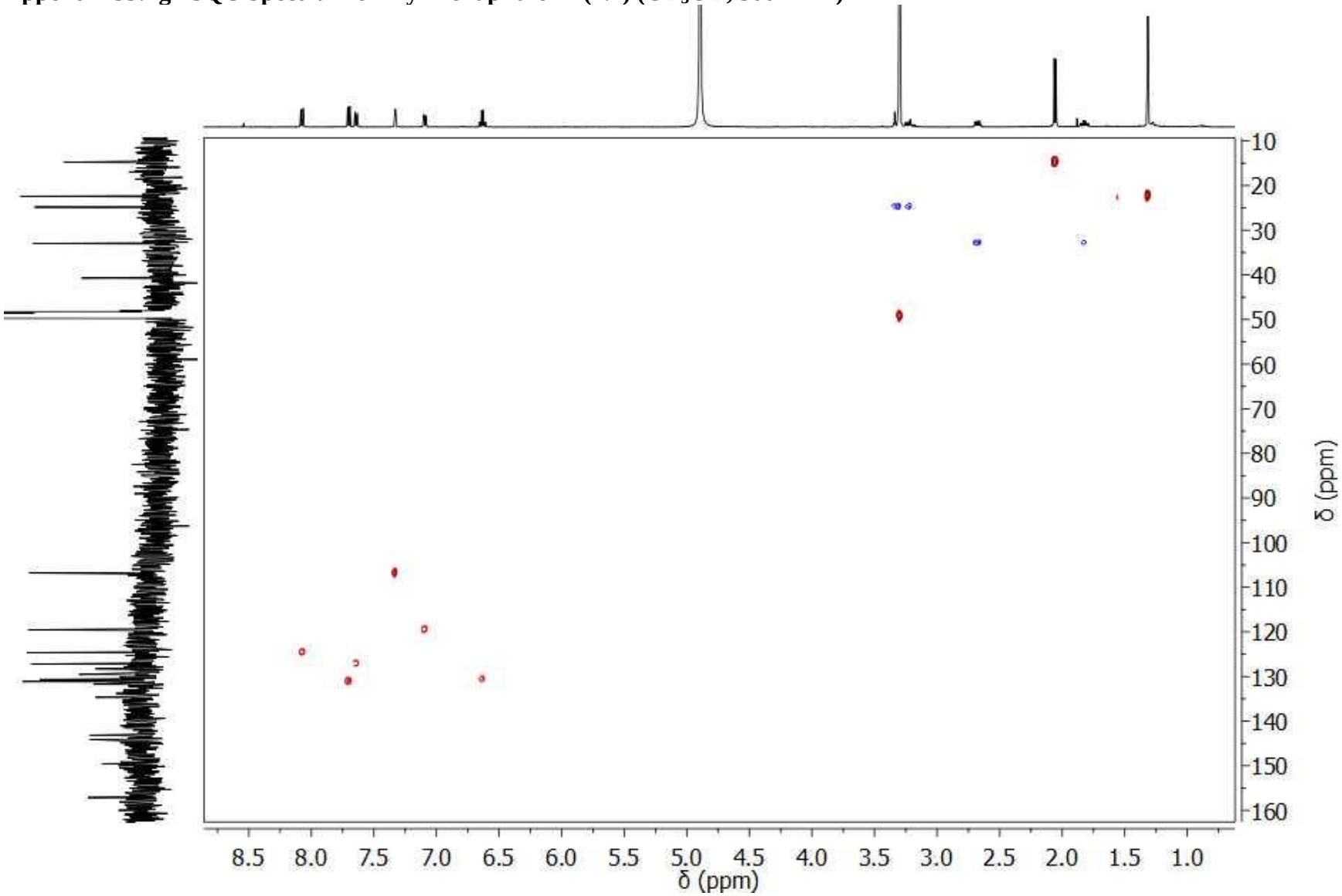

Appendix 34: gDQCOSY Spectrum of Myrmenaphthol A (4.1) (CD_3OD, 500 MHz)

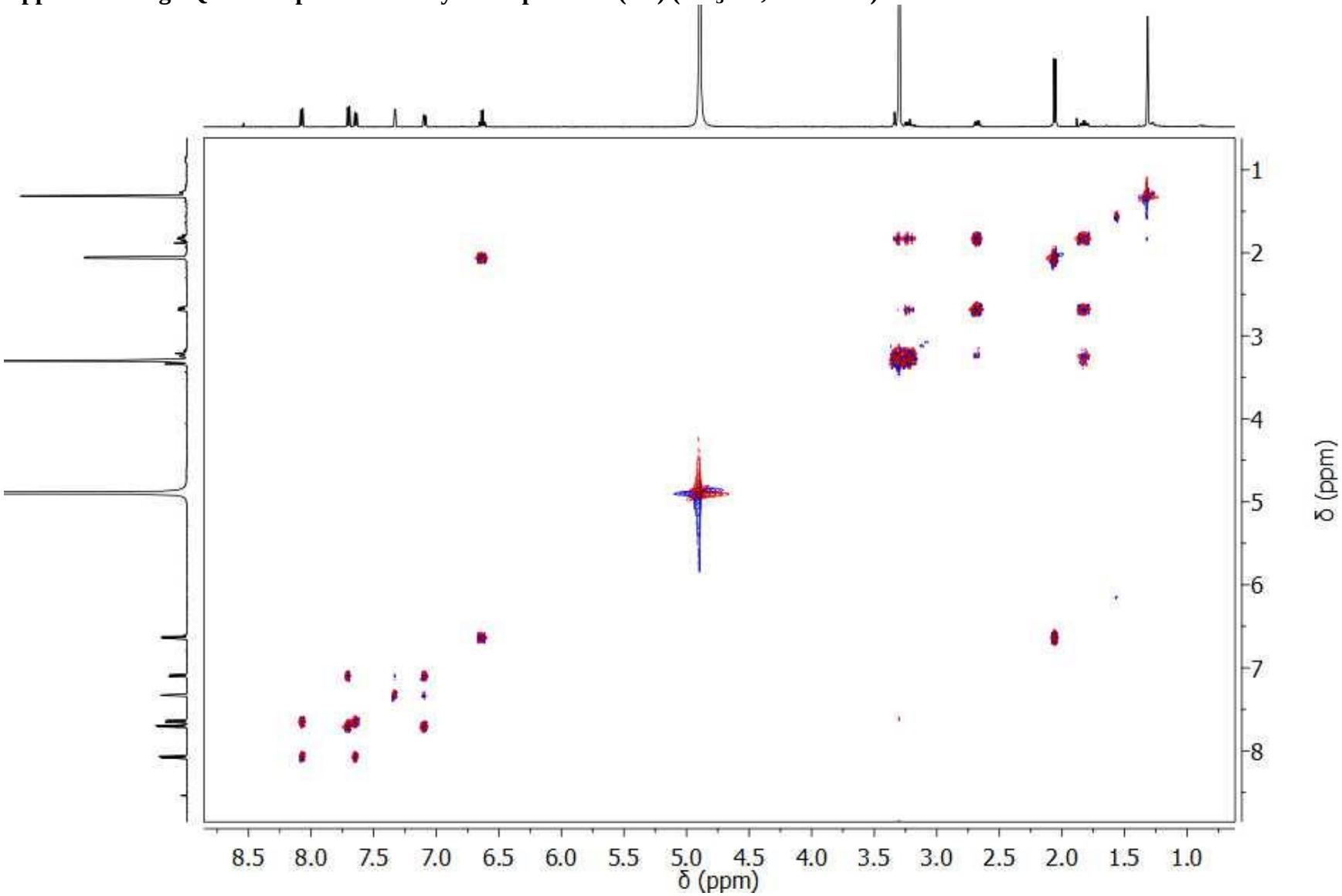

Appendix 35: gHMBC Spectrum of Myrmenaphthol A (4.1) (CD_3OD, 500 MHz)

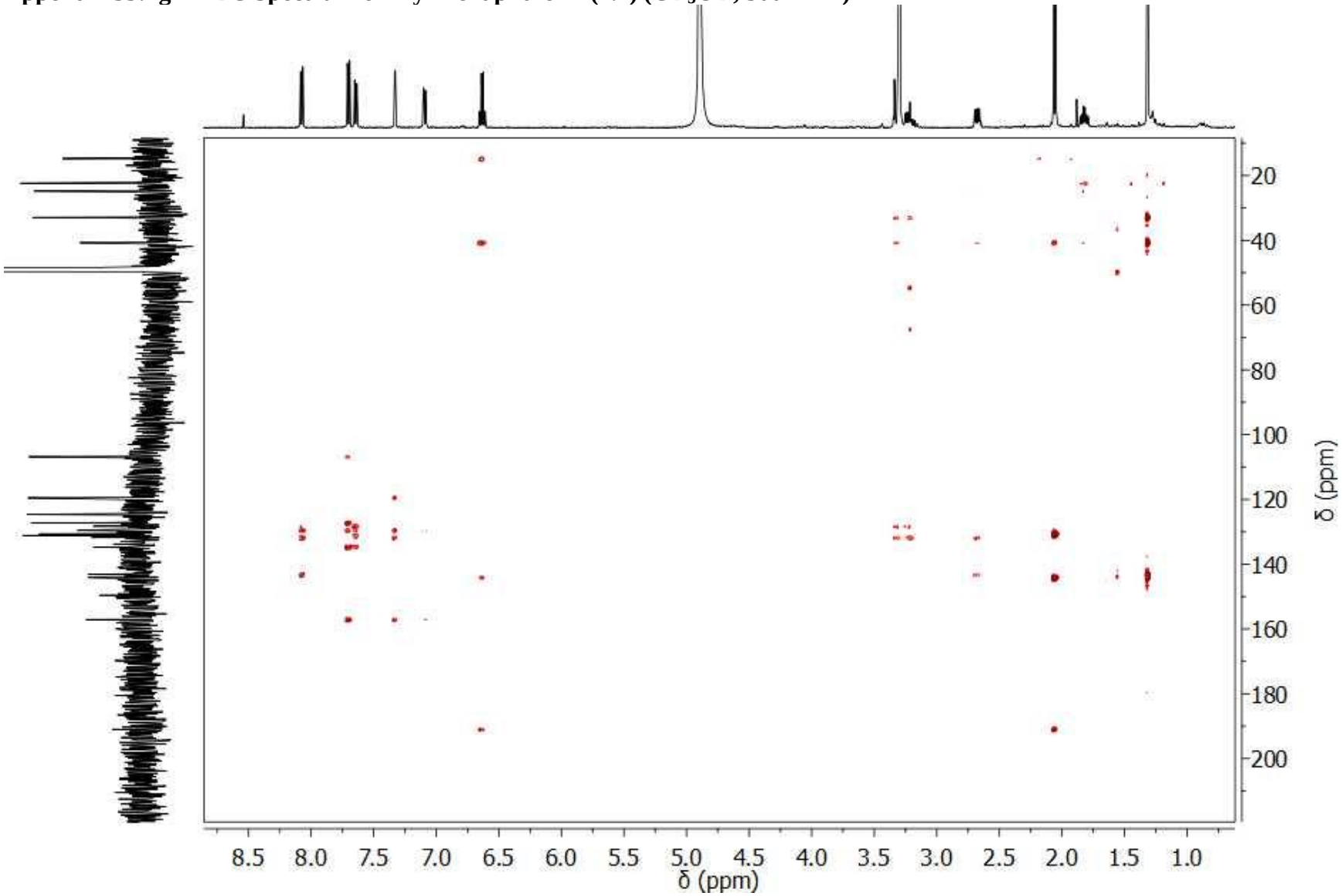

Appendix 36: ROESY Spectrum of Myrmenaphthol A (4.1) (CD_3OD, 500 MHz)

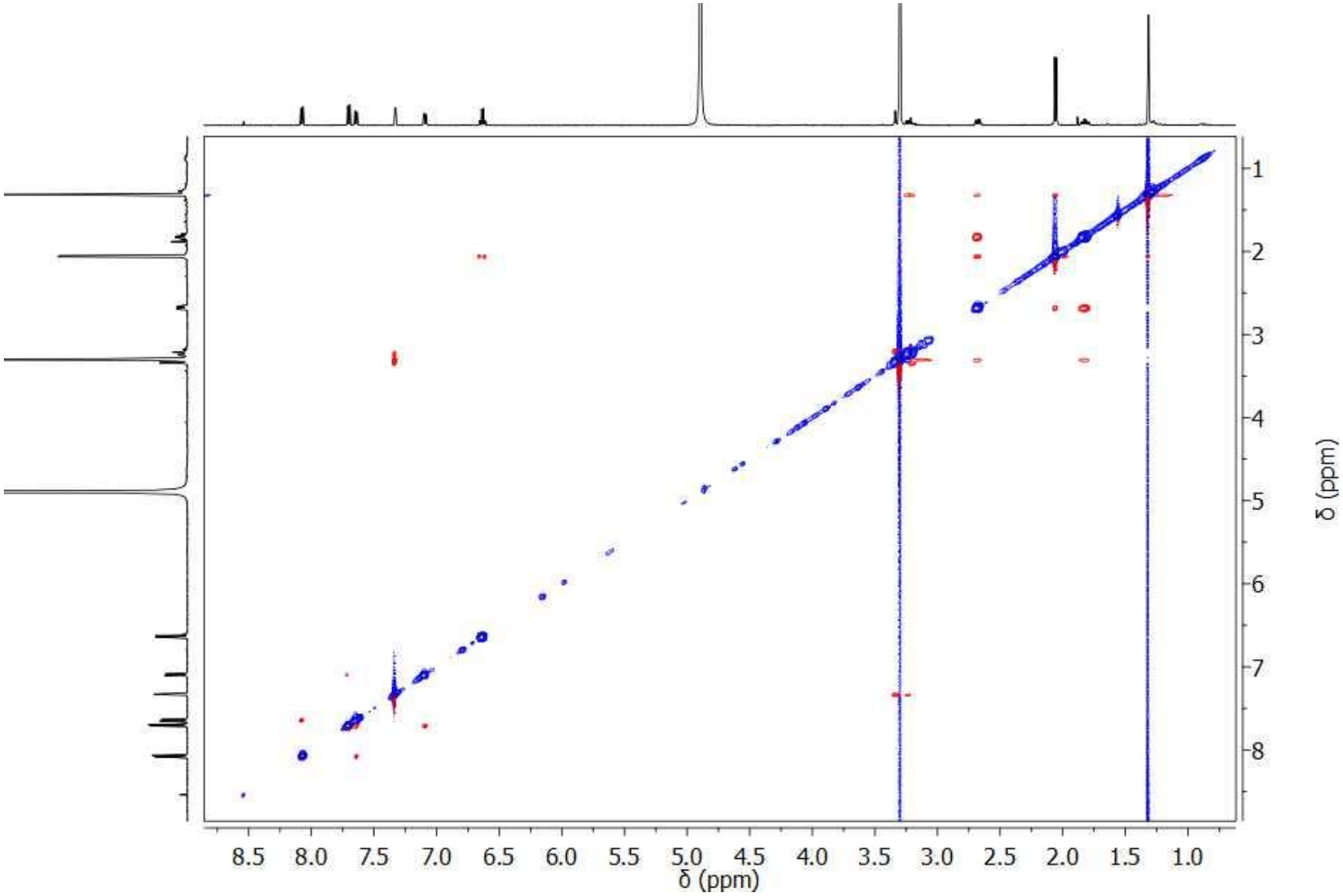

Appendix 37: ^{1}H NMR Spectrum of Cinanthrenol A (4.2) (CD_3OD, 500 MHz)

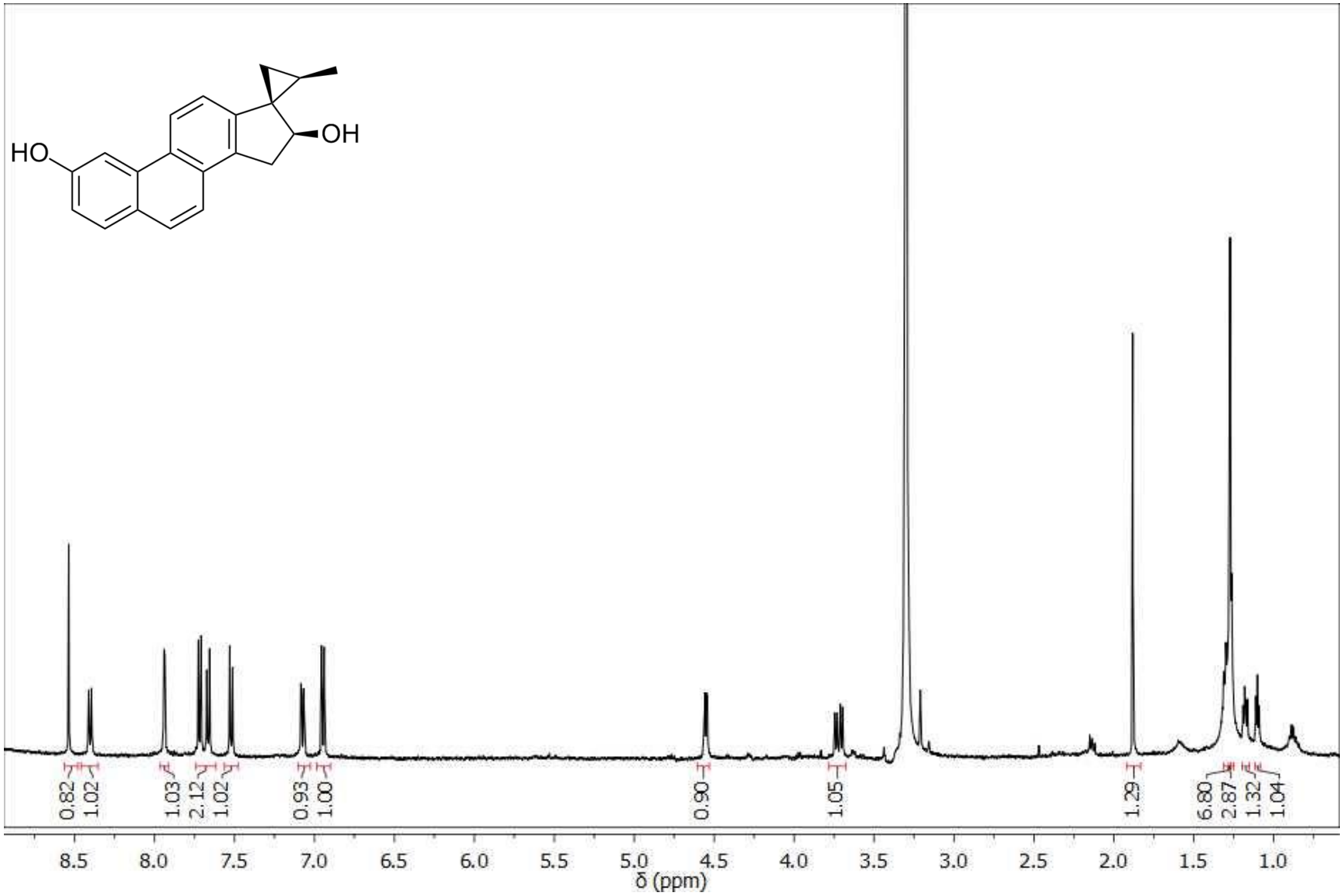

Appendix 38: gHSQC Spectrum of Cinanthrenol A (4.2) (CD_3OD, 500 MHz)

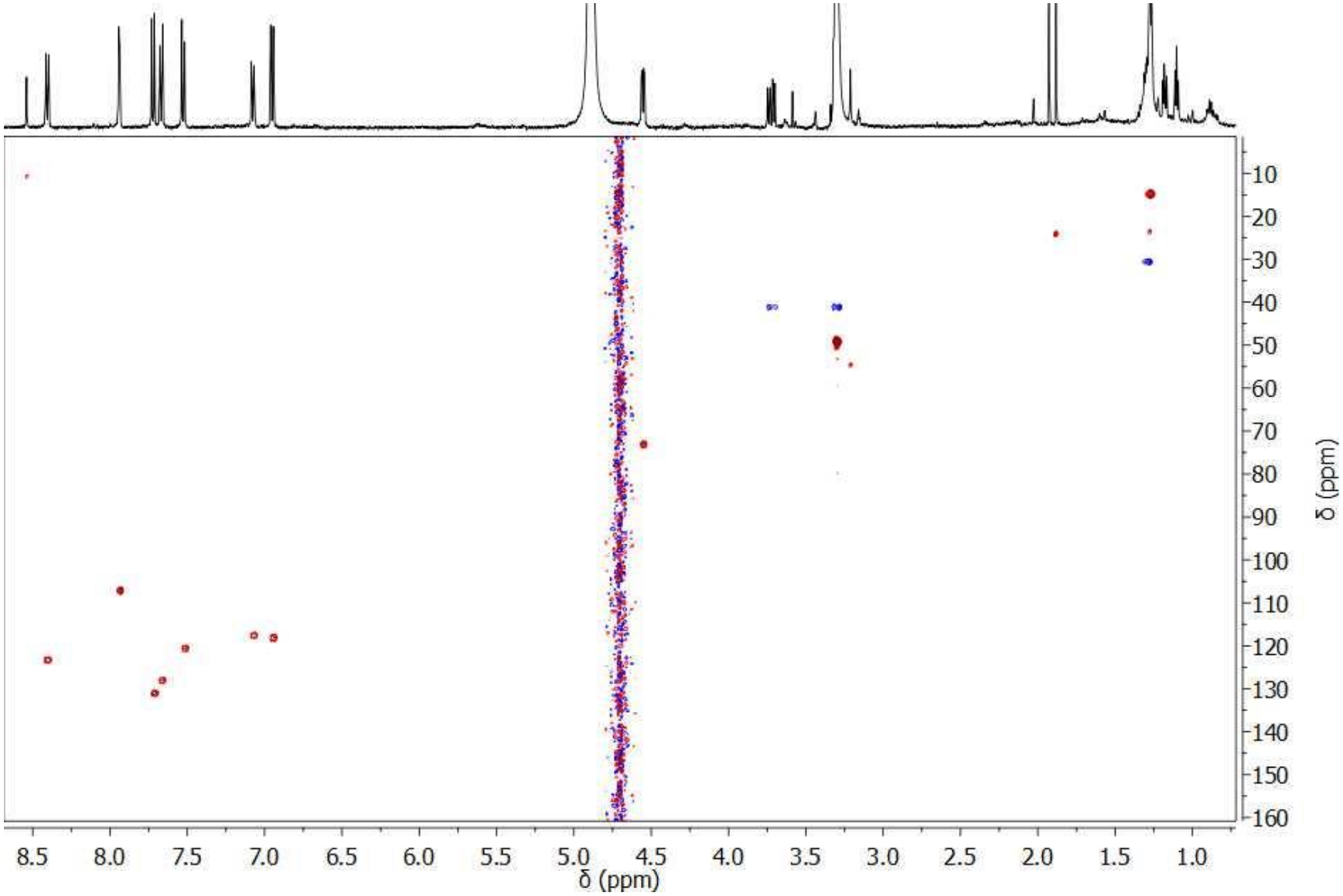

Appendix 39: gHMBC Spectrum of Cinanthrenol A (4.2) (CD_3OD, 500 MHz)

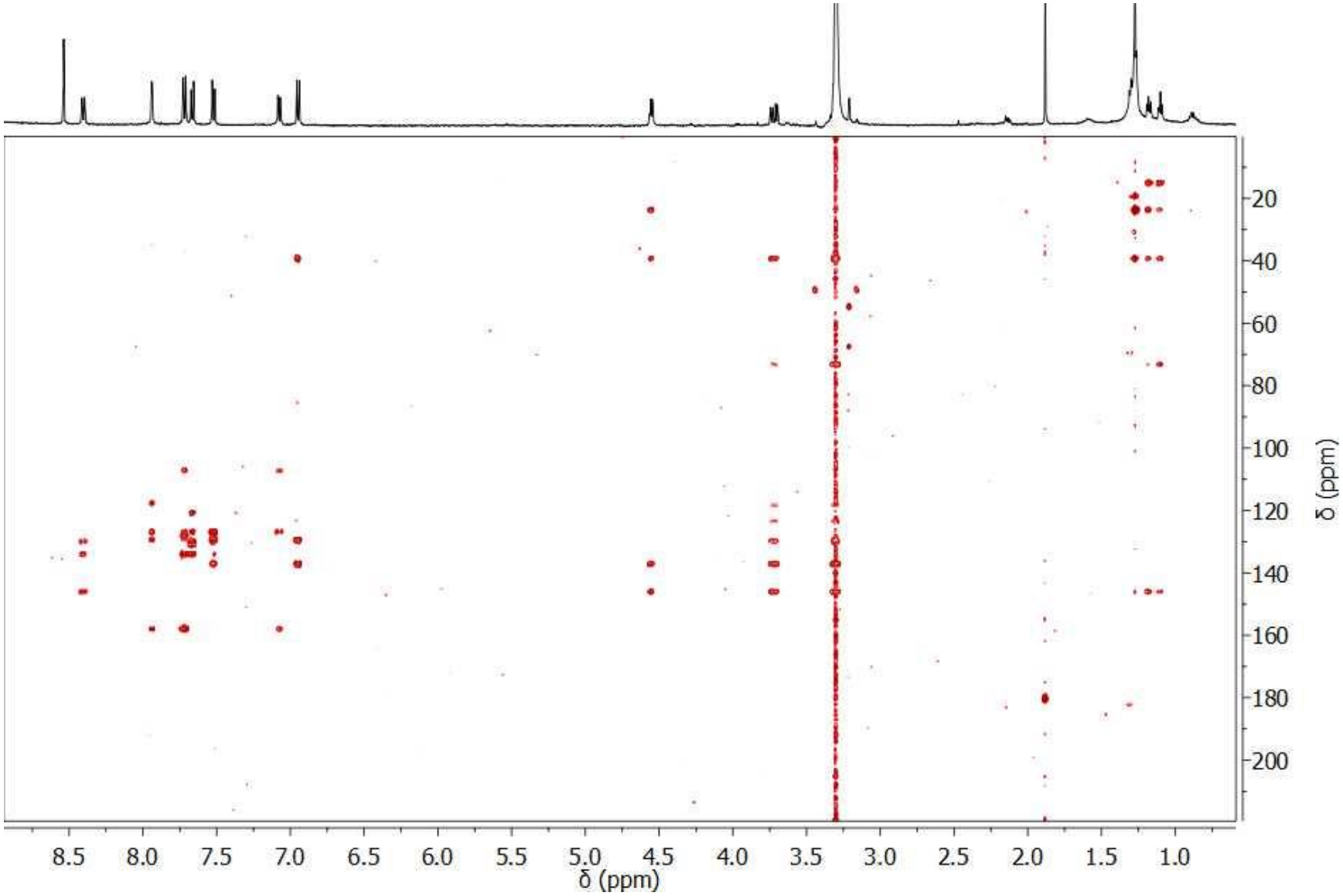

Appendix 40: Image of *Myrmekioderma* sp.

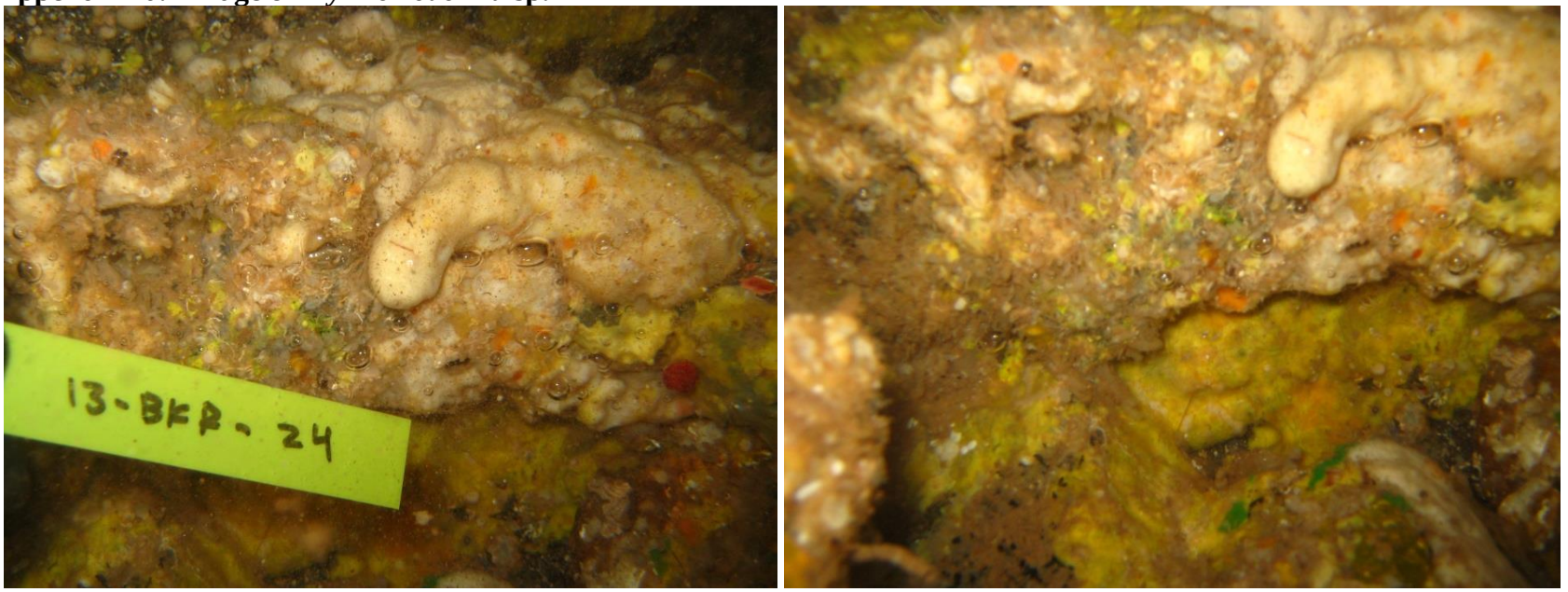

Appendix 41: ^{1}H NMR Spectrum of Impure 3,4-dihydroxypregna-5,17-diene-10,2-carbolactone (4.3) (CD_3OD, 500 MHz)

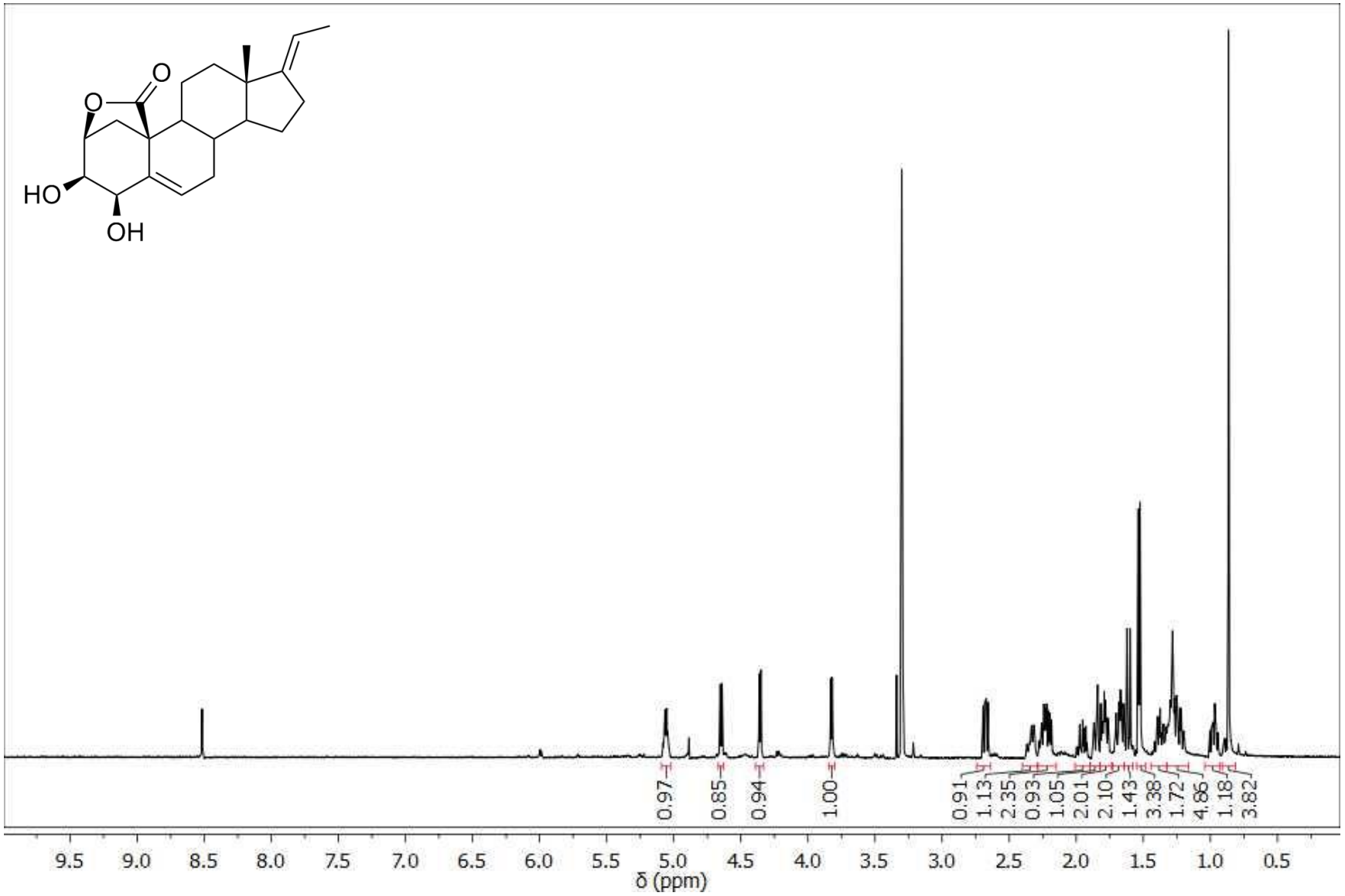

Appendix 42: ^{1}H NMR Spectrum of 3,4-dihydroxypregna-5,20-diene-10,2-carbolactone (4.4) (CD_3OD, 500 MHz)

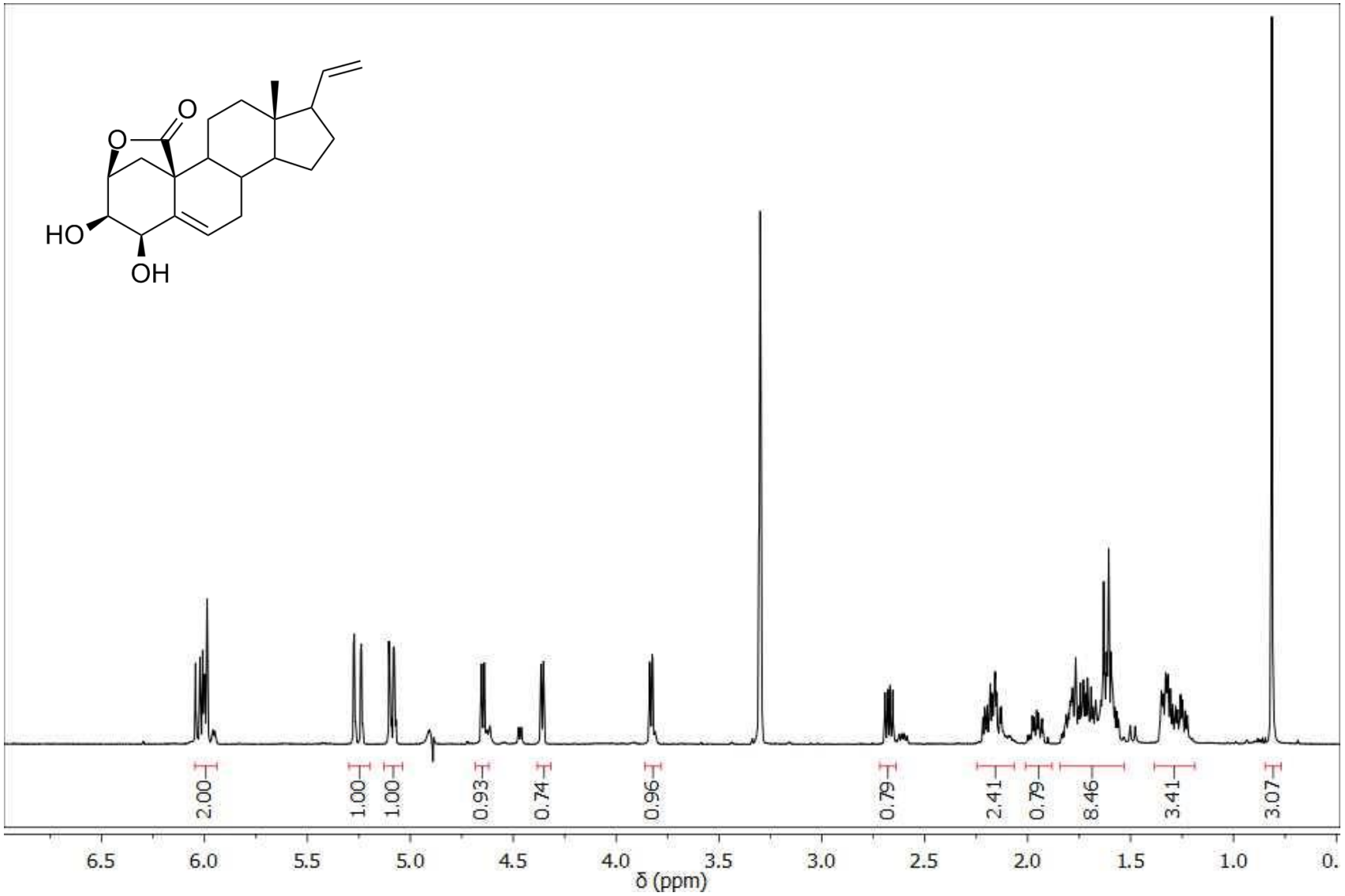

Appendix 43: ^{1}H NMR Spectrum of Avarol (5.1) (CD_3OD, 500 MHz)

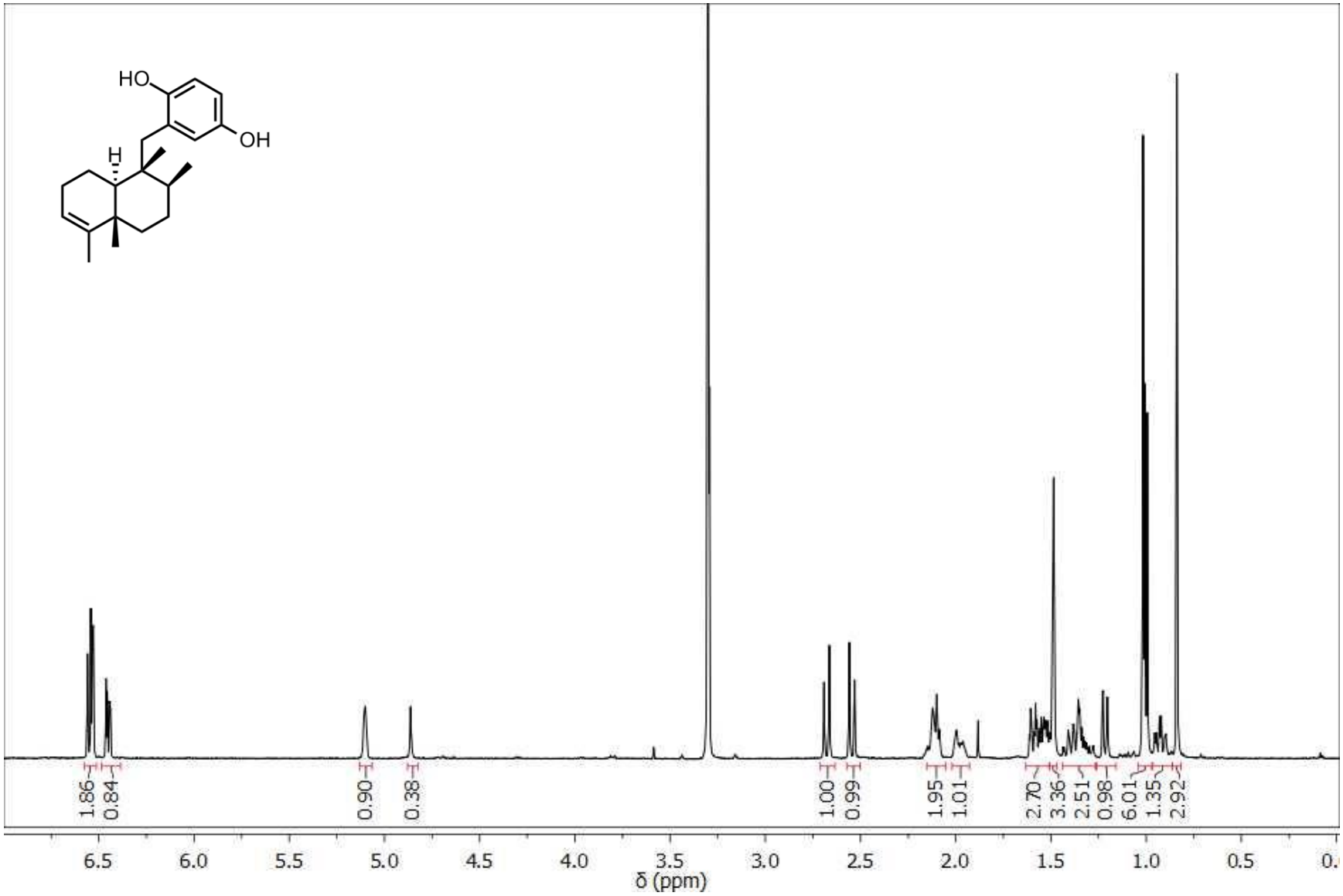

Appendix 44: ^{13}C NMR Spectrum of Avarol (5.1) (CD_3OD, 125 MHz)

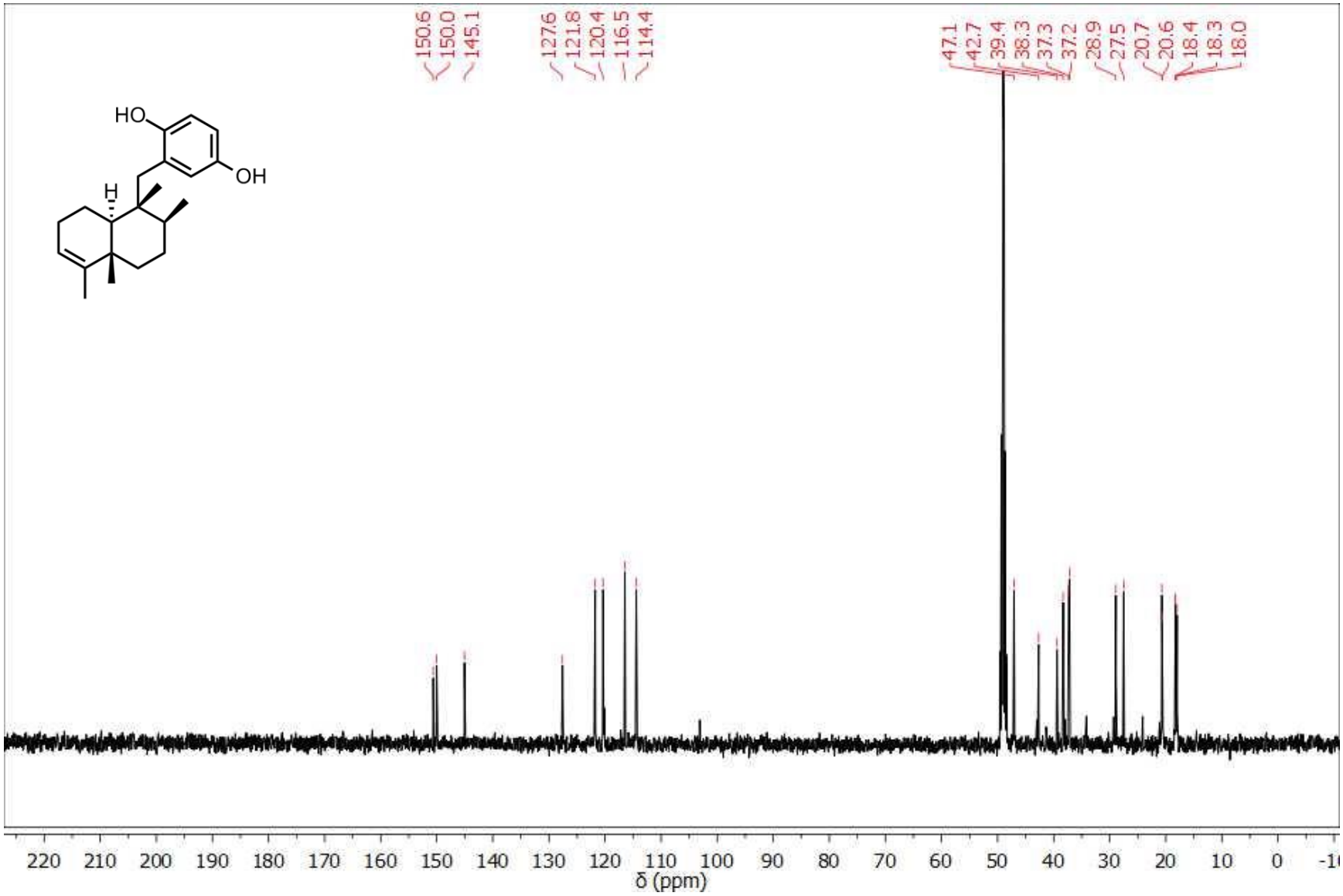

Appendix 45: ^{1}H NMR Spectrum of Isoavarol (5.2) (CD_3OD, 500 MHz)

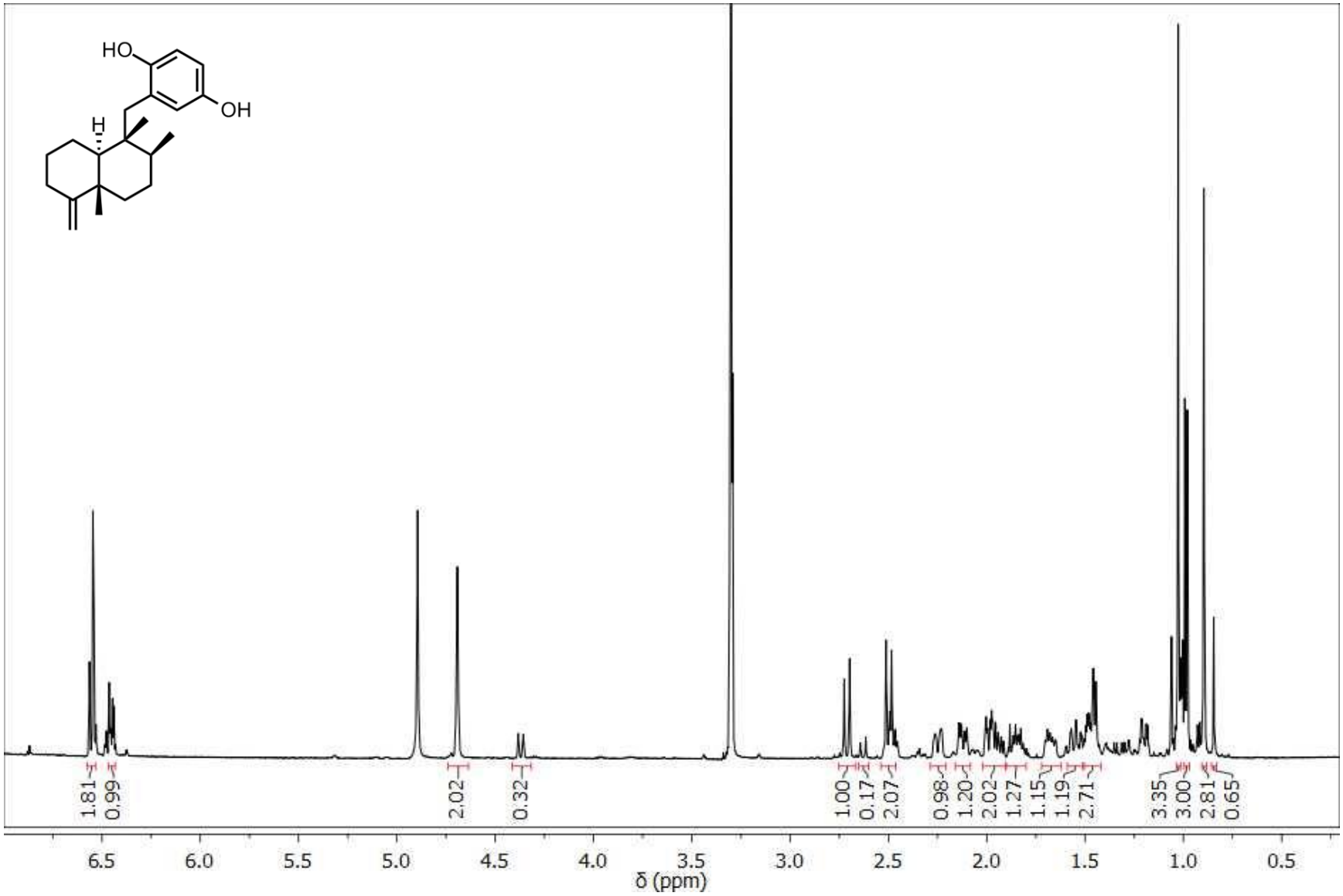

Appendix 46: ^{13}C NMR Spectrum of Isoavarol (5.2) (CD_3OD, 125 MHz)

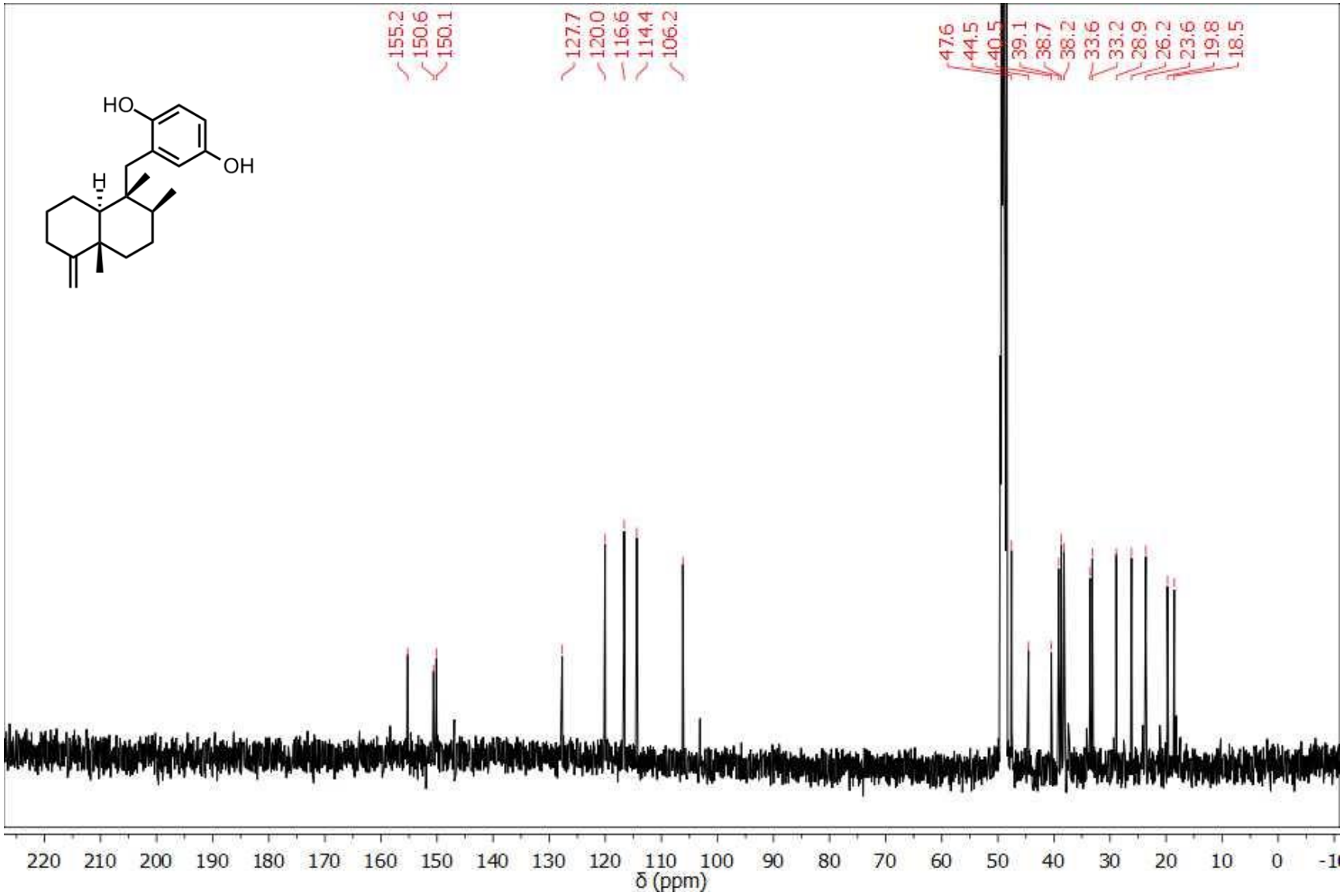

Appendix 47: ^{1}H NMR Spectrum of Avarol Monoacetate (5.3) ($CDCl_3$, 500 MHz)

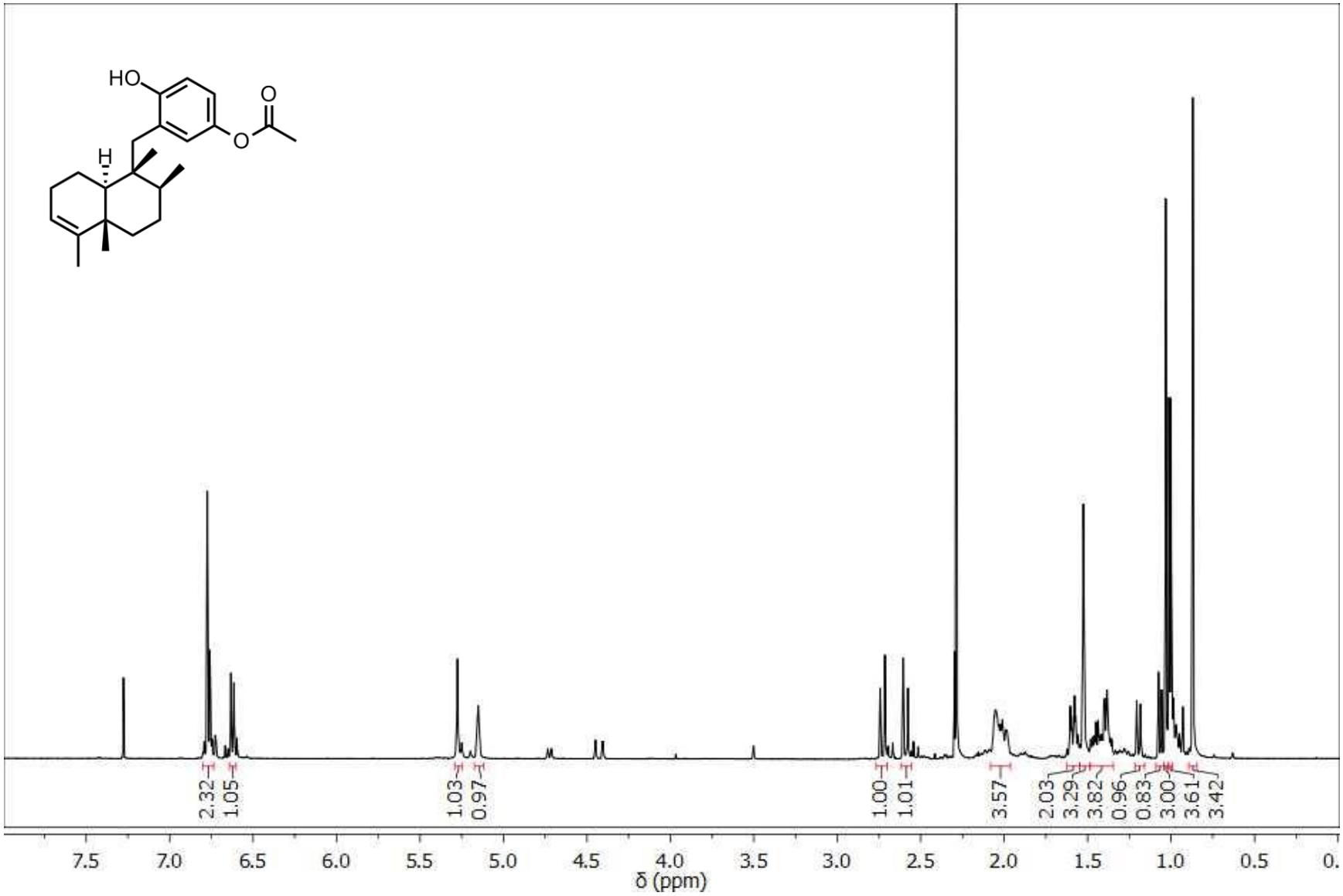

Appendix 48: ^{13}C NMR Spectrum of Avarol Monoacetate (5.3) ($CDCl_3$, 125 MHz)

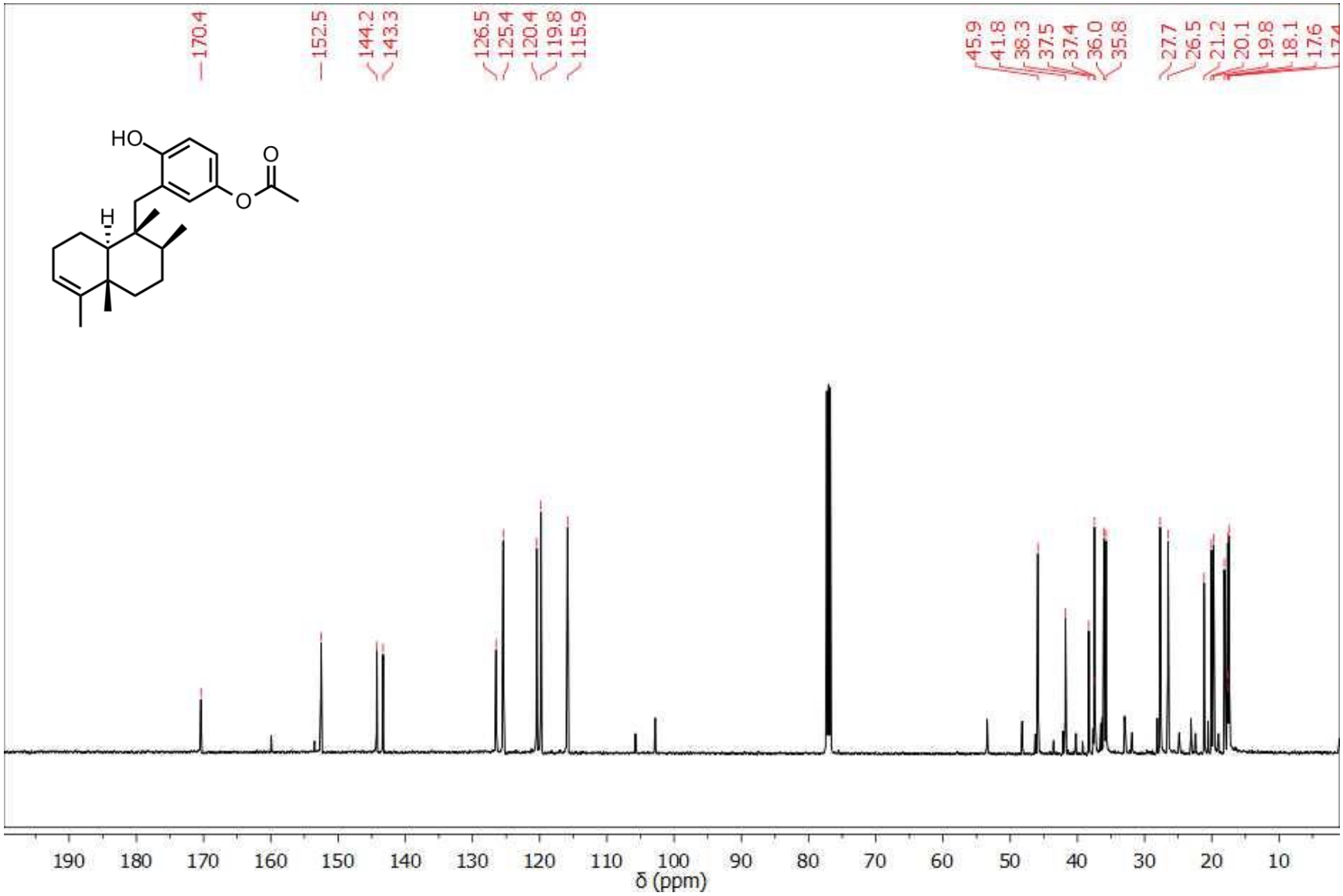

Appendix 49: ^{1}H NMR Spectrum of Avarone (5.4) ($CDCl_3$, 500 MHz)

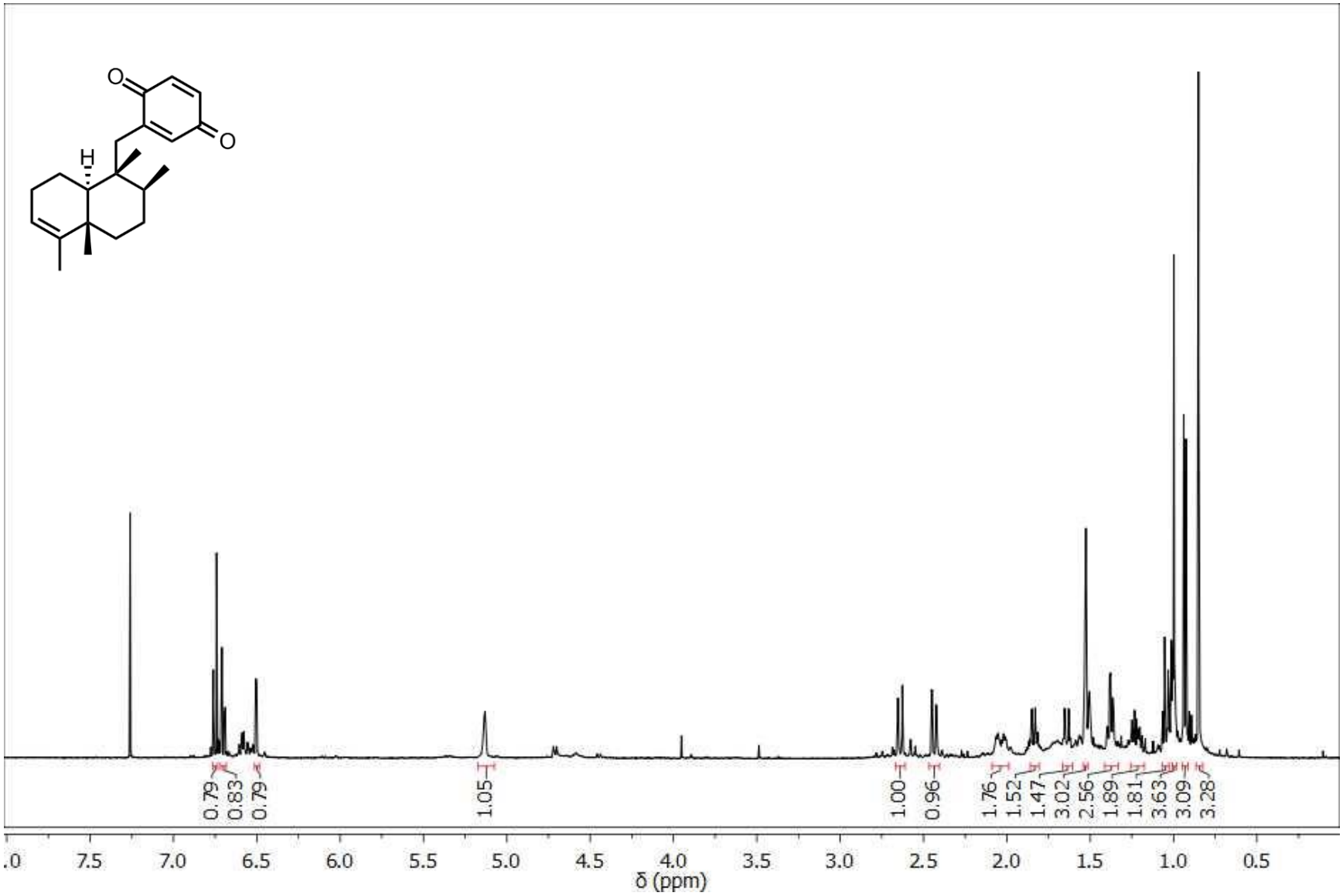

Appendix 50: ^{1}H NMR Spectrum of 3α-hydroxyisoavarol (5.5) (CD_3OD, 500 MHz)

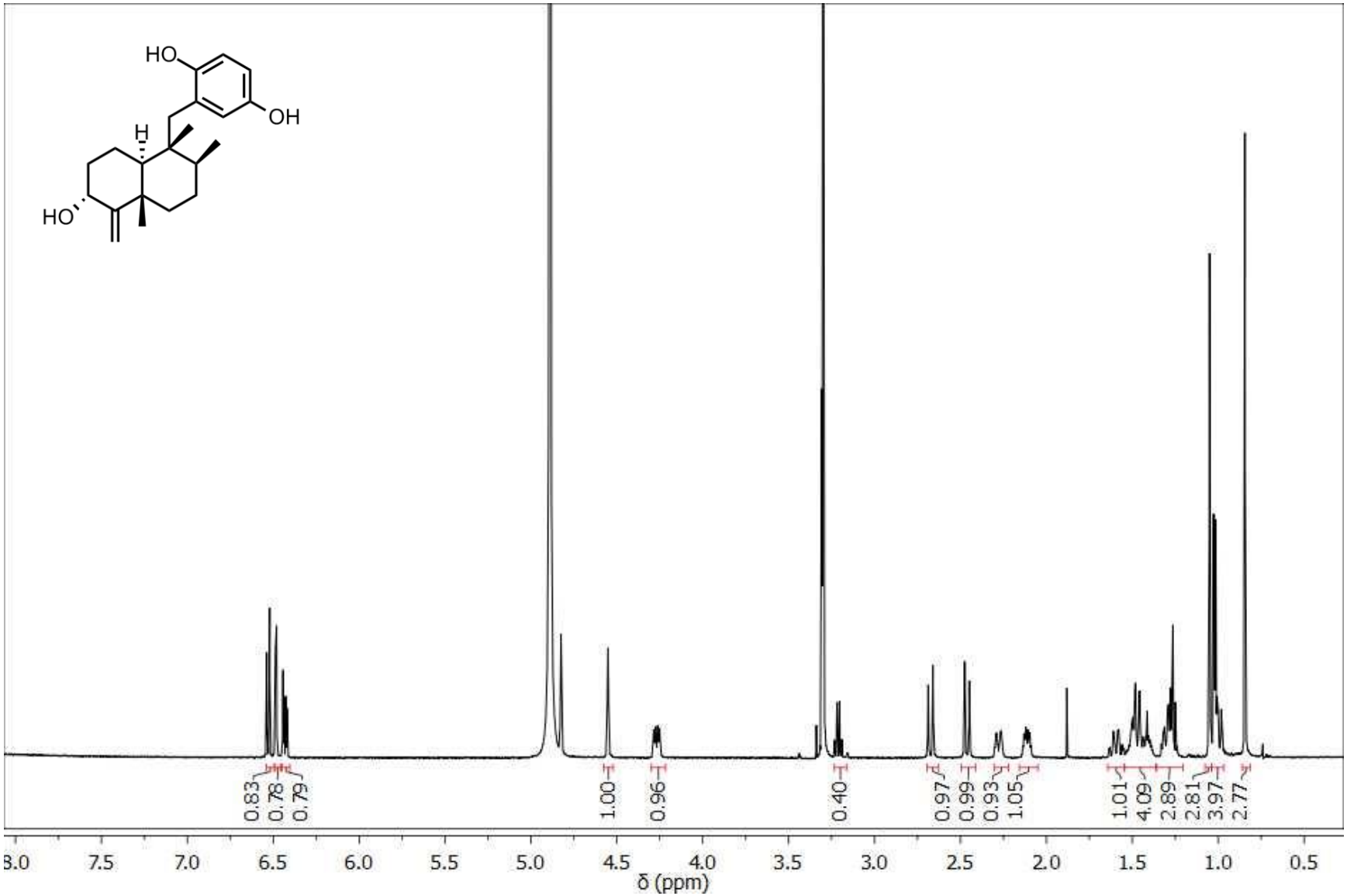

Appendix 51: ^{13}C NMR Spectrum of 3α-hydroxyisoavarol (5.5) (CD_3OD, 125 MHz)

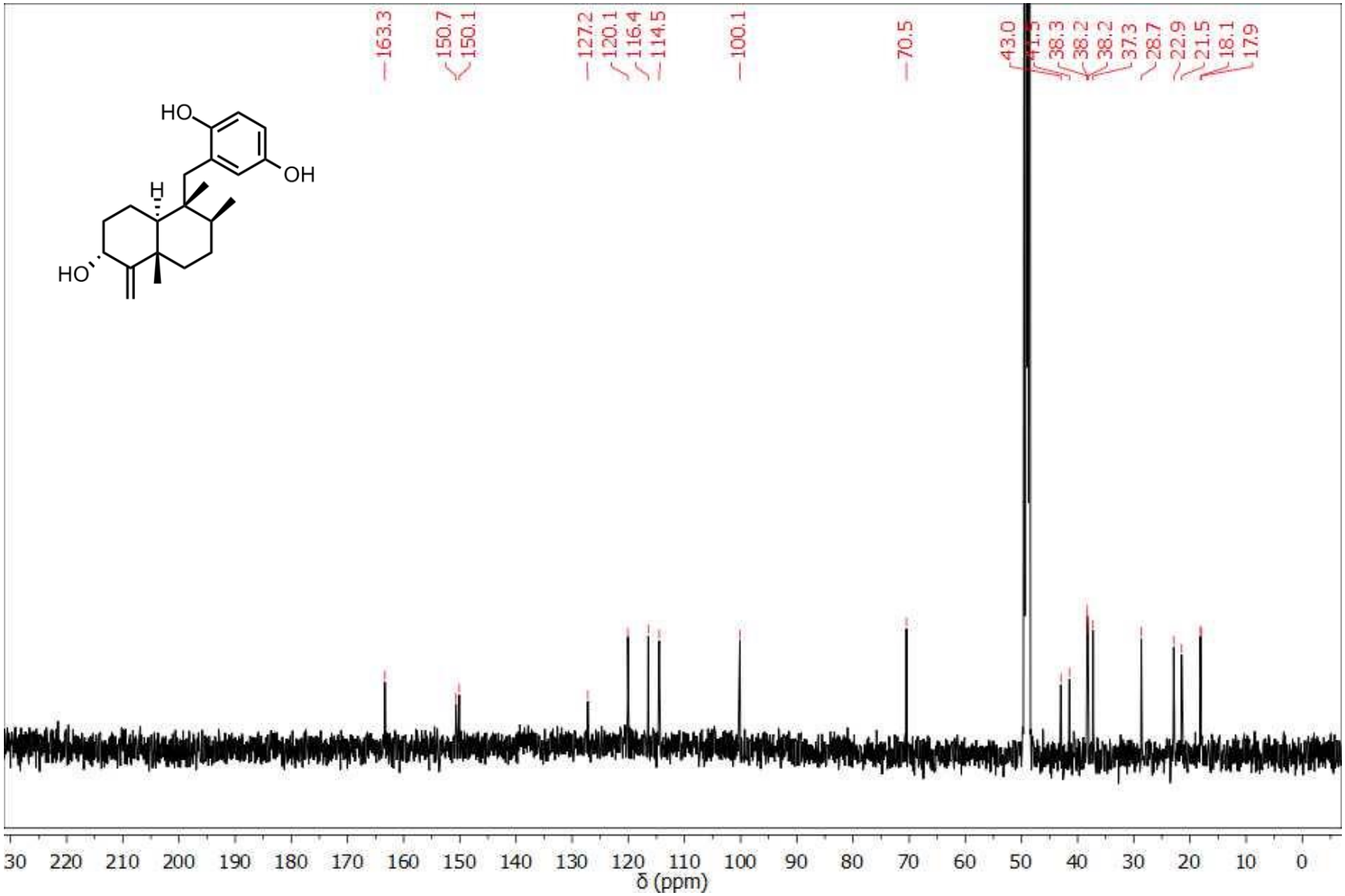

Appendix 52: gHSQC Spectrum of 3α-hydroxyisoavarol (5.5) (CD_3OD, 500 MHz)

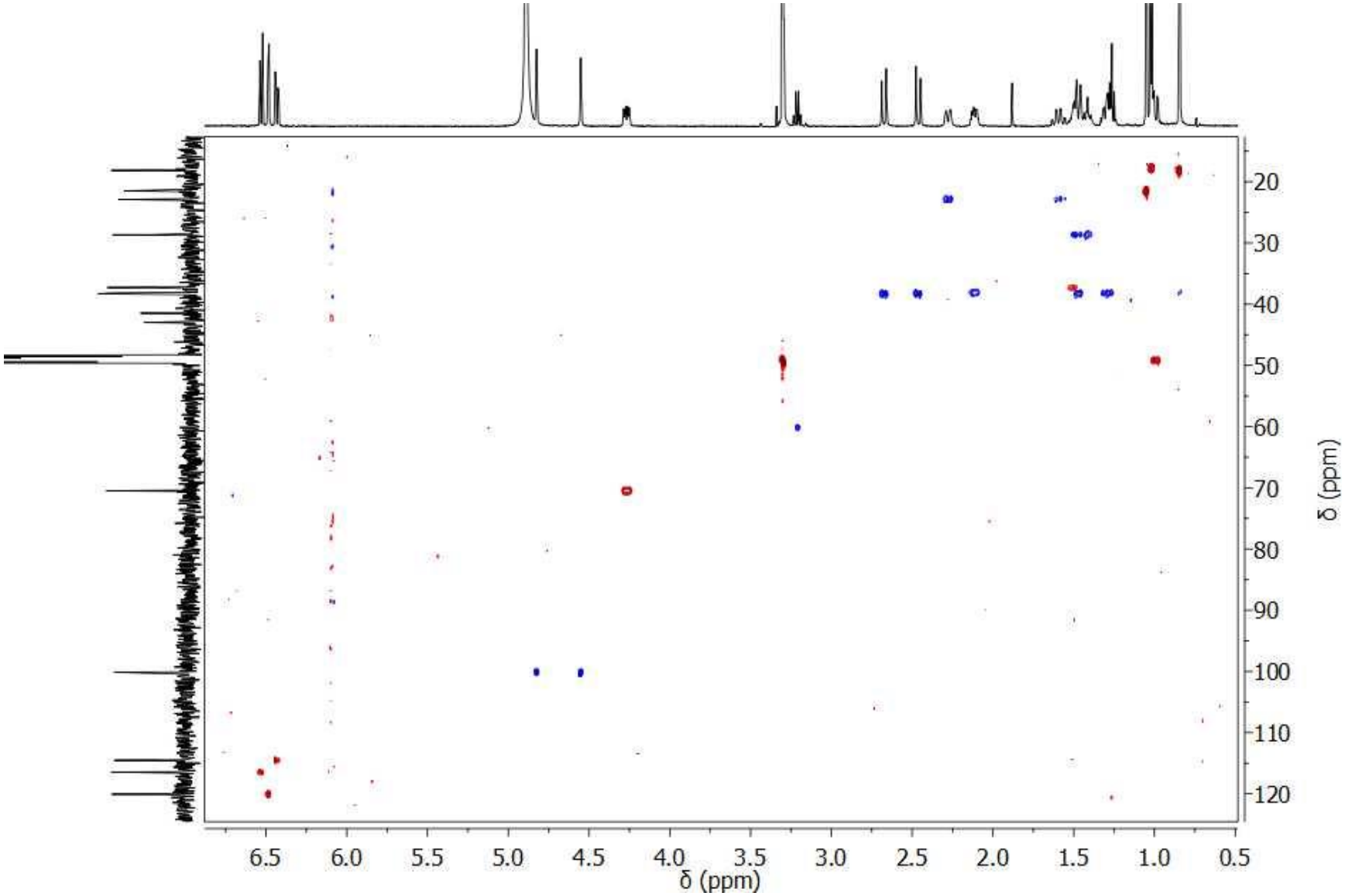

Appendix 53: gDQCOSY Spectrum of 3α-hydroxyisoavarol (5.5) (CD_3OD, 500 MHz)

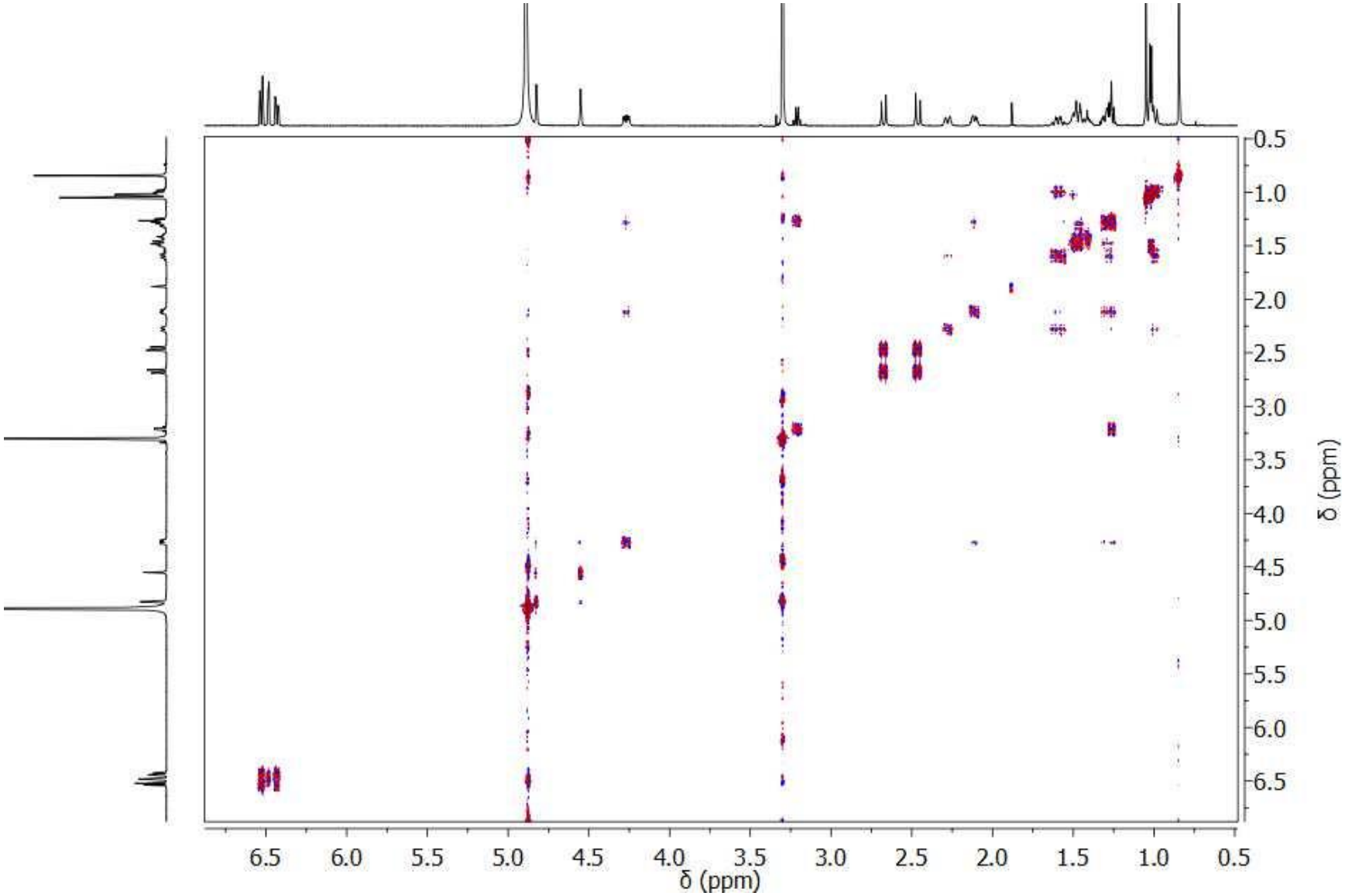

Appendix 54: gHMBC Spectrum of 3α-hydroxyisoavarol (5.5) (CD_3OD, 500 MHz)

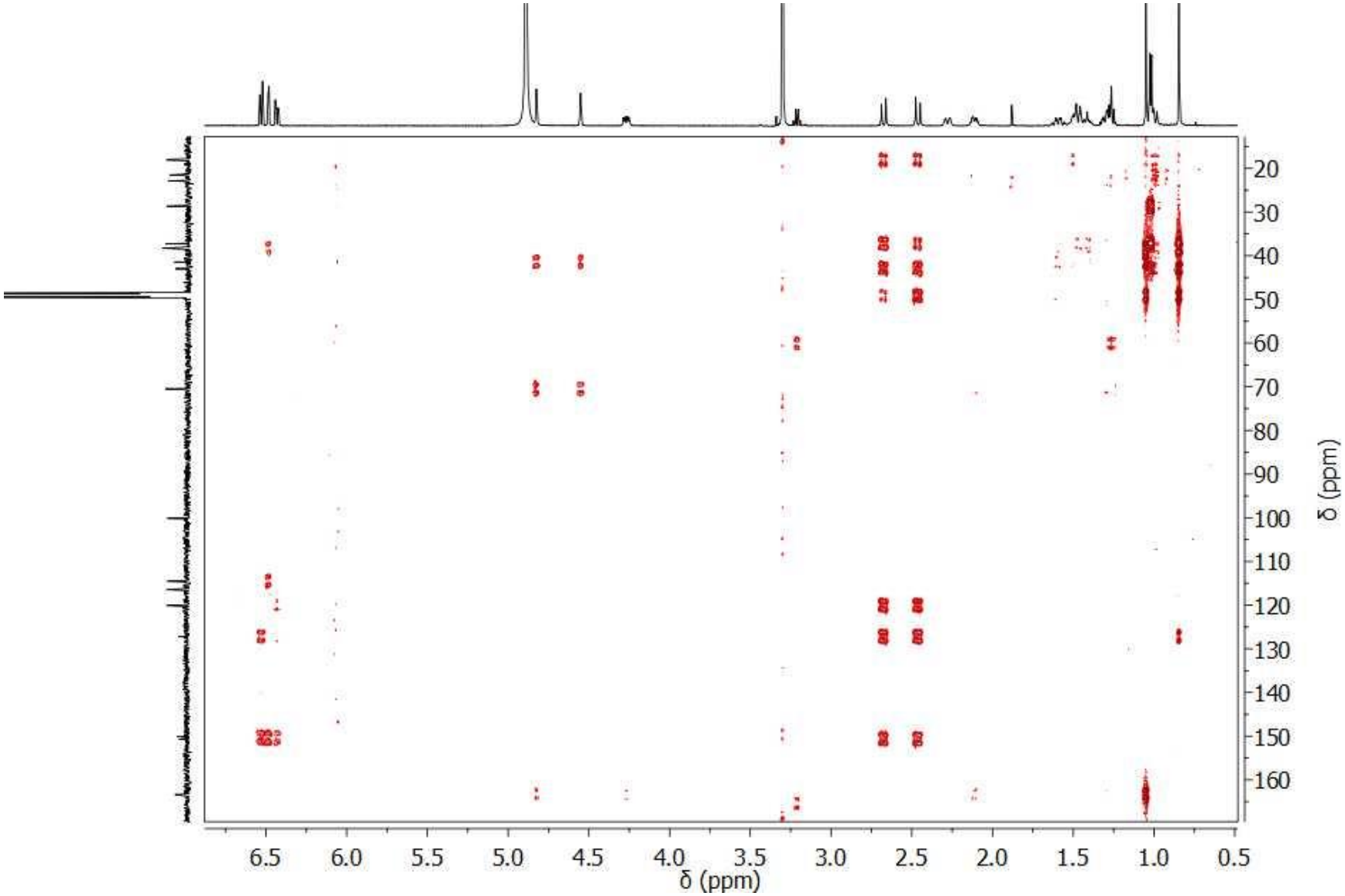

Appendix 55: NOE Spectrum of 3α-hydroxyisoavarol (5.5) Irradiated at δ_H 0.84 ppm (CD_3OD, 500 MHz)

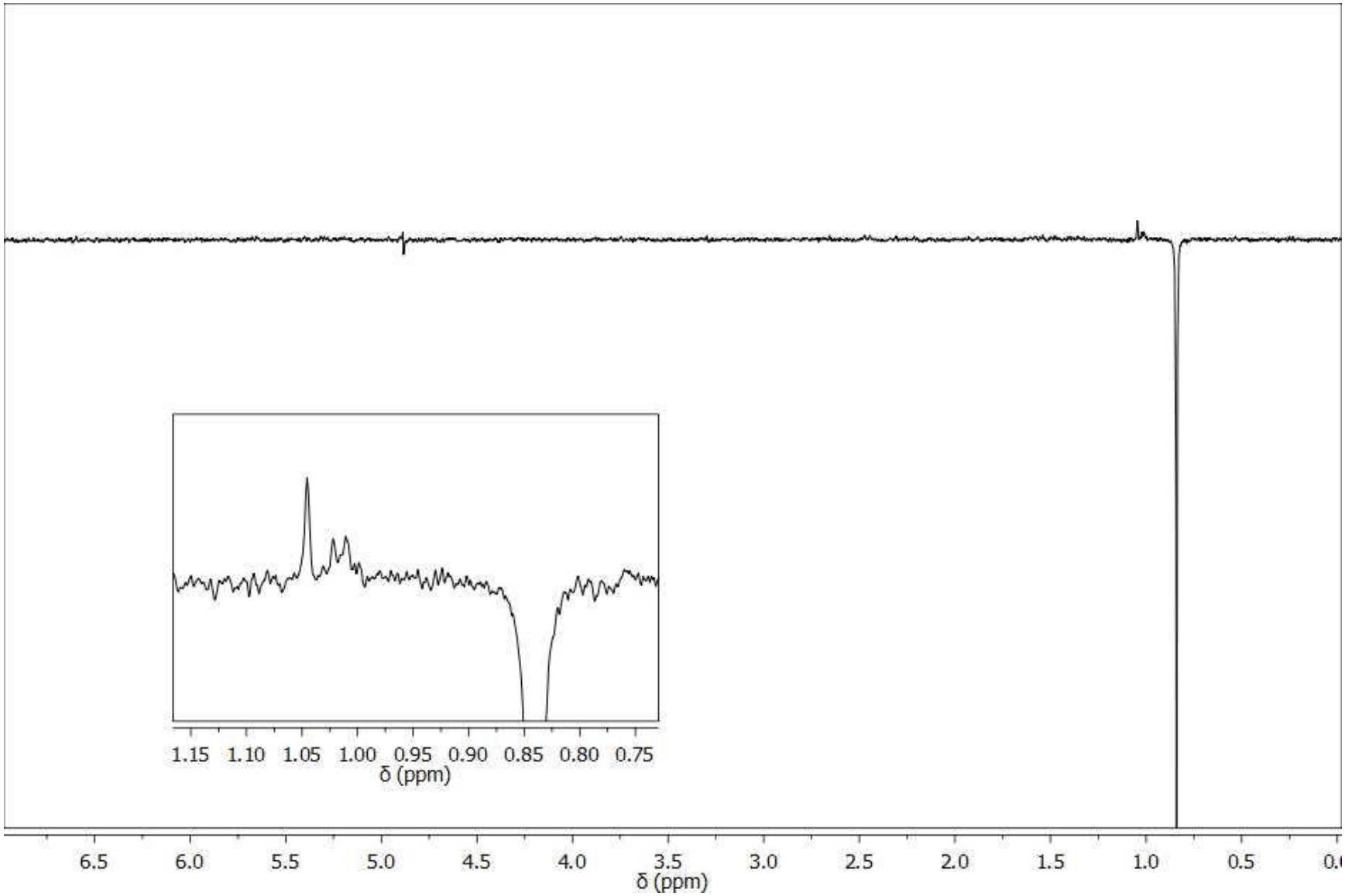

Appendix 56: NOE Spectrum of 3α-hydroxyisoavarol (5.5) Irradiated at δ_H 1.05 ppm (CD_3OD, 500 MHz)

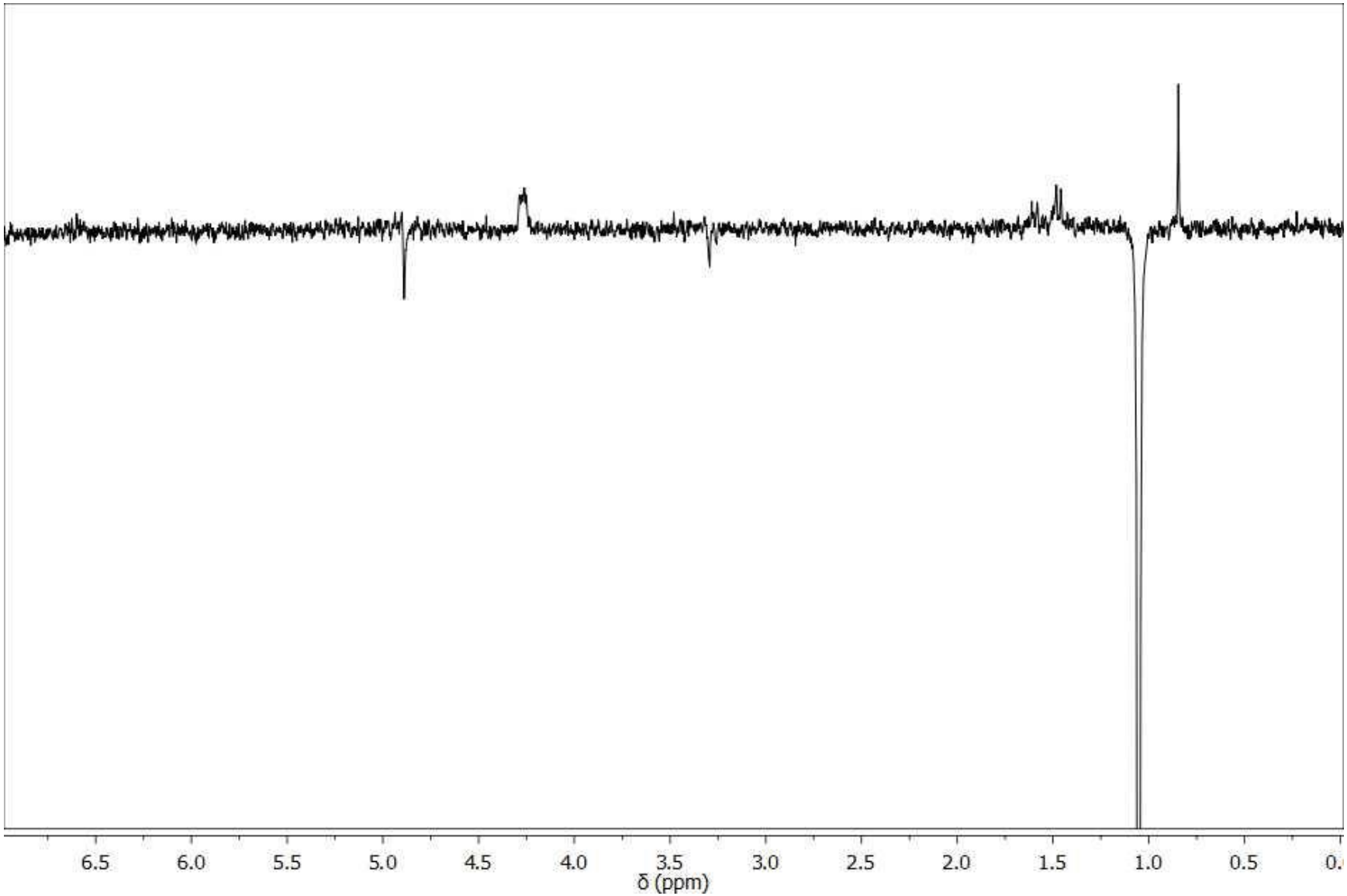

Appendix 57: ^{1}H NMR Spectrum of 2-oxoavarol (5.6) (CD_3OD, 500 MHz)

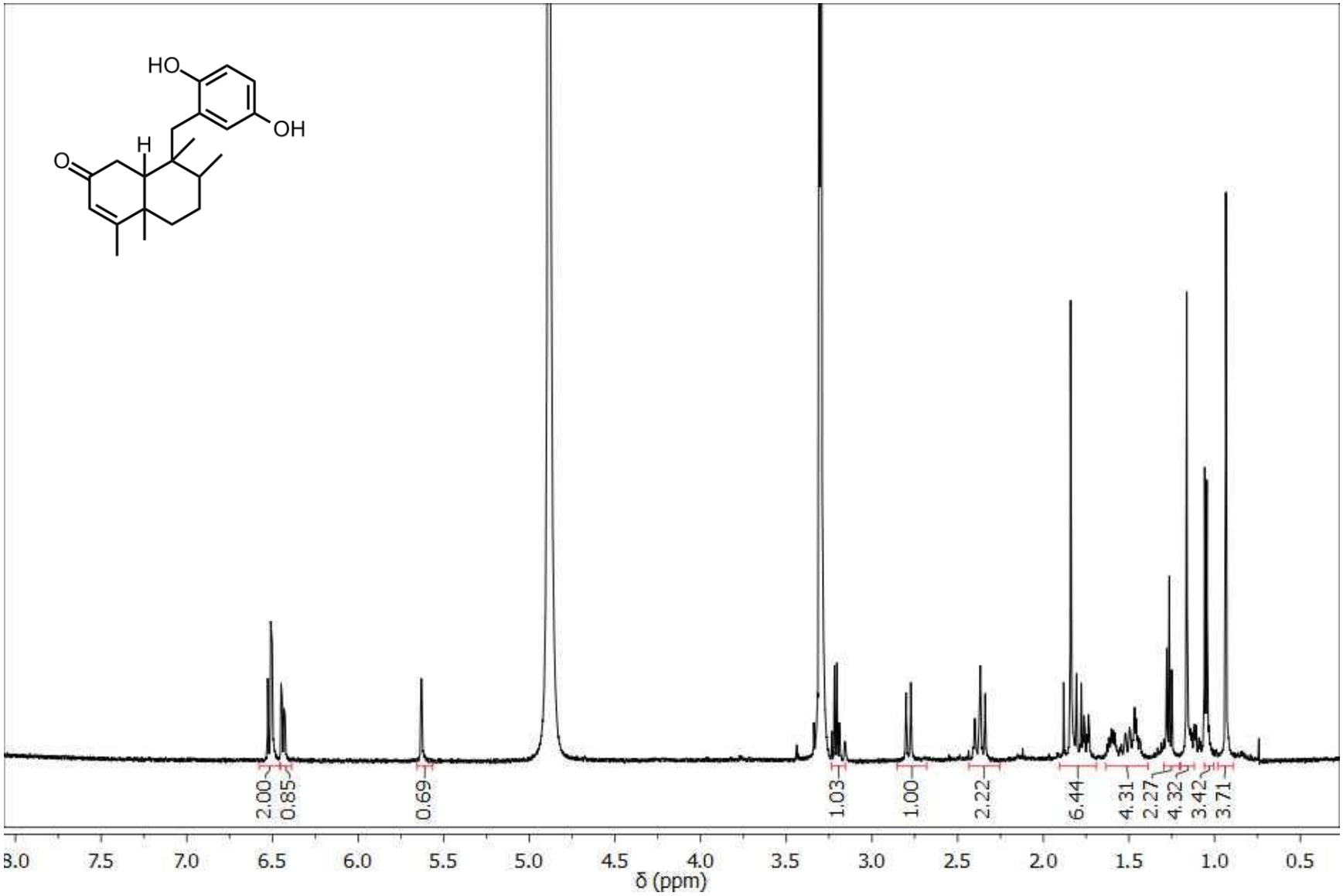

Appendix 58: ^{13}C NMR Spectrum of 2-oxoavarol (5.6) (CD_3OD, 125 MHz)

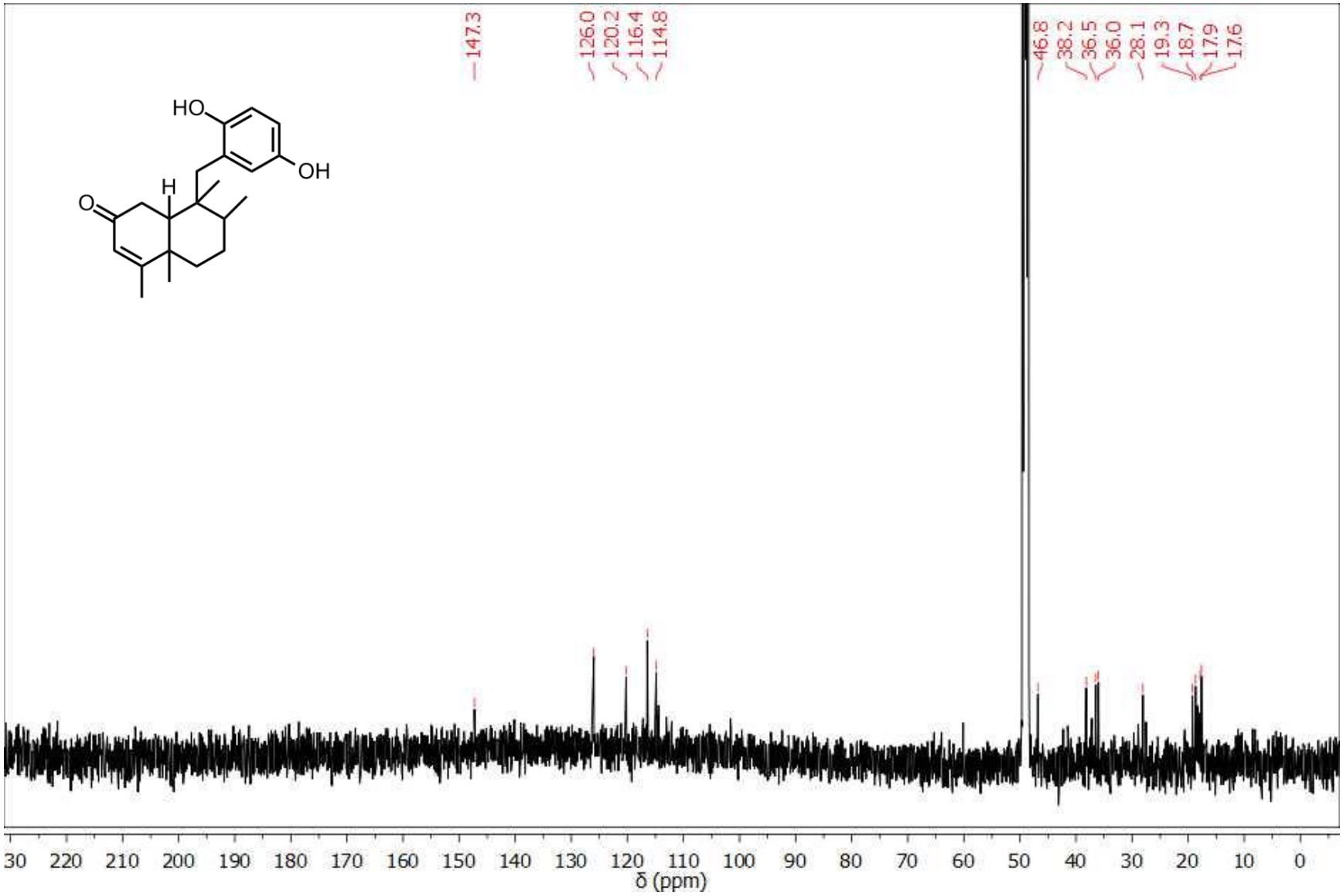

Appendix 59: ^{1}H NMR Spectrum of 2-oxoavarol (5.6) (CD_3OD, 500 MHz)

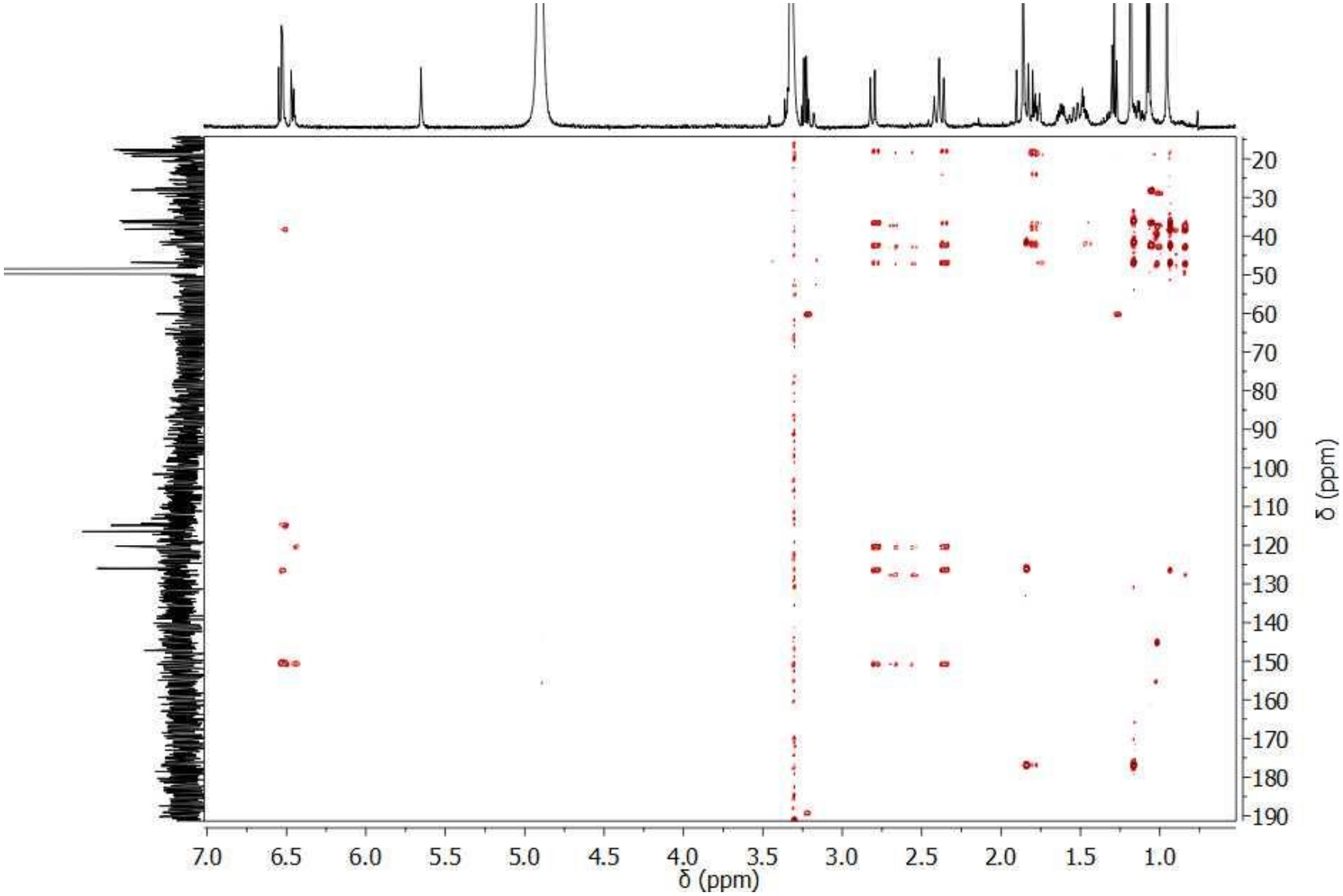

Appendix 60: ^{1}H NMR Spectrum of 2-oxoavarol (5.6) ($CDCl_3$, 500 MHz) (Presat at 1.57 ppm)

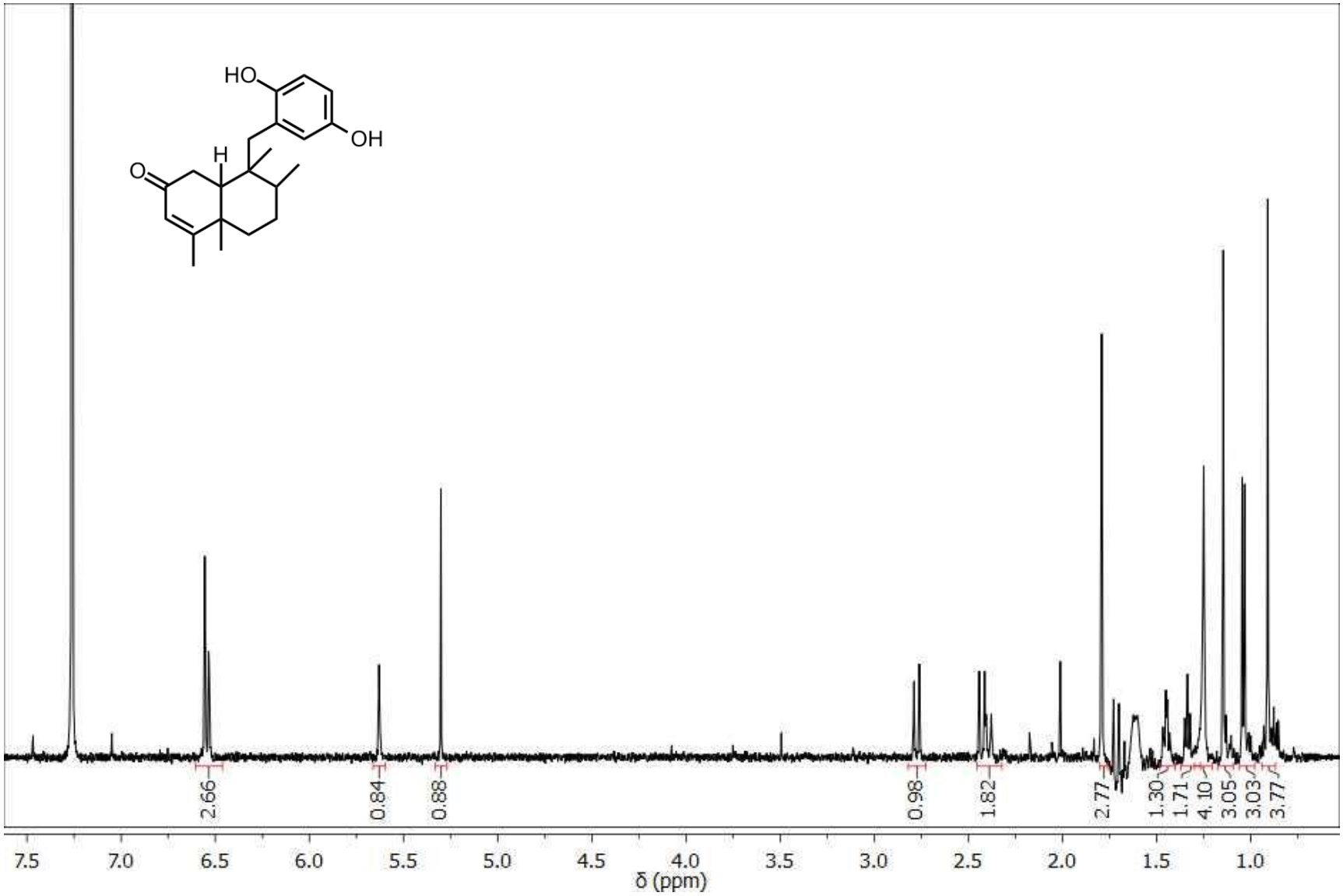

Appendix 61: gDQCOSY Spectrum of 2-oxoavarol (5.6) ($CDCl_3$, 500 MHz)

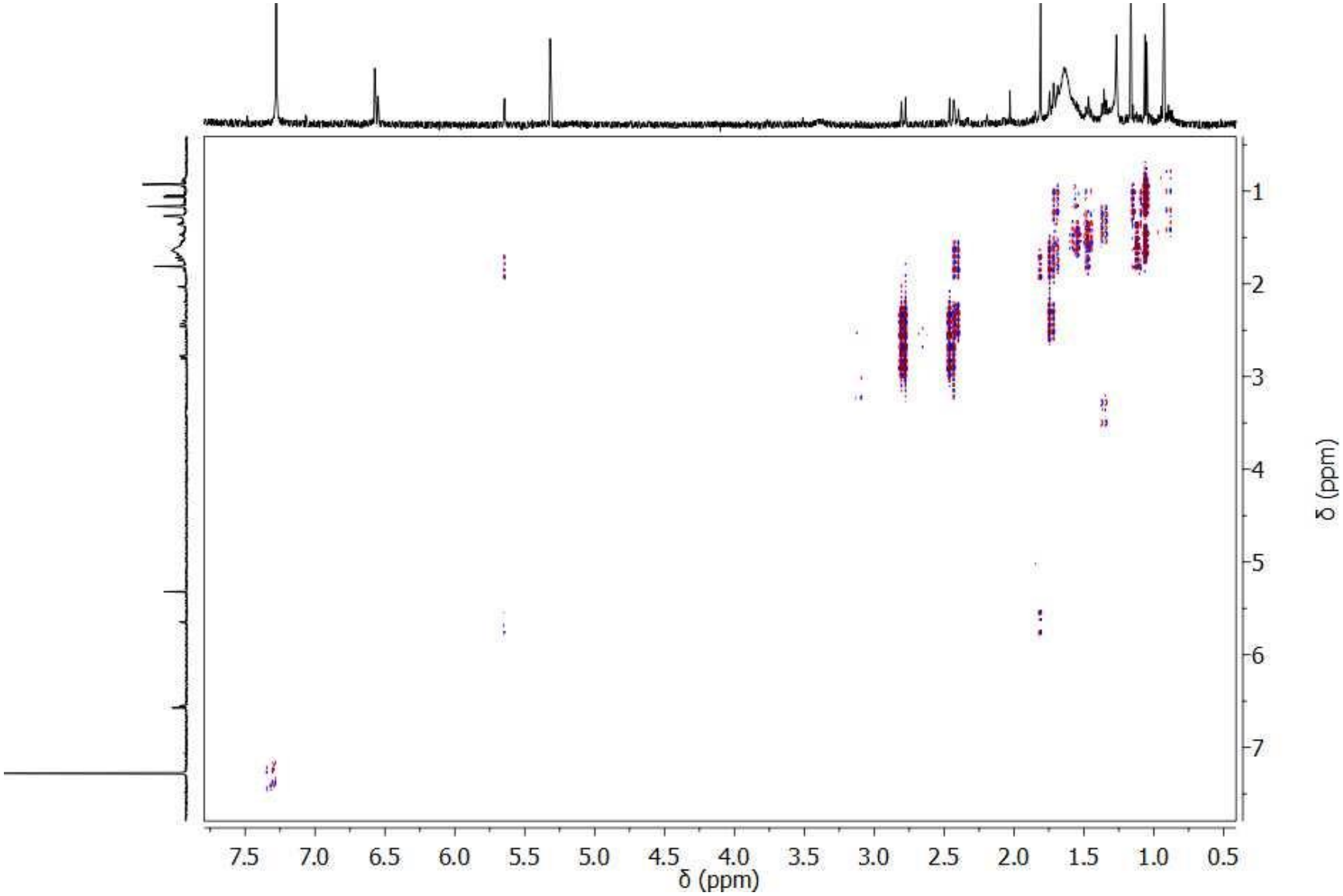

Appendix 62: gHSQC Spectrum of 2-oxoavarol (5.6) (CD_3OD, 500 MHz)

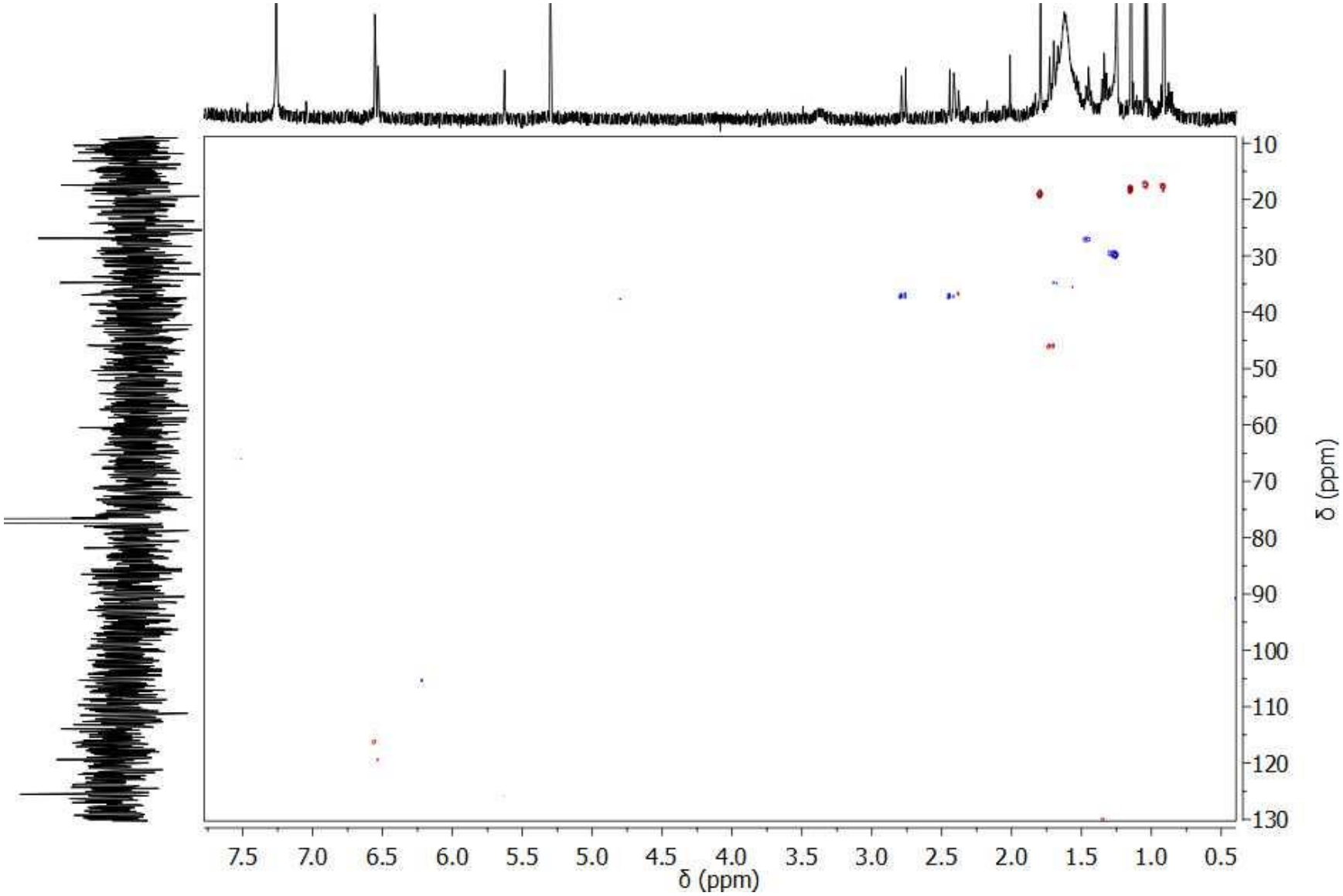

Appendix 63: gHMBC Spectrum of 2-oxoavarol (5.6) (CD_3OD, 500 MHz)

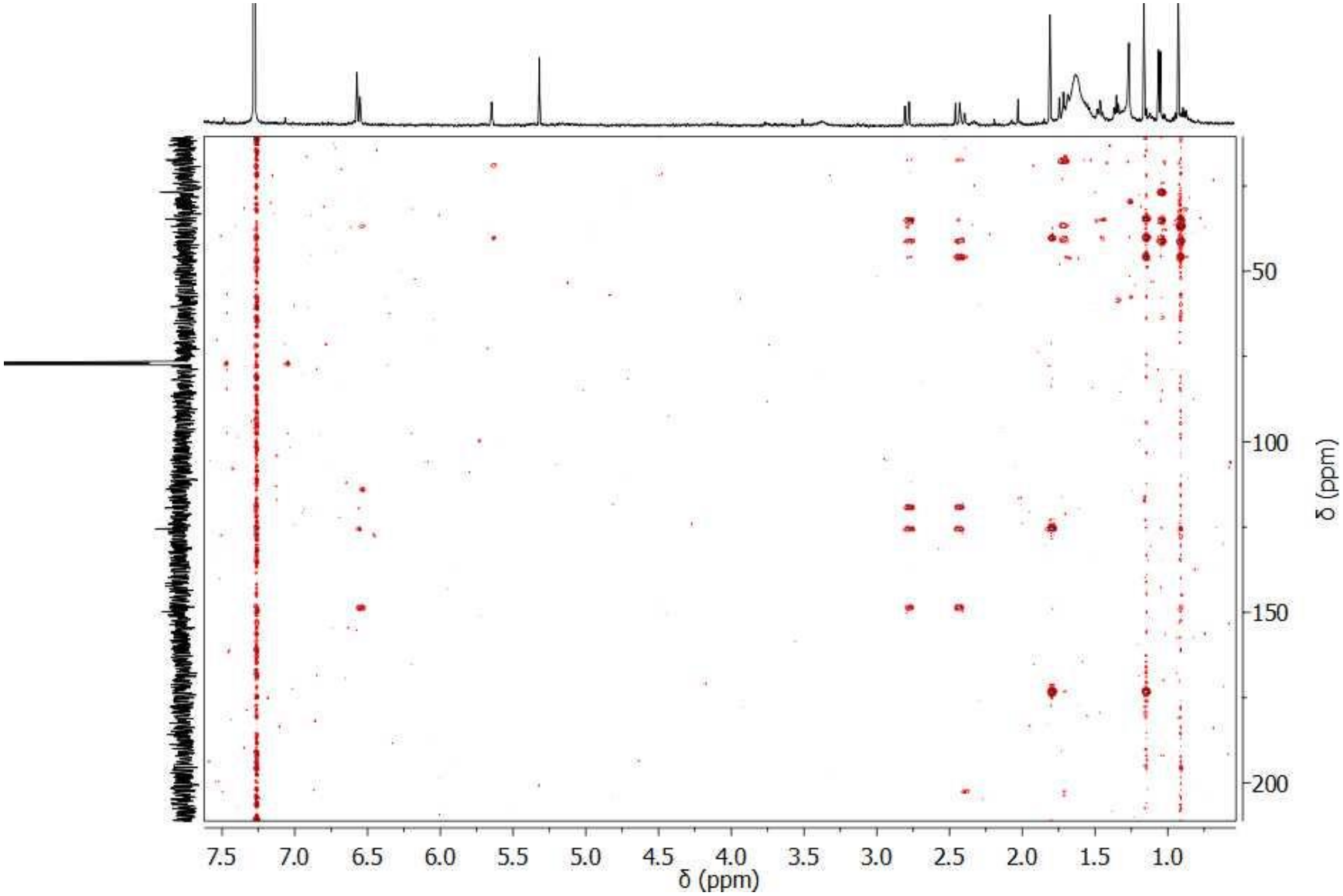

Appendix 64: Image of Unidentified Hawaiian Sponge

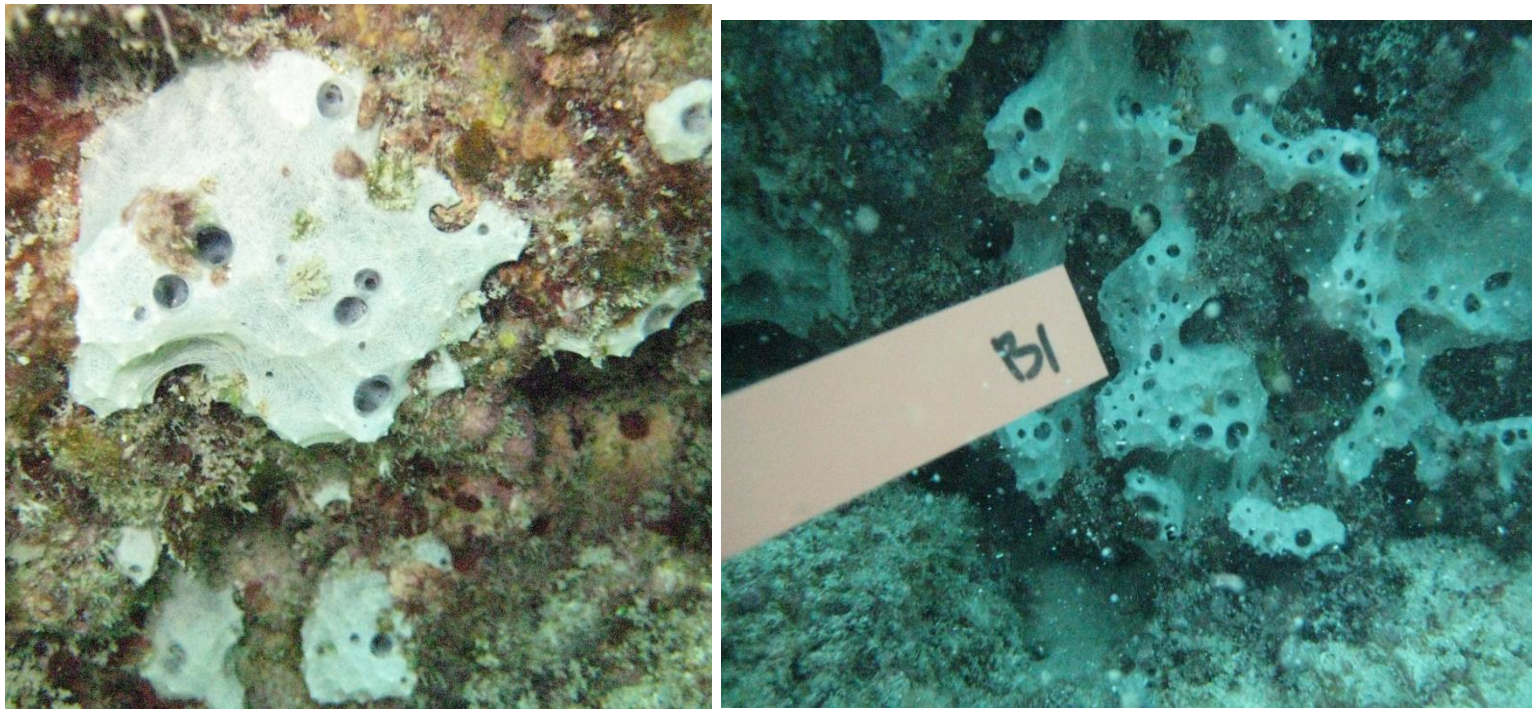

References:

[1] The introductory chapter is an updated product from my master's thesis with pripr permission of the committee. Parrish, S. M. "METABOLITES ISOLATED FROM *MOOREA PRODUCENS, NOSTOC SPHAERICUM, AND SPONGIA* SP." University of Hawai'i at Mānoa, **2013**.

[2] Moore, R. E.; Scheuer, P. J. *Science*. **1971**, *172*, 495-498.

[3] Spande, T. F.; Garraffo, H. M.; Edwards, M. W.; Yeh, H. J. C.; Pannell, L.; Daly, J. W. *J. Am. Chem. Soc.* **1992**, *114*, 3475-3478.

[4] Aboelsoud, N. H. *J. Med. Plants Res*. **2010**, *4*, 82-86.

[5] Karch, Steven B. A Brief History of Cocaine: From Inca Monarchs to Cali Cartels: 500 Years of Cocaine Dealing. Boca Raton, FL, CRC Press, 2006.

[6] Sertürner, F. W. A. *Trommsdorff. J. Pharm.* **1806**, *14*, 47-93.

[7] Stone, E. *Phil. Trans.* **1763**, *53*, 195-200.

[8] Fleming, A. *Br. J. Exp. Pathol.* **1929**, *10*, 226-236.

[9] Duggar, B. M. *Ann. N. Y. Acad. Sci.* **1948**, *51*, 177-181.

[10] National Center for Health Statistics. *Vital and Health Stat*. **1972** series 3 No. 16.

[11] Hoyert, D. L. *NCHS Data Brief*. **2012**, No.88.

[12] Wani, M. C.; Taylor, H. L.; Wall, M. E.; Coggon, P.; McPhail, A. T. *J. Am. Chem. Soc.* **1971**, *93*, 2325-2327.

[13] Arcamone, F.; Franceschi, G.; Orezzi, P.; Cassinelli, G.; Barbieri, W.; Mondelli, R. *J. Am. Chem. Soc.* **1964**, *86*, 5334-5335.

[14] Wall, M. E.;.Wani, M. C; Cook, C. E.; Palmer, K. H.; McPhail, A. T.; Sim, G. A. *J. Am. Chem. Soc.* **1966**; 88, 3888-3890.

[15] Klayman, D. L. *Science.* **1985**, *228*, 1049-1055.

[16] Endo, A.; Kuroda, M.; Tanzawa, K. *FEBS Lett.* **1976**, *72*, 323-326.

[17] Blunt, J. W.; Copp, B. R.; Hu, W. P.; Munro, M. H. G.; Northcote, P. T.; Prinsep, M. R. *Nat. Prod. Rep.* **2009**, *26*, 170-244.

[18] Food and Drug Administration (US). http://www.fda.gov/;

[19] Rinehart, K. L.; Holt, T. G.; Fregeau, N. L.; Stroh, J. G.; Keifer, P. A.; Sun, F.; Li, L. H.; Martin, D. G. *J. Org. Chem.* **1990**, *55*, 4512-4515.

[20] Olivera, B. M.; Cruz, L. J.; de Santos, V.; LeCheminant, G. W.; Griffin, D.; Zeikus, R.; McIntosh, J. M.; Galyean, R.; Varga, J.; Gray, W. R.; et al. *Biochemistry* **1987**, *26*, 2086–2090.

[21] Mayer, A. M. S.; Glaser, K. B.; Cuevas, C.; Jacobs, R. S.; Kem, W.; Little, R. D.; McIntosh, J. M.; Newman, D. J.; Potts, B. C.; Shuster, D. R. *Trends in Pharmacological Sciences.* **2010,** *31*, 255-265.

[22] Mayer, A. M. S. http://marinepharmacology.midwestern.edu/clinPipeline.htm

[23] Newman, D; Cragg, G. *J. Nat. Prod.* **2016**, *79*, 629-661.

[24] Alzheimer's & Dementia. **2016**, *12*, 1-80.

[25] Maccioni, R. B.; Farias, G.; Morales, I. Navarrette, L. *Archives of Medical Research.* **2010**, *41*, 226-231.

[26] Lee, V. M. Y.; Goedert, M.; Trojanowski, J. Q. *Annu. Rev. Neurosci.* **2001**, *24*, 1121-1159.

[27] Grundke-Iqbal I.; Iqbal K.; Tung Y. C.; Quinlan H. M.; Binder L. I. *Proc Natl Acad Sci USA* **1986**, *83*,4913-4917.

[28] Maeda, S.; Sahara, N.; Saito, Y.; Murayama, S.; Ikai, A.; Takashima, A. *Biochemistry*. **2007**, *46*, 3856-3861.

[29] Fernandez, J.; Rojo, L. E.; Kuljis, R. O.; Maccioni, R. B. *J Alzheimers Dis* **2008**, *14*, 329-333.

[30] Hardy, J. Alzheimers Dis., **2006**, *9*, 151-153.

[31] Hardy, J. *J. Neurochem.* **2009**, *110*, 1129-1134.

[32] Sherrington, R et al. *Nature.* **1995**, *375*, 754-60.

[33] Fiuza, U-M.; Arias, A. M. *J. of Endocrinology*. **2007**, *194*, 459–474.

[34] Roberds, S. L. et al. *Hum. Mol. Genet.* **2001**, 10, 1317–1324.

[35] Scarpini, E.; Schelterns, P.; Feldman, H. *Lancet Neurology.* **2003**, *2*, 539-547.

[36] Alzheimer's Disease Medications Fact Sheet. NIH Publication No. 08-3431.

[37] Reference in part, reprinted with permission from Parrish, S. M.; Yoshida, W.; Yang, B.; Williams, P. G. *J. Nat. Prod*. **2017**, *80*, 726-730. Copyright 2017, American Chemical Society.

[38] Roesener, J.; Scheuer, P. *J. Am. Chem. Soc*. **1986**, *108*, 846-847.

[39] Fusetani, N.; Yasumuro, K.; Matsunaga, S. Hashimoto, K. *Tetrahedron Lett.* **1989**, *30*, 2809-2812.

[40] Matsunaga, S.; Fusetani, N.; Hashimoto, K. *J. Org. Chem*. **1989**, *54*, 1360-1363.

[41] Tanaka, J.; Choi, J.; Bai, J.; Yan, Y.; Klenchin, V. A.; Rayment, I.; Marriott, G. *Proc. Nat. Acad. Sci.* **2003**, *100*, 13851-13856.

[42] Klenchin, V. A.; Allingham, J.; King, R.; Tanaka, J.; Marriott, G.; Rayment, I. *Nat. Struct. Bio*. 2003, *10*, 1058-1063.

[43] Allingham, J. S.; Tanaka, J.; Marriott, G.; Rayment, I. *Org.Lett*. **2004**, *6*, 597-599.

[44] Attempts at collecting ^{13}C data on a 600 MHz NMR with cryoprobe and 850 MHz with TCI probe were unsuccessful.

[45] Carmeli, S.; Moore, R. E.; Patterson, G. M. L. *J. Nat. Prod.* **1990**, *53*, 1533-1542.

[46] Ishibashi, M.; Moore, R. E.; Patterson, G. M. L.; Xu, C; Clardy, J. *J. Org. Chem.* **1986**, *51*, 5300-5306.

[47] Kitamura, M.; Schupp P. J.; Nakano, Y.; Uemura, D. *Tetrahedron Lett.* **2009**, *50*, 6606-6609.

[48] Jansen, R.; Steinmetz, H.; Sasse, F.; Schubert, W. D.; Hagelüken, G.; Albrecht, S. C.; Müller, R. *Tetrahedron Lett.* **2008**, *49*, 5796-5799.

[49] Pattenden, G.; Ashweek, N. J.; Baker-Glenn, C. A. G.; Walker, G. M.; Yee, J. G. K. *Angew. Chem. Int. Ed.* **2007**, *46*, 4356-4363.

[50] Dalisay, D. S.; Rogers, E. W.; Edison, A. S.; Molinski, T. F. *J. Nat. Prod.* **2009**, *72*, 732-738.

[51] Matsunaga, S.; Liu, P.; Celatka, C. A.; Panek, J. S.; Fusetani, N. *J. Am. Chem. Soc*. **1999**, *121*, 5605-5606.

[52] Pawlik, J. R.; Kernan, M. R.; Molinski, T. F.; Harper, M. K.; Faulkner, D. J. *J. Exp. Mar. Biol. Ecol.* **1988**, *119*, 99-109.

[53] Pettit, G. R.; Herald, C. L.; Doubek, D. L.; Herald, D. L. *J. Am. Chem. Soc.* **1982**, *104*, 6846-6848.

[54] Davidson, S. K.; Allen, S. W.; Lim, G. E.; Anderson, C. M.; Haygood, M. G. *Appl. Environ. Microbiol.* **2001**, *67*, 4531-4537.

[55] Sharp, K. H.; Davidson, S. K.; Haygood, M. G. *ISME J.* **2007**, *1*, 693-702.

[56] Zhou, Z. F.; Menna, M.; Cai, Y. S.; Guo, Y. W. *Chem. Rev.* **2015**, *115*, 1543-1596.

[57] Paul, V. J.; Fenical, W. *Tetrahedron Lett.* **1980**, *21*, 3327-3330.

[58] A) Castiello, D.; Cimino, G.; De Rosa, S.; De Stefano, S.; Sodano, G. *Tetrahedron Lett.* **1980**, *21*, 5047-5050. B) Walker, R. P.; Faulkner, D. J. *J. Org. Chem*. **1981**, *46*, 1475-1478. C) Higa, T.; Tanaka, J.; Kohagura, T.; Wauke, T. *Chem. Lett.***1990**, *19*, 145-148.

[59] Fusetani, N.; Li, H. Y.; Tamura, K.; Matsunaga, S. *Tetrahedron*. **1993**, *49*, 1203-1210.

[60] Nuzzo, G.; Ciavatta, M. L.; Villani, G.; Manzo, E.; Zanfardino, A.; Varcamonti, M.; Gavagnin, M. *Tetrahedron*. **2012**, *68*, 754-760.

[61] Patil, A. D.; Kokke, W. C.; Cochran, S.; Francis, T. A.; Tomszek, T.; Westley, J. W. *J. Nat. Prod*. **1992**, *55*, 1170-1177.

[62] Shin, J. H.; Seo, Y. W.; Cho, K. W.; Rho, J.-R.; Paul, V. J. *Tetrahedron*. **1998**, *54*, 8711-8720.

[63] Ohta, S.; Okada, H.; Kobayashi, H.; Oclarit, J. M.; Ikegami, S. *Tetrahedron Lett*. **1993**, *34*, 5935-5938.

[64] Tsukamoto, S.; Kato, H.; Hirota, H.; Fusetani, N. *J. Nat. Prod*. **1997**, *60*, 126-130.

[65] The '1-yne-3-ol' refers to nomenclature of the terminal propargylic alcohol. Depending on the molecule, systematic nomenclature sometimes requires a reversal of numbering putting the moiety at the ω terminus. This is the case for **1** and **2**, where the '1-yne-3-ol' refers to positions 30, 31, and 32.

[66] Zhou, G. X.; Molinski, T. F. *Mar. Drugs*. **2003**, 1, 46-53.

[67] El Arfaoui, D.; Listunov, D.; Fabing, I.; Oukessou, M.; Frongia, C.; Lobjois, V.; Samson, A.; Ausseil, F.; Ben-Tama, A.; El Hadrami, E.; Chauvin, R.; Génisson, Y. *ChemMedChem* **2013**, **8**, 1779-1786.

[68] Listunov, D.; Fabing, I.; Saffon-Merceron, N.; Gaspard, H.; Volovenko, Y.; Maraval, V.; Chauvin, R.; Génisson, Y. *J. Org. Chem.* **2015**, *80*, 5386-5394.

[69] Choi, H. J.; Bae, S. J.; Kim, N. D.; Jung, J. H.; Choi, Y. H. *Int. J. Mol. Med.* **2004**, *14*, 1091-1096.

[70] Kim, D. K.; Lee, M. Y.; Lee, H. S.; Lee, D. S.; Lee, J. R.; Lee, B. J.; Hung, J. H. *Cancer Lett.* **2002**, *185*, 95-101.

[71] Park, C.; Jung, J. H.; Kim, N. D.; Choi, Y. H. *Int. J. Oncol.* **2007**, *30*, 291-298.

[72] Park, C.; Kim, G. Y.; Kim, G. D.; Lee, W. H.; Cheong, J. H.; Kim, N. D.; Bae, J. H.; Choi, Y. H. *Oncol. Rep.* **2006**, *16*, 171-176.

[73] Lang, G.; Mayhudin, N. A.; Mitova, M. I.; Sun, L.; van der Sar, S.; Blunt, J. W.; Cole, A. L. J.; Ellis, G.; Laatsch, H.; Munro, M. H. G. *J. Nat. Prod*. **2008**, *71*, 1595-1599.

[74] Nakao, Y.; Uehara, T.; Matsunaga, S.; Fusetani, N.; van Soest, R. W. M. *J. Nat. Prod.* **2002**, *65*, 922-924.

[75] Li, H. Y.; Matsunaga, S.; Fusetani, N. *J. Nat. Prod.* **1994**, *57*, 1464-1467.

[76] Takada, K.; Okada, S.; Matsunaga, S. *Fish. Sci.* **2014**, *80*, 1057-1064.

[77] Fleming, I.; Harley-Mason, J. *J. Chem. Soc.* **1963**, 4771-4777. B) Fleming, I.; Owen, C. R. *J. Chem. Soc. B* **1971**, 1293-1299. C) Fleming, I.; Ramarao, C. *Org. Biomol. Chem.* **2004**, *2*, 1504-1510.

[78] Minto, R. E.; Blacklock, B. *J. Prog. Lipid Res*. **2008**, *47*, 233-306.

[79] Corgiat, J. M.; Scheuer, P. J.; Steiner, J. L. R.; Clardy, J. *Tetrahedron* **1993**, *49*, 1557-1562.

[80] D'Auria, M. V.; Minale, L.; Riccio, R. *Chem. Rev.* **1993**, *93*, 1839-1895.

[81] Kerr, R. G.; Baker, B. J. *Nat. Prod. Rep.* **1991**, *8*, 465-497.

[82] Blackman, A. J,; Heaton, A.; Skelton, B. W.; White, A. H. *Aust. J. Chem.* **1985**, *38*, 565-573.

[83] Dai, J.; Yoshida, W. Y.; Kelly, M.; Williams, P. *J. Nat. Prod.* **2016**, *79*, 1464-1467.

[84] Tomono, Y.; Hirota, H.; Imahara, Y.; Fusetani, N. *J. Nat. Prod.* **1999**, *62*, 1538-1541.

[85] Kittakoop, P.; Suttisri, R.; Chaichantipyuth C.; Vethchagarum, S.; Suwanborirux, K. *J. Nat. Prod.* **1999**, *62*, 318-320.

[86] Machida, K.; Abe, T.; Arai, D.; Okamoto, M.; Shimizu, I.; de Voogd, N. J.; Fusetani, N.; Nakao, Y.. *Org. Lett.* **2014**, *16*, 1539-1541.

[87] Moffitt, W.; Woodward, R. B.; Moscowitz, A.; Klyne, W.; Djerassi, C. *J. Am. Chem. Soc.* **1961**, *83*, 4013-4018.

[88] Gross, E. K. U.; Dobson, J. F.; Petersilka, M. *Top. Curr. Chem*. **1996**, *181*, 81-172.

[89] Runge, E.; Gross, E. K. U. *Phys. Rev. Lett.* **1984**, *52*, 997-1001.

[90] Nugroho, A. F.; Morita, H. *J. Nat. Med.* **2014**, *68*, 1-10.

[91] Zhu, L.; Tong, R. *J. Antibiotics.* **2016**, *69*, 280-286.

[92] Girard, A.; Sandulesco, G.; Fridenson, A. *Compt. Rend. Acad. Sci.* **1932**, *195***,** 981-983.

[93] Grogan, D. W.; Cronan, J .E. Jr. *Microbiol. Mol. Biol. Rev.* **1997**, *61*, 429-441.

[94] Minale, L.; Riccio, R.; Sodano, G. *Tetrahedron Letters*. **1974**, *38*, 3401-3403.

[95] Luibrand, R. T.; Erdman, T. R.; Vollmer, J. J.; Scheuer, P. J.; Finer, J.; Clardy, J. *Tetrahedron*. **1979**, *35*, 609-612

[96] Müller, W. E. G.; Sobel, C.; Diehl-Seifert, B.; Maidhof, A.; Schroder, H. C. *Biochem. Pharmacol.*, **1987**, *36*, 1489-1494.

[97] Božić, T.; Novaković, I.; Gašić, M. J.; Juranic, Z.; Stanojkovic, T.; Tufegdzic, S.; Kljajic, Z.; Sladić, D. *Eur. J. Med. Chem.* **2010**, *45*, 923-929.

[98] Monks, T. J.; Hanzlik, R. P.; Cohen, G. M.; Ross, D.; Graham, D. G. *Toxicol. Appl. Pharmacol.* **1992**, *112*, 2-16.

[99] O'Brien, P. J. *Chem. Biol. Interact*. **1991**, *80*, 1-41.

[100] Schröder, H. C.; Wenger, R.; Gerner, H.; Reuter, P.; Kuchino, Y.; Müller, W. E. G. *Cancer Res.* **1989**, *49*, 2069-2076.

[101] Sladić, D.; Gašić, M. J. *J. Serb. Chem. Soc*. **1994**, *59*, 915-920.

[102] Sladić, D.; Novaković, I.; Vujčić, Z.; Božić, T.; Božić, N.; Milić, D.; Šolaja, B.; Gašić, M. J. *J. Serb. Chem. Soc*. **2004**, *69*, 901-907.

[103] Novaković, I.; Vujčić, Z.; Božić, T.; Božić, N.; Milosavić, N.; Sladić, D. *J. Serb. Chem. Soc.* **2003**, *68*, 243-248.

[104] Gordaliza, M.; *Mar. Drugs*. **2010**, *8*, 2849-2870.

[105] Sladić, D.; Gašić, M. J. *Molecules*. **2006**, *11*, 1-33

[106] Marcos, I.S.; Conde, A.; Moro, R.F.; Basabe, P.; Diez, D.; Urones, J.G. *Mini Rev. Org. Chem*. **2010**, 7, 230-254.

[107] Pretsch book pg 130

[108] Yong, K. W. L.; Jankam, A.; Hooper, J. N. A.; Suksamrarn, A.; Garson, M. J. *Tetrahedron* **2008**, *64*, 6341-6348.

[109] Hagiwara, K.; Garcia Hernandez, J. E.; Harper, M. K.; Carroll, A.; Motti, C. A.; Awaya, J.; Nguyen, H. Y.; Wright, A. D. *J. Nat. Prod.* **2015**, *78*, 325-329.

[110] Cimino, G.; De Stefano, S.; Minale, L. *Experientia*. **1975**, *31*, 1117-1118.

[111] Shen, Y. C.; Liaw, C. C.; Ho, J. R.; Khalil, A. T.; Kuo, Y. H. *Nat. Prod. Res.* **2006**, *20*, 578-585.

[112] Frisch, M. J.; Trucks, G. W.; Schlegel, H. B.; Scuseria, G. E.; Robb, M. A.; Cheeseman, J. R.; Scalmani, G.; Barone, V.; Mennucci, B.; Petersson, G. A.; Nakatsuji, H.; Caricato, M.; Li, X.; Hratchian, H. P.; Izmaylov, A. F.; Bloino, J.; Zheng, G.; Sonnenberg, J. L.; Hada, M.; Ehara, M.; Toyota, K.; Fukuda, R.; Hasegawa, J.; Ishida, M.; Nakajima, T.; Honda, Y.; Kitao, O.; Nakai, H.; Vreven, T.; Montgomery, J. A.; Peralta, J. E.; Ogliaro, F.; Bearpark, M.; Heyd, J. J.; Brothers, E.; Kudin, K. N.; Staroverov, V. N.; Kobayashi, R.; Normand, J.; Raghavachari, K.; Rendell, A.; Burant, J. C.; Iyengar, S. S.; Tomasi, J.; Cossi, M.; Rega, N.; Millam, J. M.; Klene, M.; Knox, J. E.; Cross, J. B.; Bakken, V.; Adamo, C.; Jaramillo, J.; Gomperts, R.; Stratmann, R. E.; Yazyev, O.; Austin, A. J.; Cammi, R.; Pomelli, C.; Ochterski, J. W.; Martin, R. L.; Morokuma, K.; Zakrzewski, V. G.; Voth, G. A.; Salvador, P.; Dannenberg, J. J.; Dapprich, S.; Daniels, A. D.; Farkas; Foresman, J. B.; Ortiz, J. V.; Cioslowski, J.; Fox, D. J., Gaussian 09, Revision B.01. Wallingford CT, 2009.

[113] Cammi, R.; Tomasi, J. *J. Comput. Chem.* **1995**, *16*, 1449-1458

[114] Miertuš, S.; Tomasi, J. *Chem. Phys.* **1982**, *65*, 239-245.

[115] Naqvi, T. J. *Biomol. Screen.* **2004**, *9*, 298–408

[116] Shubina, L. K.; Fedorov, S. N.; Stonik, V. A. *Chem. Nat. Compd.* **1990**, *26*, 296-298.

[117] Crispino, A.; De Giulio, A.; De Rosa, S.; Strazzullo, G. *J. Nat. Prod.* **1989**, *52*, 646-648.

[118] Feng, B. Y.; Simeonov, A.; Jadhav, A.; Babaoglu, K.; Inglese, J.; Shoichet, B. K.; Austin, C. P. *J. Med. Chem.* **2007**, *50*, 2385-2390.